Toward New Era of Photonuclear Reactions

Hiroaki Utsunomiya
(Konan University)

Content

Lecture 1 : Past of Photonuclear Reactions
- 1.1 γ-ray sources
- 1.2 Nuclear physics – (γ,n) for GDR
- 1.3 Compilations of experimental data- Atlas, IAEA, CDFE, EXFOR

Lecture 2 : Present of Photonuclear Reactions
- 2.1 Laser Compton-scattering γ-ray beam
- 2.2 Nuclear Physics (γ,γ') for PDR
- 2.3 Nuclear Astrophysics
  - a. p-process – (γ,n)
  - b. s-process - gamma-ray strength function for (γ,n) and (n,γ)

Lecture 3: Present and Future of Photonuclear Reactions

2.3 Nuclear Astrophysics

c. reciprocity theorem – photodisintegration of D, ^{9}Be, ^{16}O

2.4 Evaluated Nuclear Data Library – ENDF, JEFF, JENDL

Reference Input Parameter Library - RIPL

3. ELI-NP project

3.1 ELI-NP vs HIGS and NewSUBARU

3.2 p-process – rare isotopes

3.3 Precision Era of Nuclear Physics

a. PDR above neutron threshold

b. GDR – (γ,γ), (γ,n) $(\gamma,2n)$, $(\gamma,3n)$ cross sections

3.4 Special topic

Photoreactions on isomers – laser-gamma combined experiment

γ-ray sources: radioisotopes

Green and Donahue, PR 135, B701 (1964)

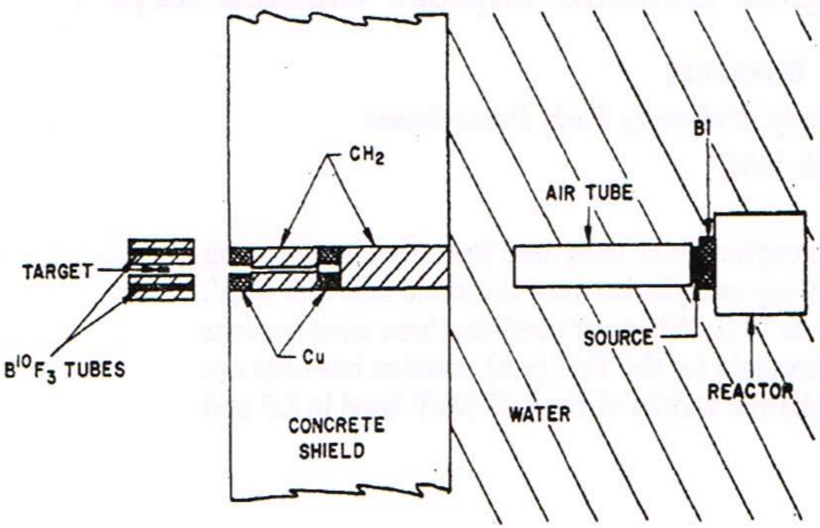

FIG. 1. Neutron counter and source arrangement.

TABLE I. Measured gamma-ray intensities.

Source	Energy[a] (MeV)	Intensity $\times 10^{-4}$ (γ rays/cm^2-sec)
Aluminum	7.72	8.1 $\pm$0.7
Copper	7.91	14.0 $\pm$1.4
	7.63	6.4 $\pm$0.6
Chlorine	8.56	2.3 $\pm$0.3
	7.77	6.0 $\pm$0.7
	7.42	6.9 $\pm$0.8
Nitrogen	10.83	0.49$\pm$0.03
	8.31	0.10$\pm$0.03
Nickel	9.00	19.8 $\pm$2.1
	8.53	9.1 $\pm$0.9
Chromium	9.72	2.5 $\pm$0.4
	8.88	6.2 $\pm$0.9
Iron	7.64	22.0 $\pm$2.8
	9.30	1.9 $\pm$0.2
	6.03+5.92	11.3 $\pm$1.5
Lead	7.38	1.9 $\pm$0.3
Sulphur	5.43	10.2 $\pm$1.4
	8.64	0.6 $\pm$0.1
	7.78	0.8 $\pm$0.2
Titanium	6.75	18.9 $\pm$2.2
	6.41	12.5 $\pm$1.5
	6.61[b]	33.7 $\pm$2.7
Manganese	7.16[c]	19.0 $\pm$1.7
Zinc	7.88	4.5 $\pm$0.5

Lecture 1 : Past of Photonuclear Reactions

TABLE II. Summary of measured cross sections (millibarns).

Source	Energy[a] (MeV)	Targets Ta^{181}	Li^{7}	Li^{6}	C^{13}	B^{10}
Aluminum	7.72	4.1± 0.4	0.06 ±0.01	1.13±0.12	1.7 ±0.2	···
Copper	7.91	10.8±1.0	0.07 ±0.01	1.1 ±0.2	0.97±0.13	···
Chlorine	8.56	29 ± 6	0.17 ±0.12	···	···	···
Nickel	9.00	44 ± 6	0.16 ±0.06	1.6 ±0.3	0.6 ±0.1	0.11±0.01
Nitrogen	10.83	121 ±12	1.07 ±0.25	···	4 ±2	0.9 ±0.2
Chromium	9.72	84 ±25	0.55 ±0.25	···	···	0.23±0.05
Iron	7.64	0.0± 0.9	0.079±0.014	1.3 ±0.2	0.23±0.05	···
Iron	9.30	···	···	···	···	0.09±0.03
Lead	7.38	···	0.068±0.035	1.2 ±0.2	0.3 ±0.3	···
Sulphur	5.43	···	···	0.42±0.07		
Sodium	6.41	···	···	0.6 ±0.1		
Titanium	6.75	···	···	1.3 ±0.2	···	···
Titanium	6.61[b]	···	···	···	0.32±0.04	···
Manganese	7.16[c]	···	···	0.9 ±0.1	0.4 ±0.1	
Zinc	7.88	···	···	1.0 ±0.2	1.2 ±0.2	

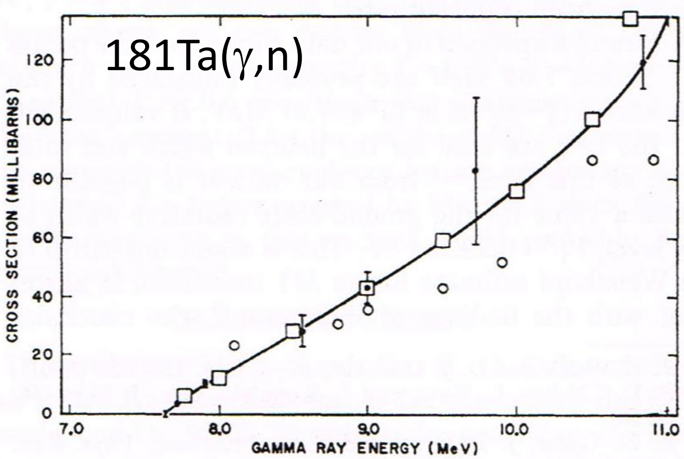

FIG. 2. Energy versus cross section, $Ta^{181}(\gamma,n)$. Boxes are data of Fuller and Weiss (Ref. 8), circles are data of Bramblett *et al.* (Ref. 1). The solid line is a smooth curve through the present cross-section measurements.

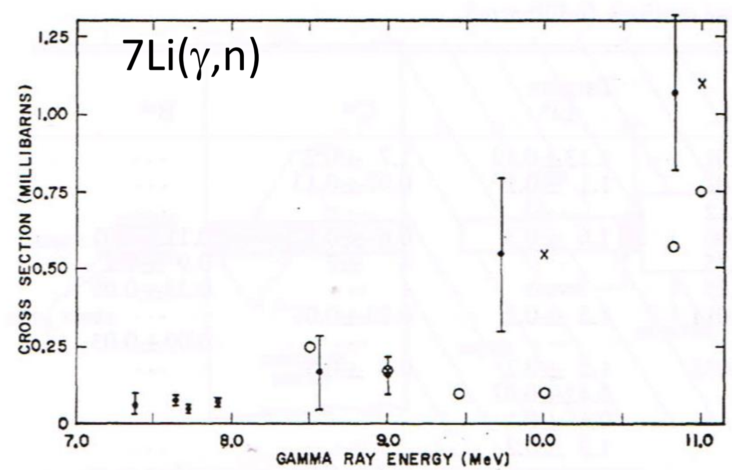

FIG. 3. Energy versus cross section, $Li^{7}(\gamma,n)$. Crosses are data of Goldemberg and Katz (Ref. 3), circles are data of Romanowski and Voelker (Ref. 12).

γ-ray sources: Nuclear reactions

$^{27}Al(p, \gamma)^{28}Si$, E_p = 992 keV resonance

Anttila et al., NIM 147, 501 (1977)

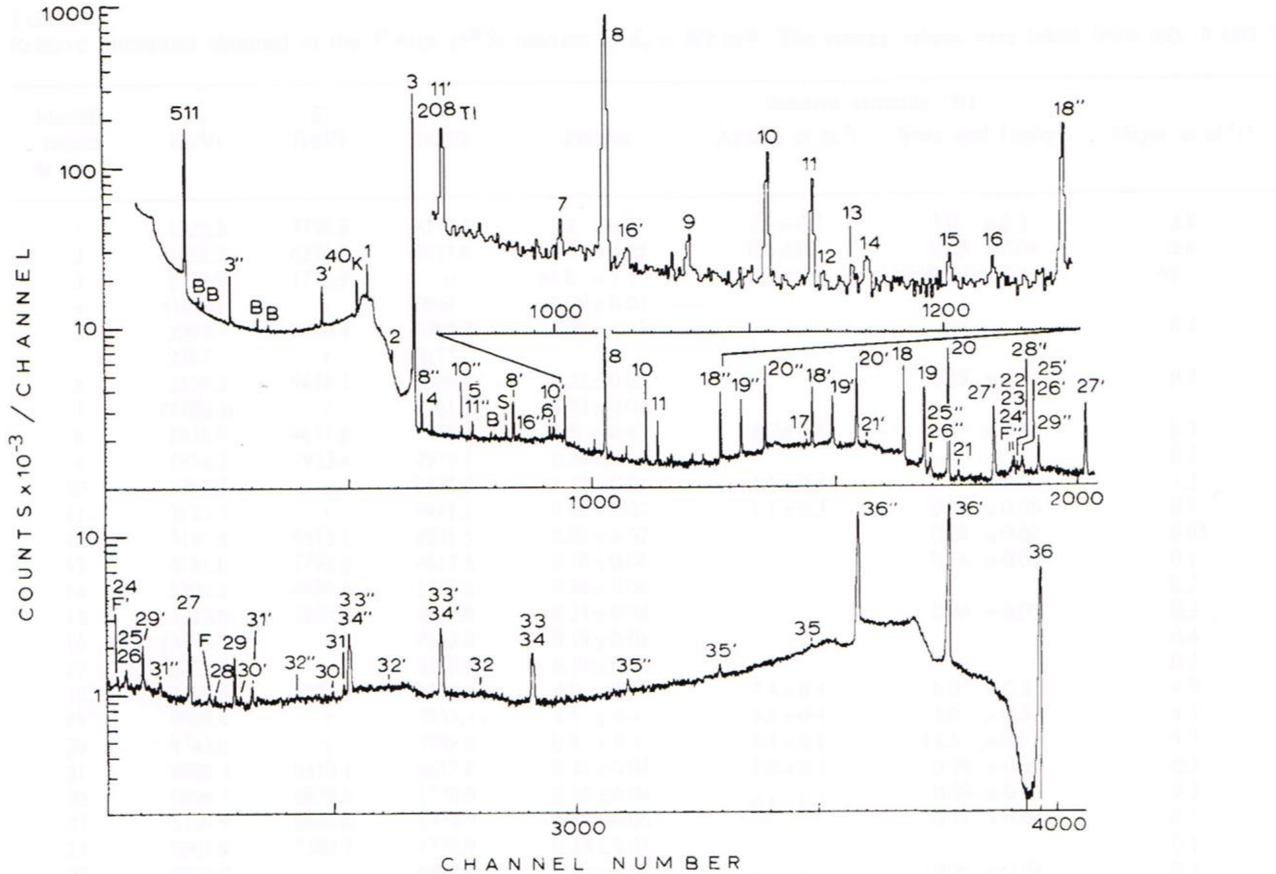

Fig. 1. Gamma-ray spectrum of the $E_p = 992$ keV resonance in the $^{27}Al(p, \gamma)^{28}Si$ reaction taken at the distance of 6 cm and at $\theta = 55°$. The prime and double-prime refer to the single-escape and double-escape peaks, respectively. B means background peak, S the sum peak of the 1779 keV and 511 keV γ-rays and F illustrates $E_\gamma = 6129$ keV energy due to the $^{19}F(p, \alpha\gamma)^{16}O$ reaction. The insert illustrates in more detail the intensity of the weak transitions.

27Al(p, γ)28Si, E_p = 992 keV resonance

TABLE 1
Relative intensities obtained in the $^{27}Al(p, \gamma)^{28}Si$ reaction at $E_p = 992$ keV. The energy values were taken from refs. 4 and 5.

Identification in fig. 2	E_γ (keV)	E_i (keV)	E_f (keV)	Relative intensity (%) Present	Azuma et al.[9]	Scott and Lusby[2]	Meyer et al.[4] [a]
1	1522.3	7798.8	6276.5	2.8 ±0.2	2.9±0.5	3.0 ±0.3	2.8
2	1658.7	6276.5	4617.8	0.52±0.05	0.6±0.1	0.49 ±0.04	0.4
3	1778.9	1778.9	0	94.8 ±1.5	94.0±9.4	94.1 ±9.4	95
4	(1874)	r	10668	0.29±0.03			
5	2099.7	9480.4	7380.7	0.24±0.02			0.2
	2267	r	10275		?		
6	2529.3	9418.1	6888.8	0.22±0.03		0.19 ±0.03	0.2
7	(2780.3)	r	9761.5	0.23±0.04			
8	2838.9	4617.8	1778.9	5.5 ±0.4	6.2±0.6	6.3 ±0.4	6.3
9	2954.3	7933.4	4979.1	0.24±0.02			0.2
10	3063.3	r	9478.5	1.15±0.11	1.1±0.3	1.2 ±0.1	1.3
11	3123.7	r	9418.1	0.70±0.07	1.1±0.3	0.80 ±0.06	0.9
12	3141.6	9418.1	6276.5	0.09±0.02		0.08 ±0.02	0.05
13	3181.0	7798.8	4617.8	0.16±0.04		0.16 ±0.06	0.1
14	3200.2	4979.1	1778.9	0.24±0.06			0.2
15	3315.6	7933.4	4617.8	0.21±0.04		0.34 ±0.05	0.3
16	(3377.9)	r	9163.9	0.19±0.05			0.4
17	3952.9	r	8588.9	0.19±0.04			0.3
18	4497.6	6276.5	1778.9	4.8 ±0.3	4.4±0.4	6.0 ±0.3	4.9
19	4608.4	r	7933.4	4.5 ±0.4	3.6±0.4	5.0 ±0.3	4.2
20	4743.0	r	7798.8	8.8 ±0.5	8.1±0.8	11.5 ±0.5	9.7
21	4800.3	9418.1	4617.8	0.31±0.04	1.0±0.3	0.29 ±0.07	0.3
22	5099.7	6878.6	1778.9	0.10±0.04	0.6±0.2	0.30 ±0.05	0.2
23	5109.9	6888.8	1778.9	0.50±0.06		0.52 ±0.09	0.5
24	5601.8	7380.7	1778.9	0.24±0.05			0.1
25	5653.0	r	6888.8	0.40±0.04	0.9±0.3	0.36 ±0.09	0.3
26	5663.2	r	6878.6	0.58±0.06		0.89 ±0.21	0.6
27	6019.9	7798.8	1778.9	6.0 ±0.5	5.9±0.6	7.8 ±0.4	6.8
28	6154.5	7933.4	1778.9	0.26±0.05		0.55 ±0.07	0.2
29	6265.3	r	6276.5	2.1 ±0.2	2.4±0.4	3.4 ±0.2	2.4
30	6810.0	8588.9	1778.9	0.24±0.05			0.3
31	6878.6	6878.6	0	0.63±0.06	0.5±0.2	0.59 ±0.04	0.4
32	7639.2	9418.1	1778.9	0.23±0.05		0.32 ±0.06	0.2
33	7924.0	r	4617.8	4.3 ±0.4	4.9±0.9	5.2 ±0.4	4.9
34	7933.4	7933.4	0	3.7 ±0.4	3.8±0.9	3.9 ±0.3	3.4
35	9478.5	9478.5	0	0.98±0.10	1.1±0.4	1.1 ±0.1	1.1
	10275	10275	0		1.1±0.4		
36	10762.9	r	1778.9	76.6 ±1.5	77.0±7.7	72.4 ±3.6	75
	12541.8	r	0			0.022±0.009	<0.02

Response of a high-resolution and high-energy spectrometer

Harada et al., NIM in Phys. Res. A 554, 306 (2005)

Twin Ge crystals

BGO
Compton-suppression

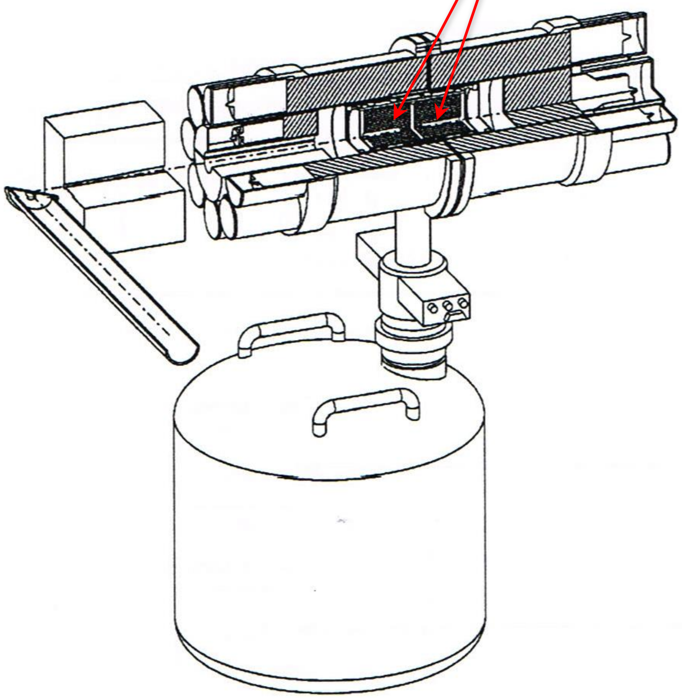

27Al(p,γ)28Si, E_p = 992 keV resonance

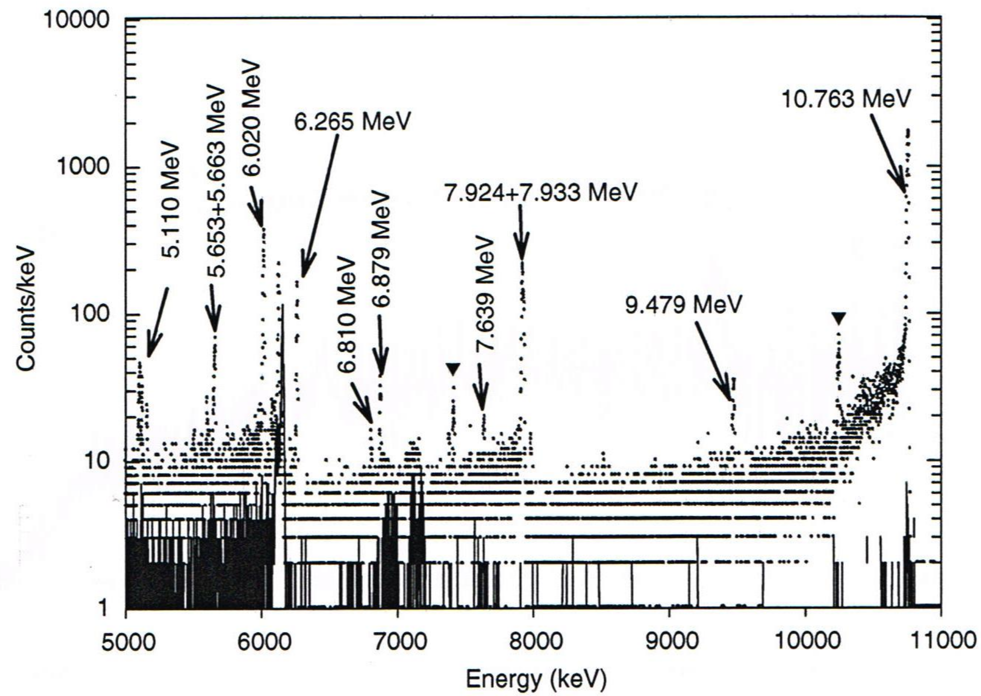

Lecture 1 : Past of Photonuclear Reactions

Ciemada et al., NIM Phys. Res. A 608, 76 (2009)

Table 1
Parameters of the (p, γ) reactions, energies (E_γ) and relative intensities (I_γ) of the γ-rays emitted by product nucleus [9,11,12].

Reaction	E_{res} (keV)	Q value (keV)	E_p (keV)	E_γ (keV)	I_γ	Target and its thickness ($\mu g/cm^2$)
$^{23}Na(p,\gamma)^{24}Mg$	1318.1	11 693	1323	1368.6(1)	1.000(2)	Na_2WO_4
				11 584.9(6)	0.960(2)	20
$^{23}Na(p,\gamma)^{24}Mg$	1416.9	11 693	1422	2754.0(1)	1.000(1)	Na_2WO_4
				8925.2(6)	0.985(1)	20
$^{27}Al(p,\gamma)^{28}Si$	767.2	11 585	770	2838.7(1)	1.0000(14)	Al
				7706.5(2)	0.9810(14)	15
$^{39}K(p,\gamma)^{40}Ca$	1346.6	8328	1351	3904.4(1)	1.000(1)	K_2SO_4
				5736.5(1)	0.965(1)	20
$^{11}B(p,\gamma)^{12}C$	675	15 957	676	4438.0(3)	1.0000(7)	$LiBO_2$
				12 137.1(3)	1.0000(7)	75
$^{7}Li(p,\gamma)^{8}Be$	441	17 255	450	17 619.0(6)	–	$LiBO_2$, 75

Nuclear data are taken from ENSDF [13]. Q values calculated by QCalc from NNDC [14].

Response of a 2” x 2” LaBr3(Ce) detector

23Na(p, γ)24Mg, E_p = 1416.9 keV

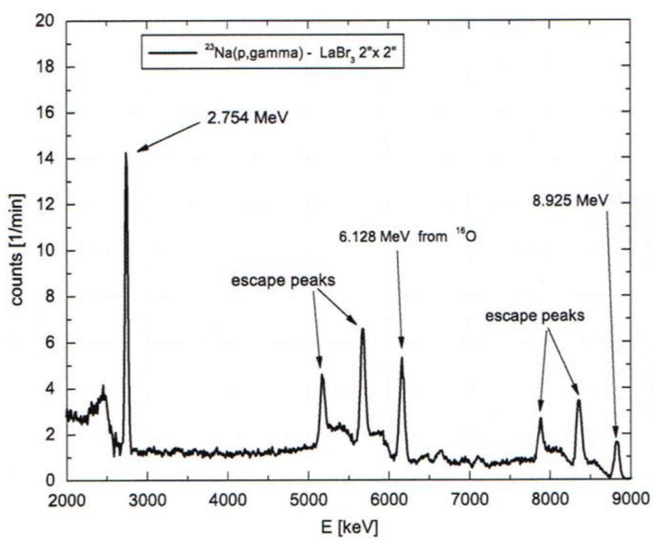

Fig. 1. Gamma-ray spectrum emitted by ^{24}Mg nuclei created in the $^{23}Na(p,\gamma)^{24}Mg$ reaction at the 1.318 MeV resonance energy, measured by a $LaBr_3$: Ce 2 in. × 2 in. scintillation detector.

7Li(p, γ)8Be, E_p = 441 keV

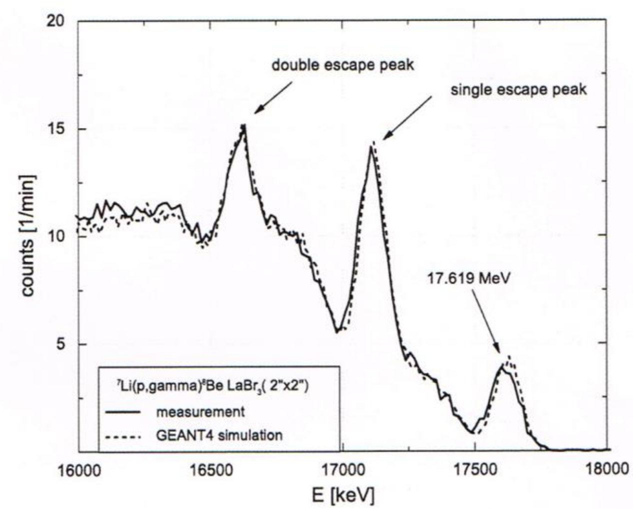

Fig. 2. Gamma-ray spectrum emitted by ^{8}Be nuclei created in the $^{7}Li(p,\gamma)^{8}Be$ reaction, measured by a $LaBr_3$: Ce 2 in. × 2 in. scintillation detector. It is compared, after normalization to the full absorption peak, to spectrum simulated using a GEANT4 code.

γ-ray sources: Bremsstrahlung

Collisional loss: Electrons lose kinetic energies in matter by colliding with atomic electrons, leading to atomic excitation and ionization.

Bremsstrahlung (Radiation loss): Electrons lose kinetic energies in matter by radiative processes.

linear stopping power of electrons for radiation loss

$$-\left(\frac{dE}{dx}\right)_r = \frac{NEZ(Z+1)e^4}{137 m_0^2 c^4}\left(4\ln\frac{2E}{m_0 c^2} - \frac{4}{3}\right)$$

Radiative losses are most important for high electron energies and for absorber materials of large atomic number.

Ratio of the specific energy losses

$$\frac{(dE/dx)_r}{(dE/dx)_c} \cong \frac{EZ}{700}$$

E in MeV

Bremsstrahlung facilities

1. Moscow State University, Nuclear Physics Institute, Moscow, Russia (microtron)
2. Joint Institute for Nuclear Research, Dubna, Russia (microtron)
3. Uzhgorod State University, Ukraine (betatron)
4. Kharkovskii Fiziko-Tekhnicheskii Institute, Kharkov, Ukraine (linear accelerator)
5. Forschungszentrum-Rossendorf (FZD), Dresden, ELBE, Germany (linear accelerator)
6. Tech. Universitaet, Darmstadt, S-DALINAC, Germany (linear accelerator)
7. Kyoto University, Kyoto, Japan (linear accelerator)
8. Pohang University of Science and Technology, Pohang, Korea (linear accelerator)
9. Bhabha Atomic Res. Centre, Trombay, India (linear accelerator)
10. Mangalore University, Mangalagangotri, Konaje, India (microtron)
11. Australian Radiat. Protect. & Nucl. Safe. Agency, Melbourne, Australia (linear accelerator)

The bremsstrahlung facility at the electron accelerator ELBE

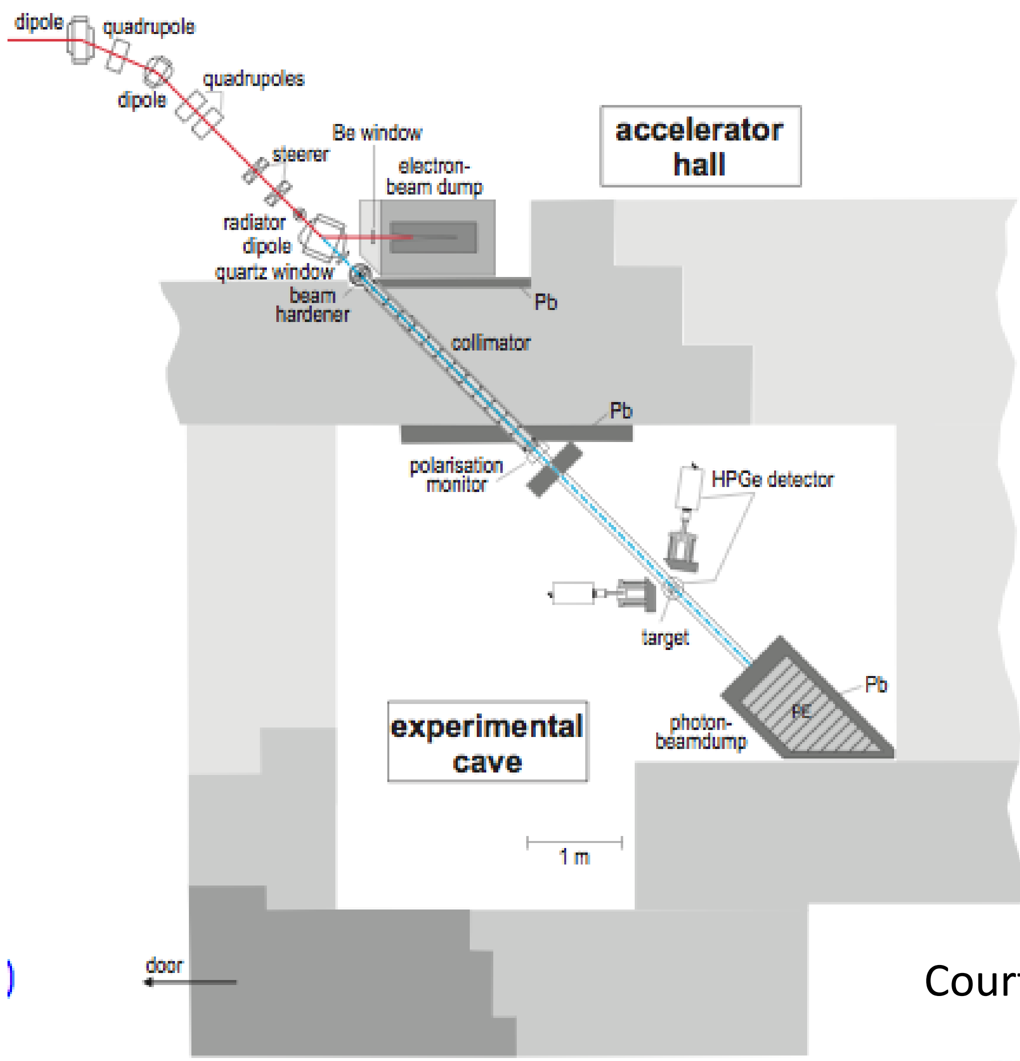

Courtesy by R. Schwenger

Yield : convolution of the photonuclear cross section with the bremsstrahlung spectrum over the photon energies.

$$Y(E_0) = N_R \int_{Threshold}^{E_0} \sigma(E_\gamma) K(E_0, E_\gamma) \frac{dE_\gamma}{E_\gamma},$$

E_0: electron beam energy; $K(E_0, E_\gamma)$: bremsstrahlung spectrum

Yield curve: obtained by changing the electron beam energy in small steps

This technique requires:
(1) Accurate knowledge of the bremsstrahlung spectrum for all electron energies
(2) Great stability in the accelerator operation and large counting statistics to accurately measure the yield curve
(3) Unfolding (differentiation) procedure of the yield curve
  (a) Photon Difference Method: difference of two bremsstrahlung spectra with slightly-different end-point energies
  (b) Penfold-Leiss Method: a set of liner equations for a given energy bin
  (c) Regularization Methods
    Tikhonov's Method, Cook's Least Structure Method, the Second Difference Method, the Statistical Regularization Method

Bremsstrahlung data

compiled in CDFE, MSU

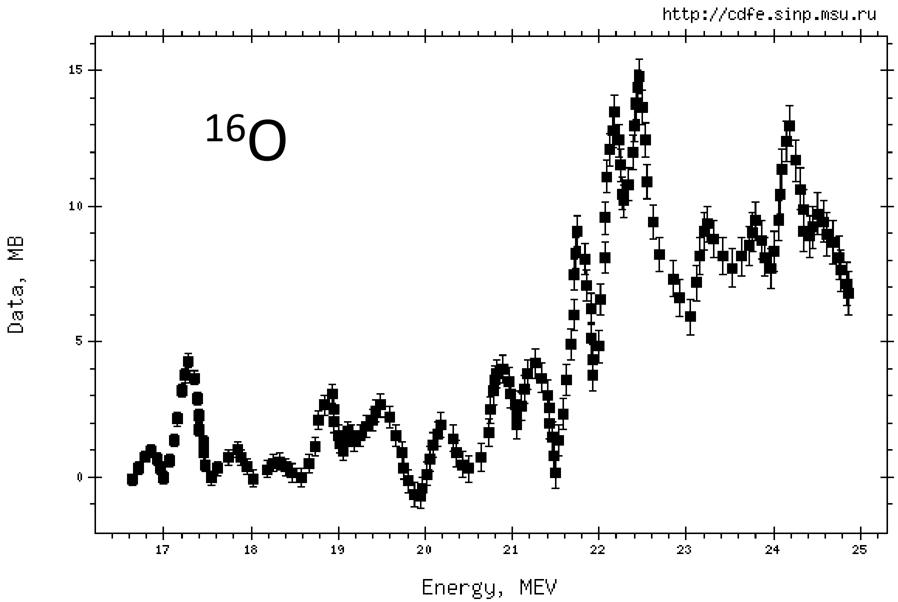

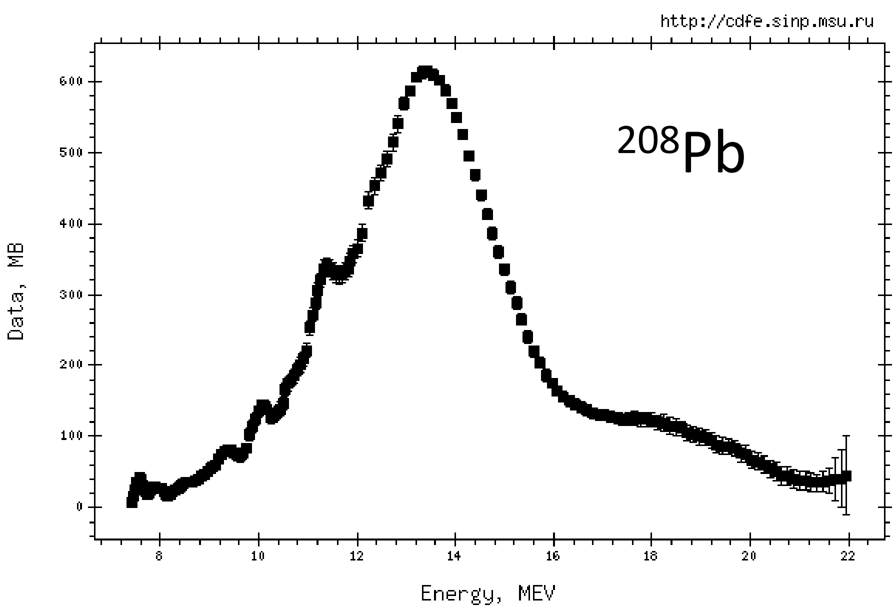

γ-ray sources: Positron annihilation in flight

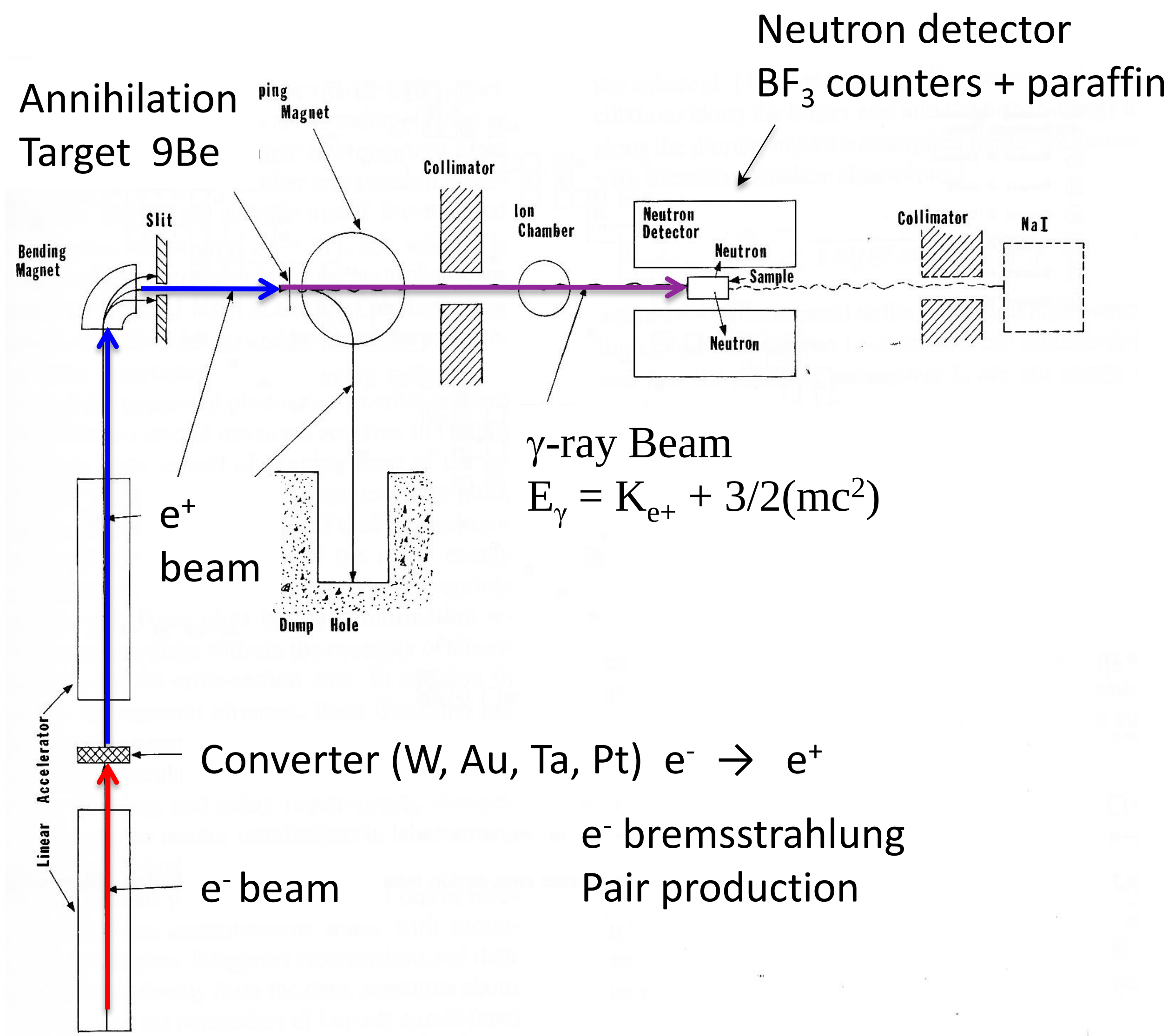

Lawrence Livermore National Laboratory (USA)

Saclay (France)

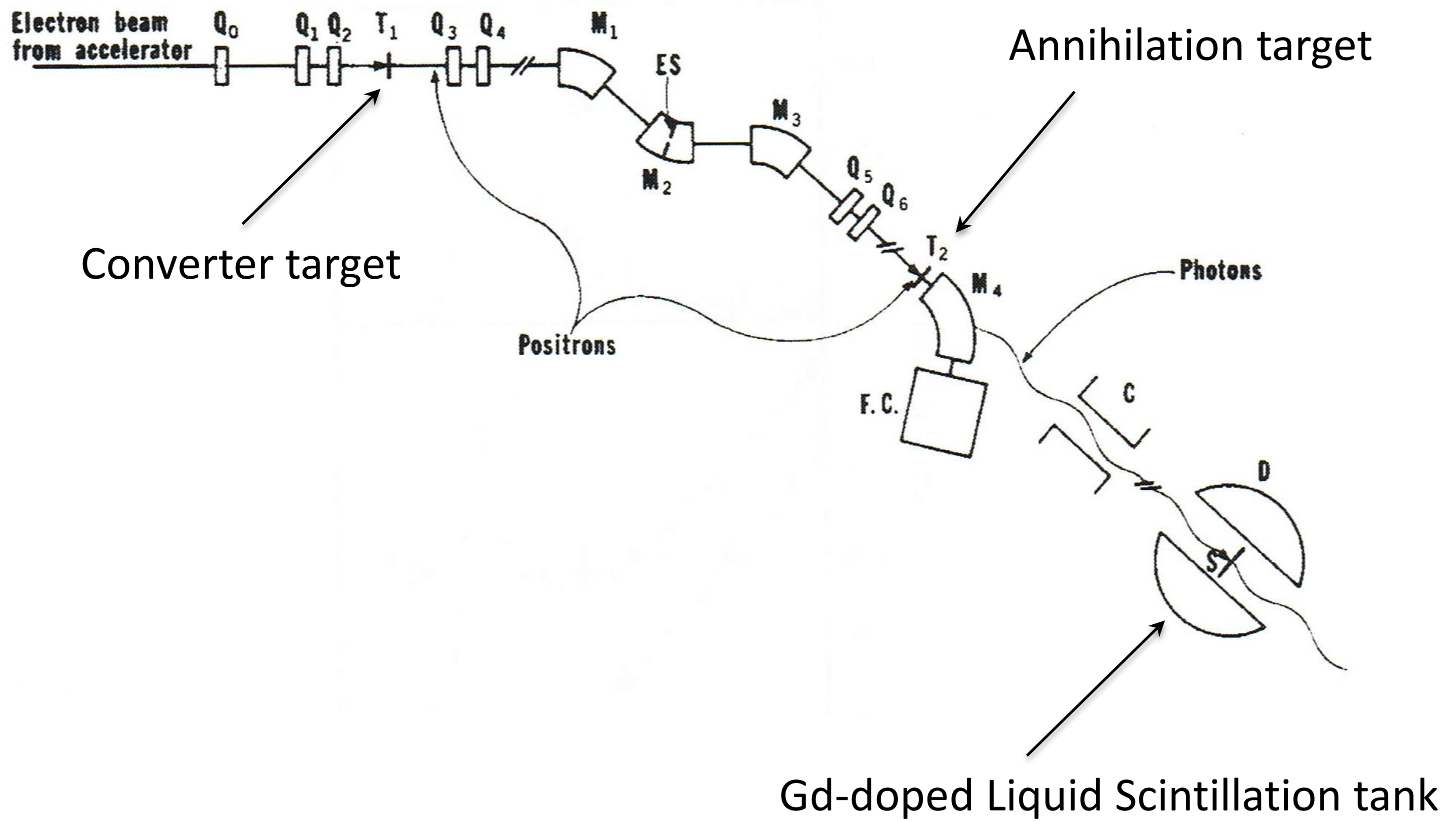

Subtracted

e^+-e^- annihilation
(quasi-monochromatic)

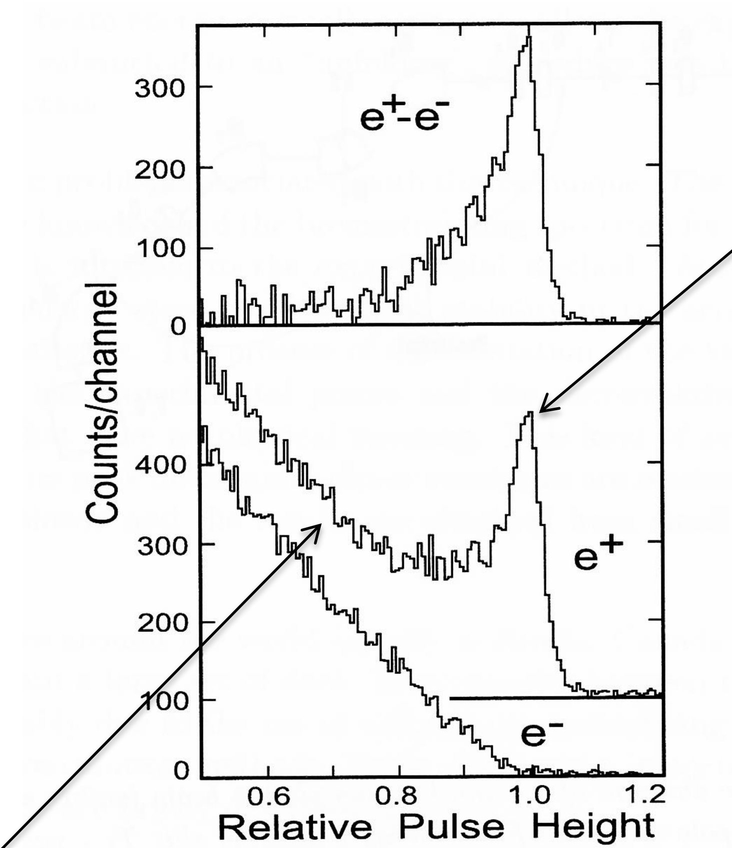

e^+ bremsstrahlung
(background)

(γ,n) cross section measurements in 1960s – 1980s

LLNL (USA)

Saclay (France)

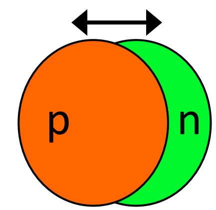

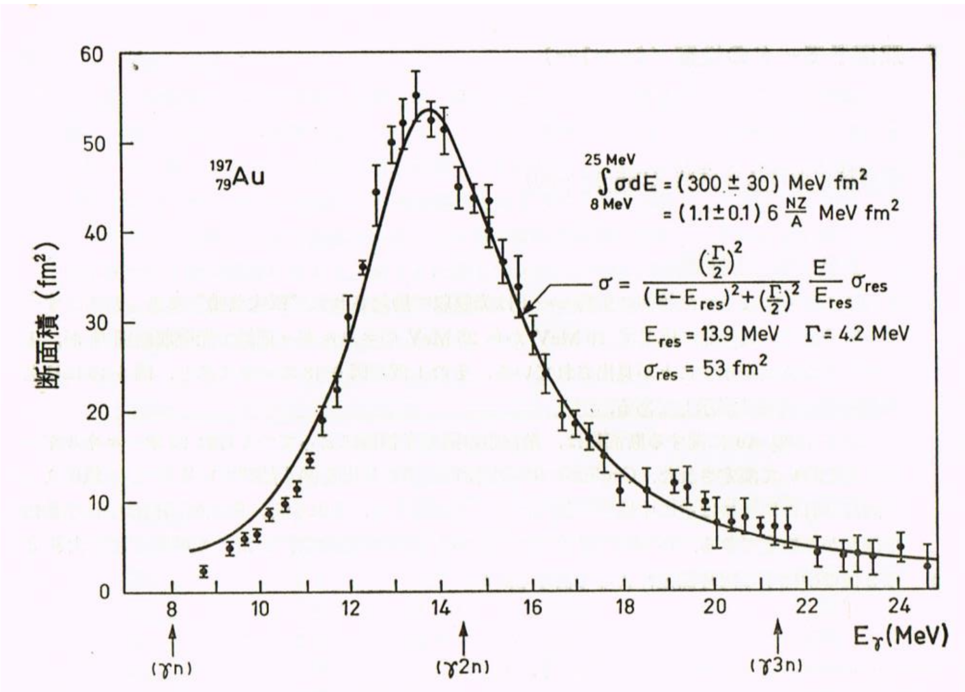

E_R=79A$^{-1/3}$ MeV

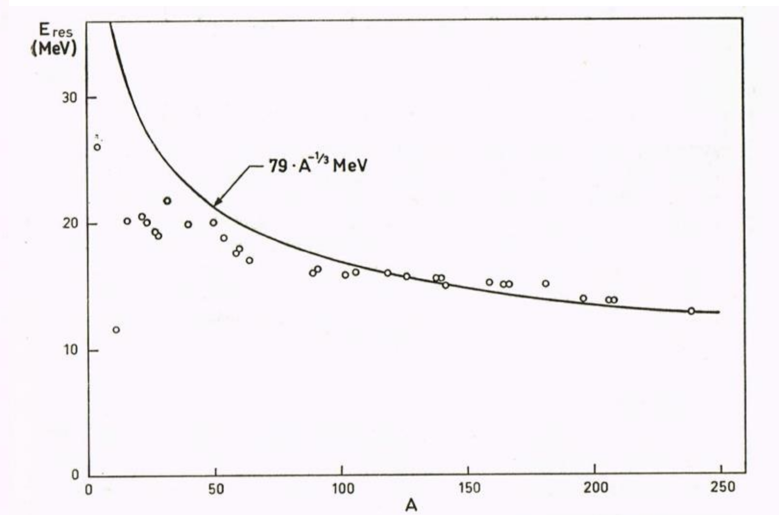

Thomas-Reiche-Kuhn sum rule (energy-weighted sum rule)

$$\int \sigma(E)dE = 60\frac{NZ}{A}[MeV \cdot mb] = \frac{16\pi^3}{9}\overline{E}\cdot B(E1)\uparrow \cdot \alpha$$

Compilations photoneutron cross sections

(1) ATLAS of photoneutron cross sections obtained with monoenergetic photons, S.S. Dietrich and B.L. Berman
Atomic Data and Nuclear Data Tables 38, 199-338 (1988)

(2) Handbook on photonuclear data for applications, Cross sections and spectra
IAEA TECDOC-1178 (2000)

International Nuclear Reaction Database in the format EXFOR

IAEA - https://www-nds.iaea.org/exfor/exfor.htm/
CDFE - http://cdfe.sinp.msu.ru/exfor/index.php/
USA NNDC - http://www.nndc.bnl.gov/exfor/exfor.htm/

Lecture 2

Present of Photonuclear Reactions

2.1 Laser Compton-scattering γ-ray beam

2.2 Nuclear Physics (γ, γ') for PDR

2.3 Nuclear Astrophysics

a. p-process – (γ,n)

b. s-process - gamma-ray strength function for (γ,n) and (n, γ)

γ-ray sources: Inverse Compton scattering

Compton scattering vs Inverse Compton scattering

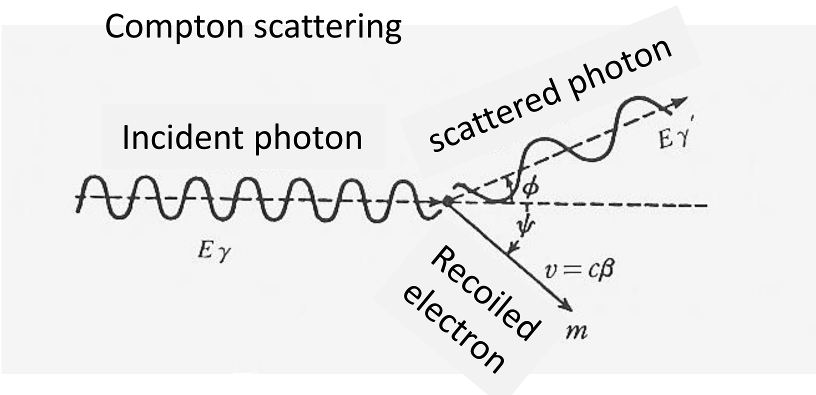

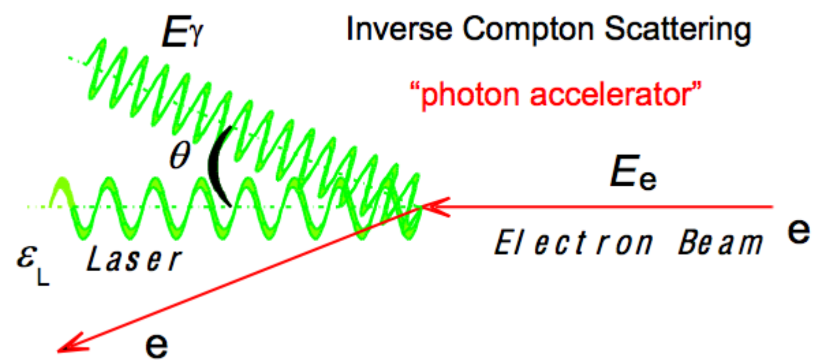

$$h\nu' = \frac{h\nu}{1 + h\nu(1-\cos\phi)/mc^2}$$

$$E_\gamma = \frac{4\gamma^2\varepsilon_L}{1 + (\gamma\theta)^2 + 4\gamma\varepsilon_L/(mc^2)}$$

$$h\nu + mc^2 = h\nu' + \sqrt{p^2c^2 + m^2c^4}$$

$$\frac{h\nu}{c} = \frac{h\nu'}{c}\cos\phi + p\cos\psi$$

$$0 = \frac{h\nu'}{c}\sin\phi - p\sin\psi$$

$\gamma = E_e/mc^2$ Lorentz factor

Laser Compton scattering γ-ray beam

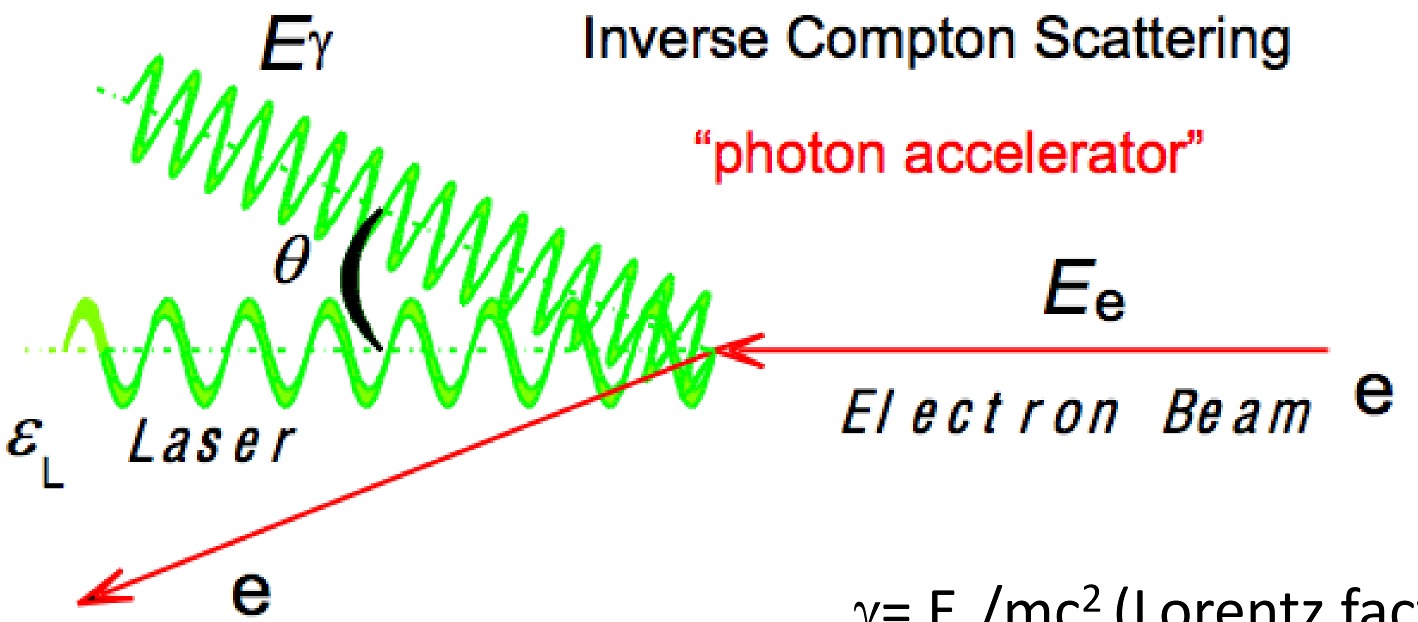

$$E_\gamma = \frac{4\gamma^2\varepsilon_L}{1 + (\gamma\theta)^2 + 4\gamma\varepsilon_L/(mc^2)}$$

$$\Delta E/E \cong \left\{\left(\frac{2\Delta E_e}{E_e}\right)^2 + \gamma^4(\theta_e^2 + \theta_c^2)^2\right\}^{1/2}$$

$\gamma = E_e/mc^2$ (Lorentz factor)

$\sim\ 2 \times 10^3$ E_e=1 GeV

Energy am

$E_\gamma/\varepsilon_L = 4\gamma^2 \sim 1.6 \times 10^7$

$\varepsilon_L \sim$ 1eV

$E_\gamma \sim$ 16 MeV

Realm of Nuclear Photonics

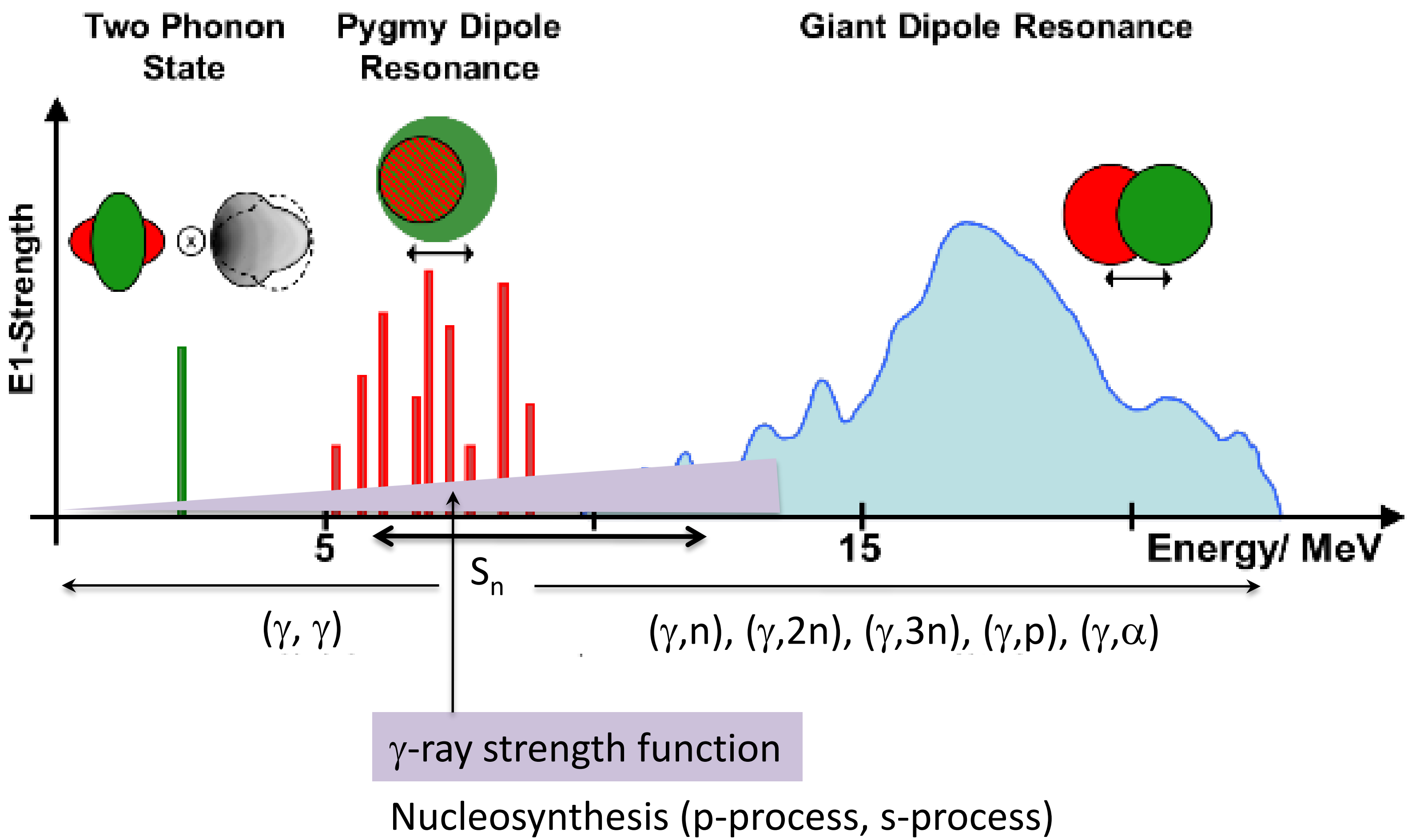

modified by H. Utsunomiya

Norbert Pietralla, TU Darmstadt ELI Workshop

"Applications" of low-lying E1 strength

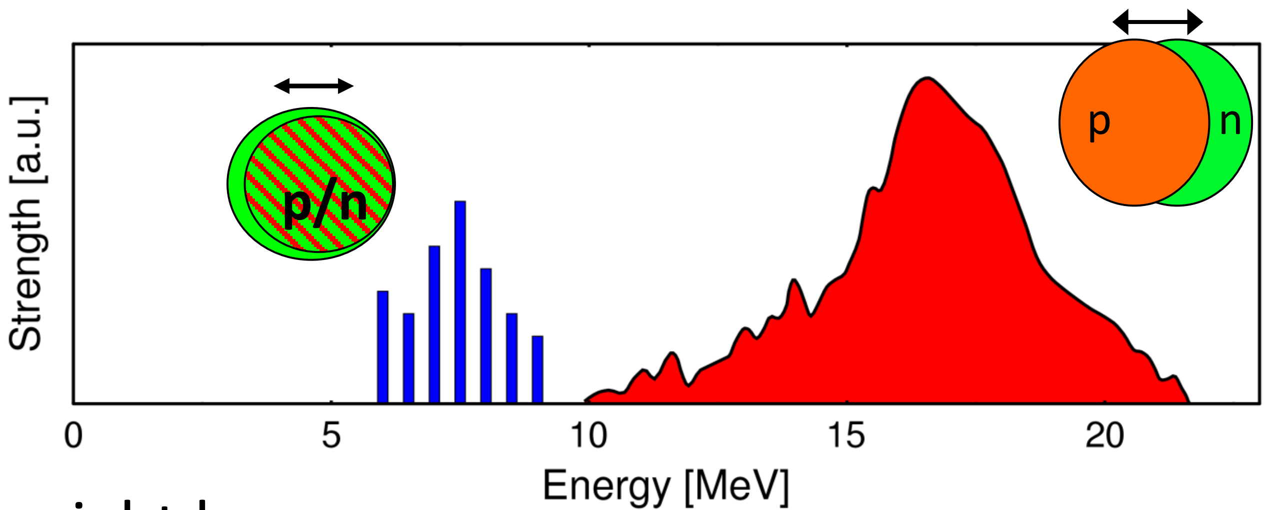

PDR is / might be

… sensitive to neutron skin thickness

… sensitive to parameters of symmetry energy

… influencing reaction rates / nucleosynthesis

➔ detailed understanding of the PDR mandatory

Courtesy by D. Savran

Photon scattering ...

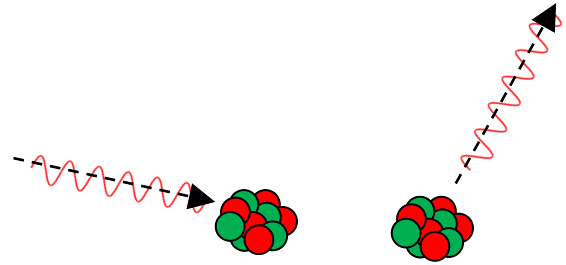

... using Bremsstrahlung

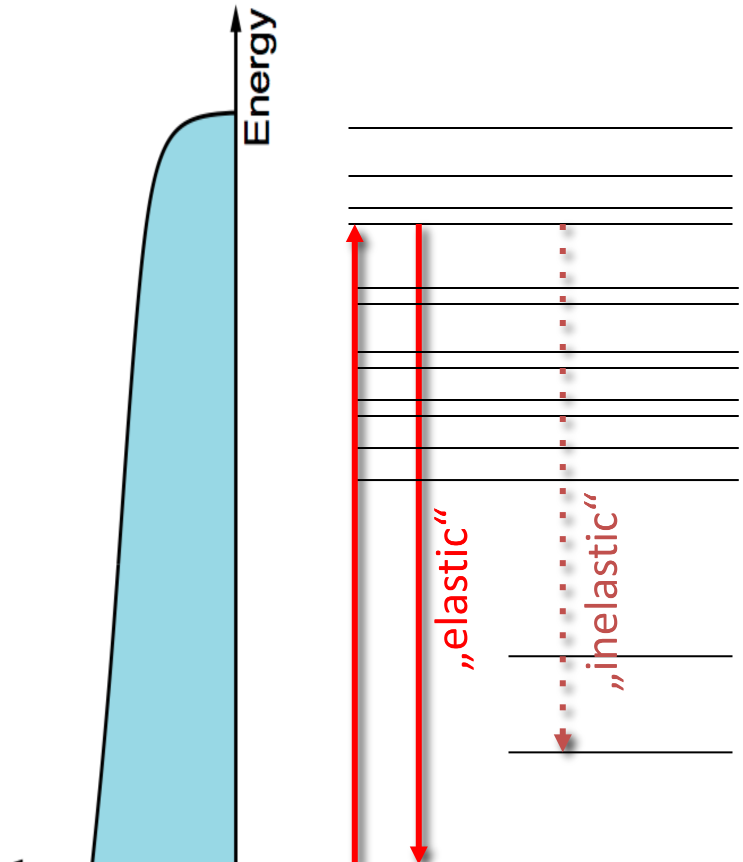

e.g. Darmstadt High Intensity Photon Setup (DHIPS):

K. Sonnabend et al., Nucl. Instr. and Meth. **A640** (2011) 6

$N_\gamma(E_\gamma) \cdot \varepsilon(E_\gamma)$

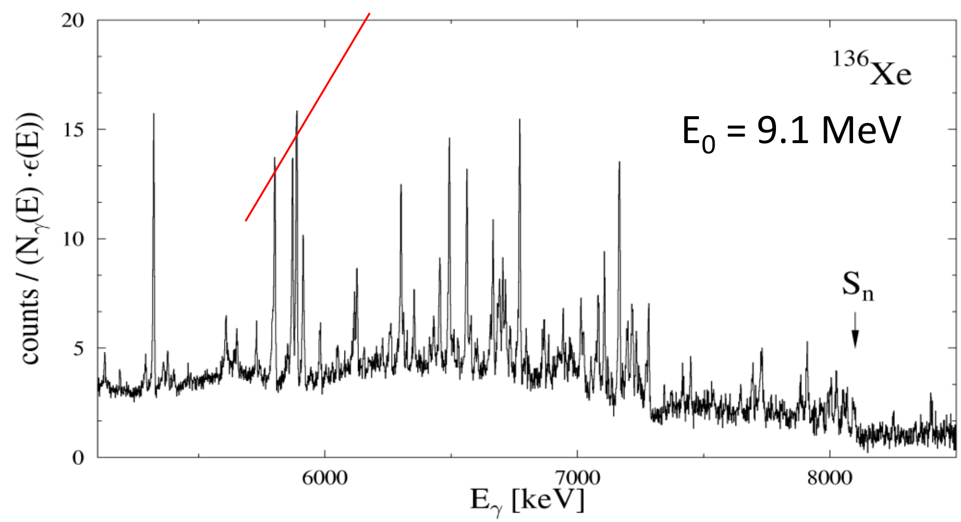

- Investigation of large energy region
- Excellent energy resolution: State-to-state analysis, investigation of fine structure

Photon scattering …

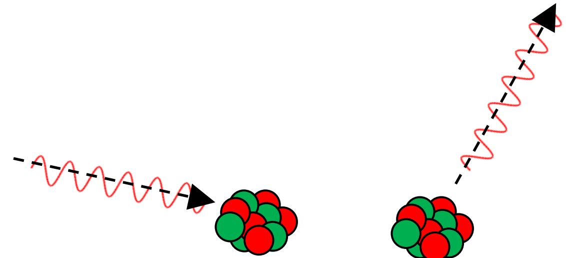

… using Laser Compton Backscattering

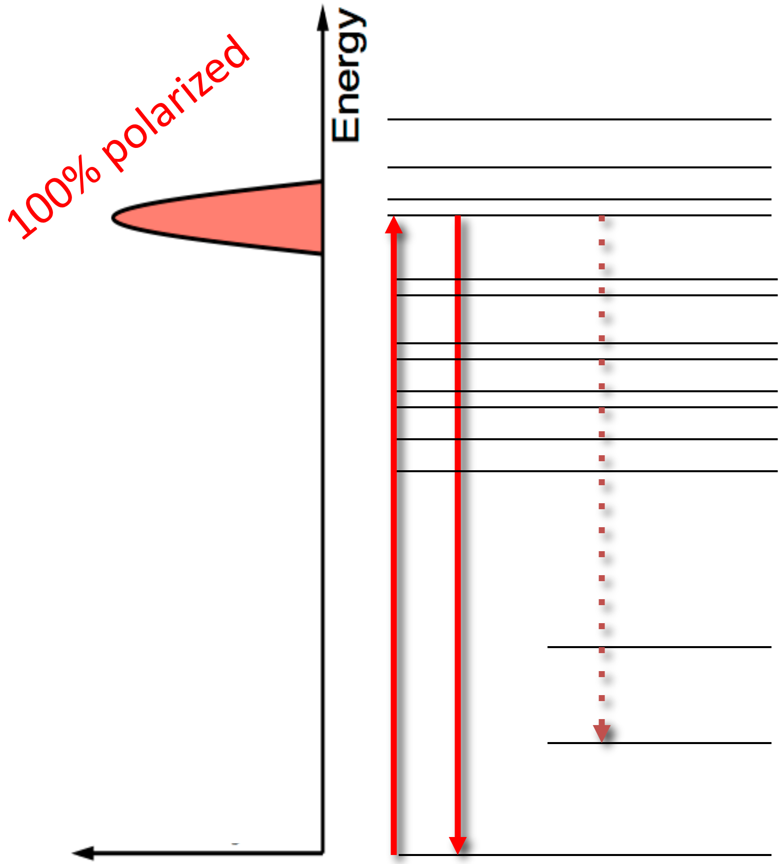

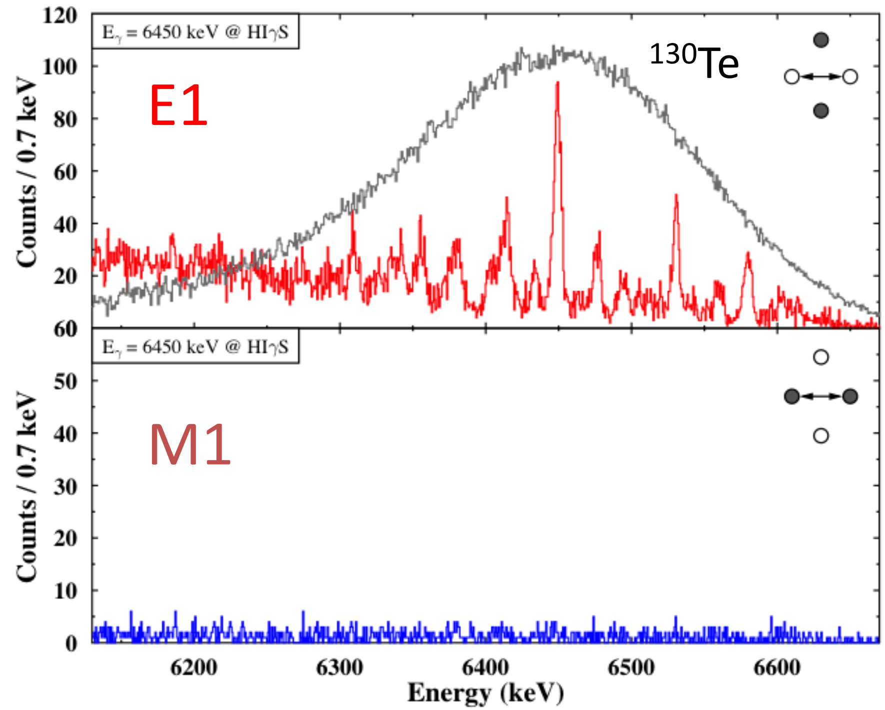

- Determination of parities

e.g. High Intensity γ-ray Source (HIγS):

H.R. Weller *et al.*, Prog. Part. Nucl. Phys. **62** (2009) 257

Cortesy by D. Savran

Lecture 2 : Present of Photonuclear Reactions

Spin and Parity Determination

^{138}Ba

Courtesy by A. Tonchev

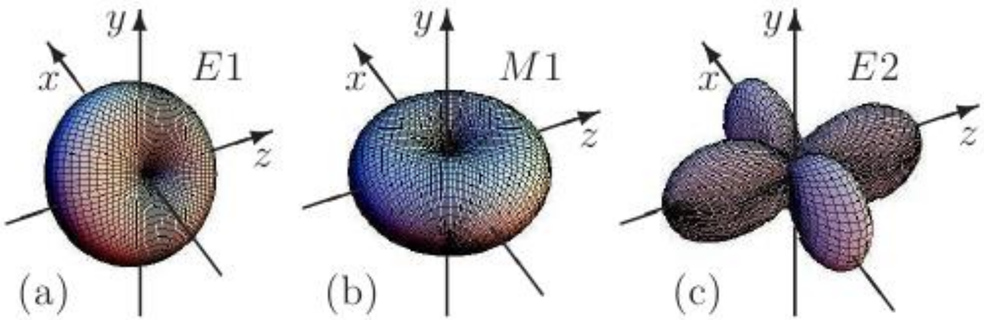

z axis: beam direction; x axis: vector of polarization

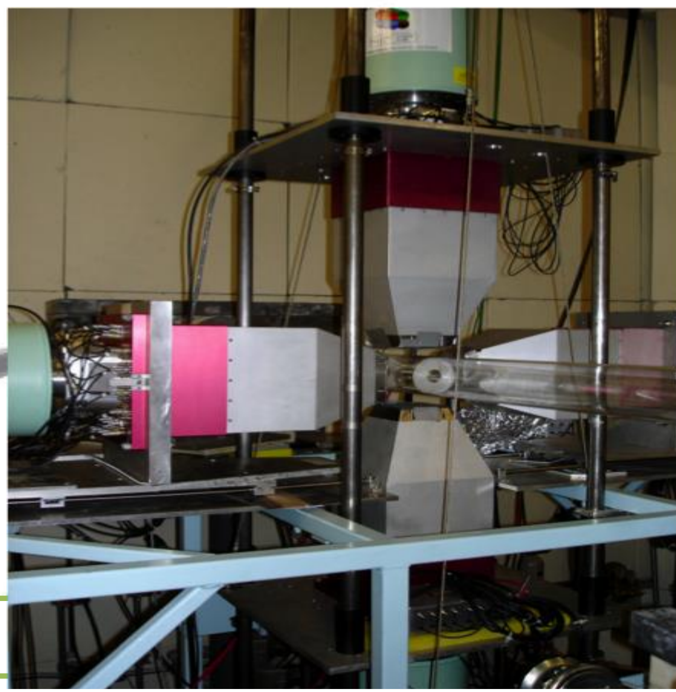

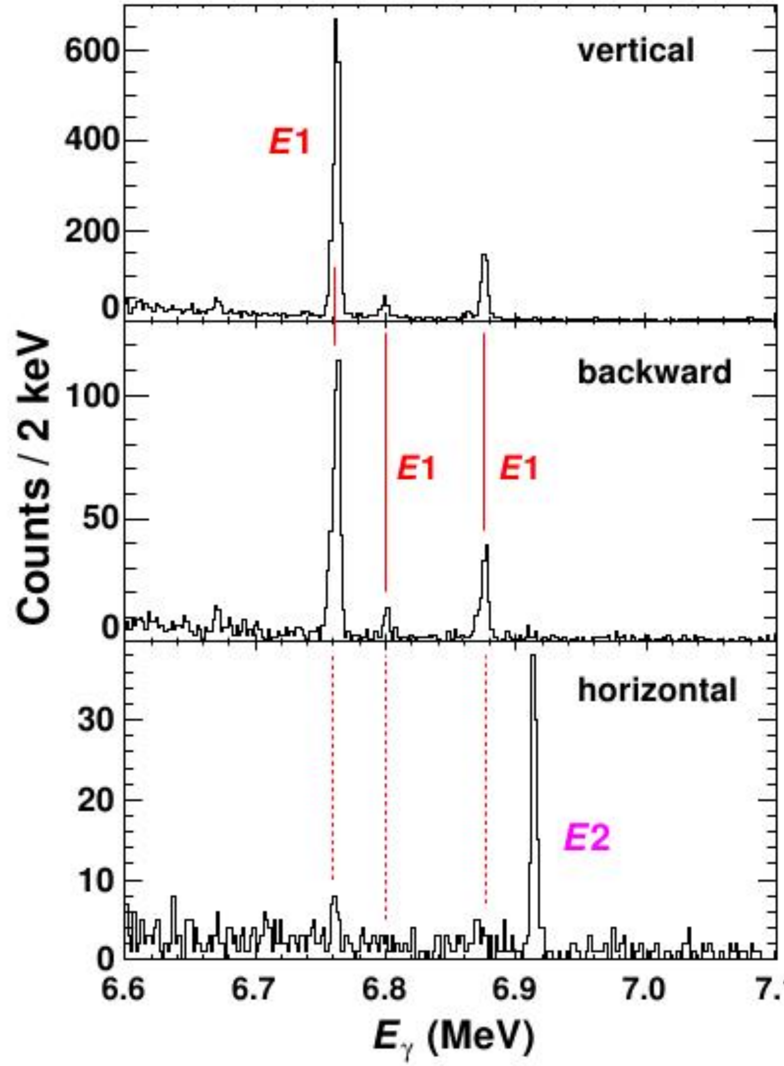

N. Pietralla, at al. PRL **88** (2002) 012502; A. Tonchev, NIM **B 241** (2005) 51474

Courtesy by A. Tonchev

Spin and Parity Determination

^{138}Ba

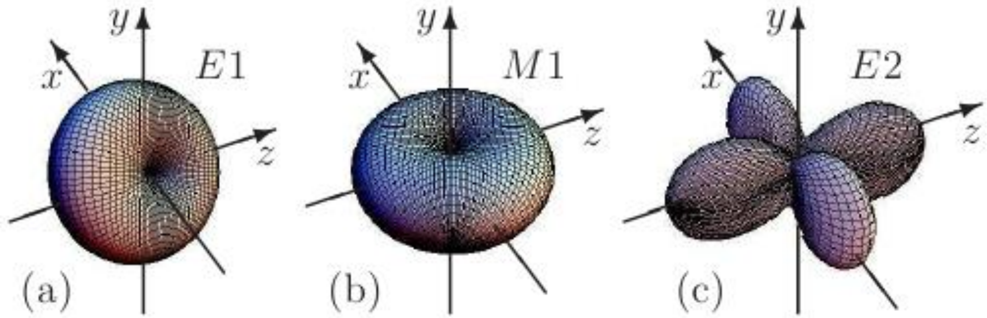

z axis: beam direction; x axis: vector of polarization

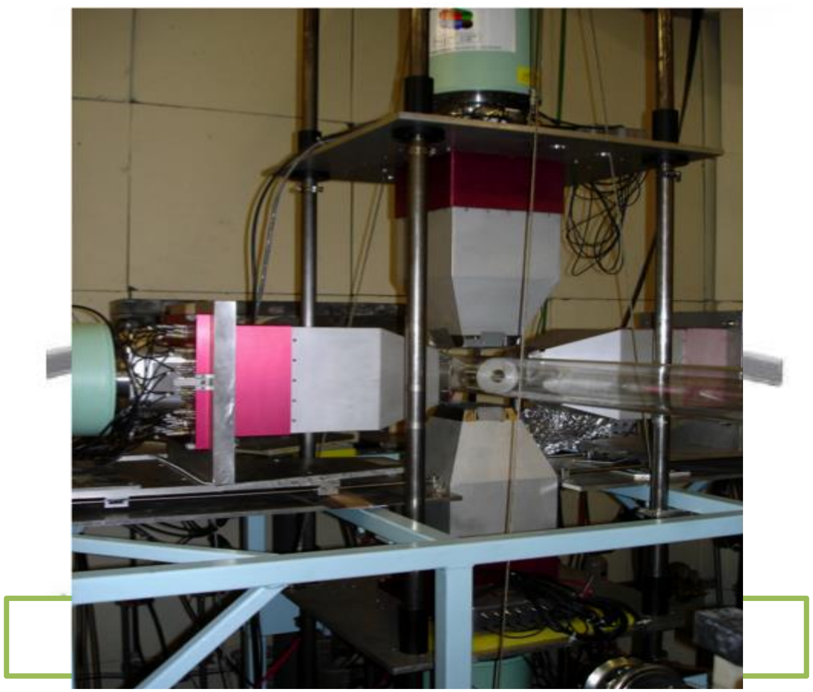

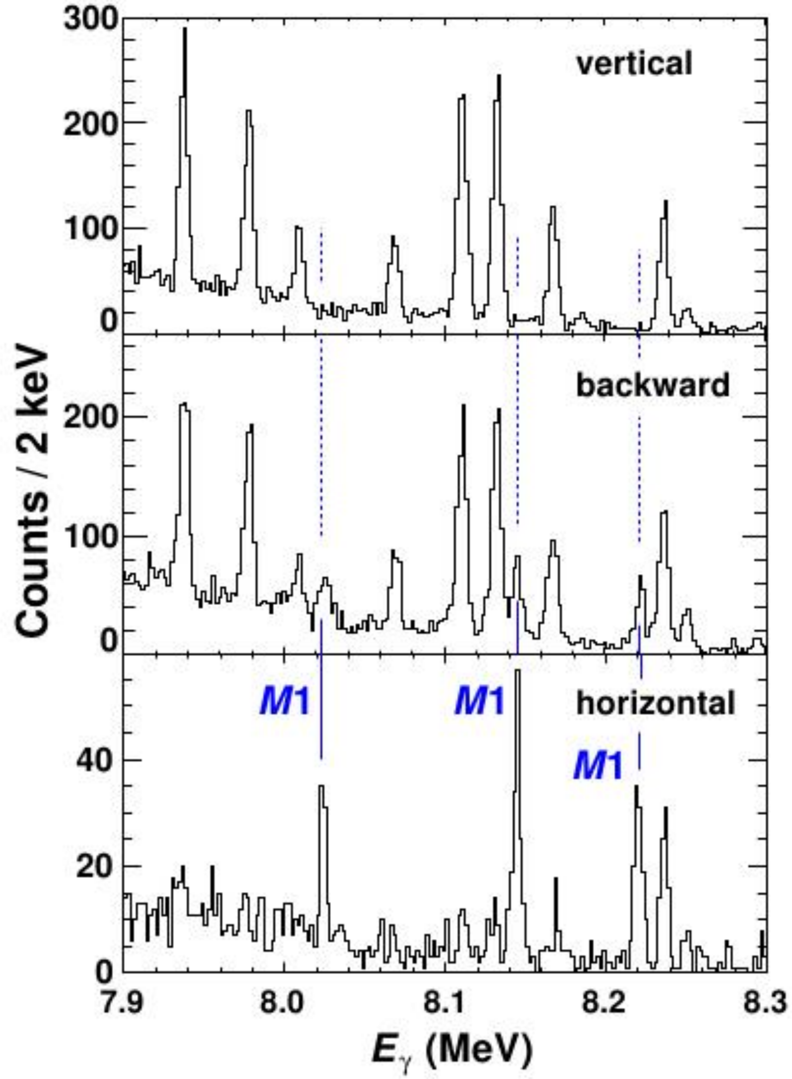

N. Pietralla, at al. PRL **88** (2002) 012502; A. Tonchev, NIM **B 241** (2005) 51474

PDR study by NRF (nuclear resonance fluorescence = photon scattering = (γ, γ')) measurements

1) Ideal to separate PDR (E1) and M1 resonance using linearly-polarized photons

2) Limited below neutron threshold (S_n)

3) Best suited to even-even nuclei
   - 0^+ ground state
   - high neutron threshold (S_n)

4) Determine partial strength
   - discrete (resolved) states
   - unresolved states: model -dependent

PDR in ^{207,208}Pb above neutron threshold

T. Kondo *et al.*, Phy. Rev. C 86, 014316 (2012)

9587 mg, 98.5%, 208Pb
3482 mg, 99.1%, 207Pb

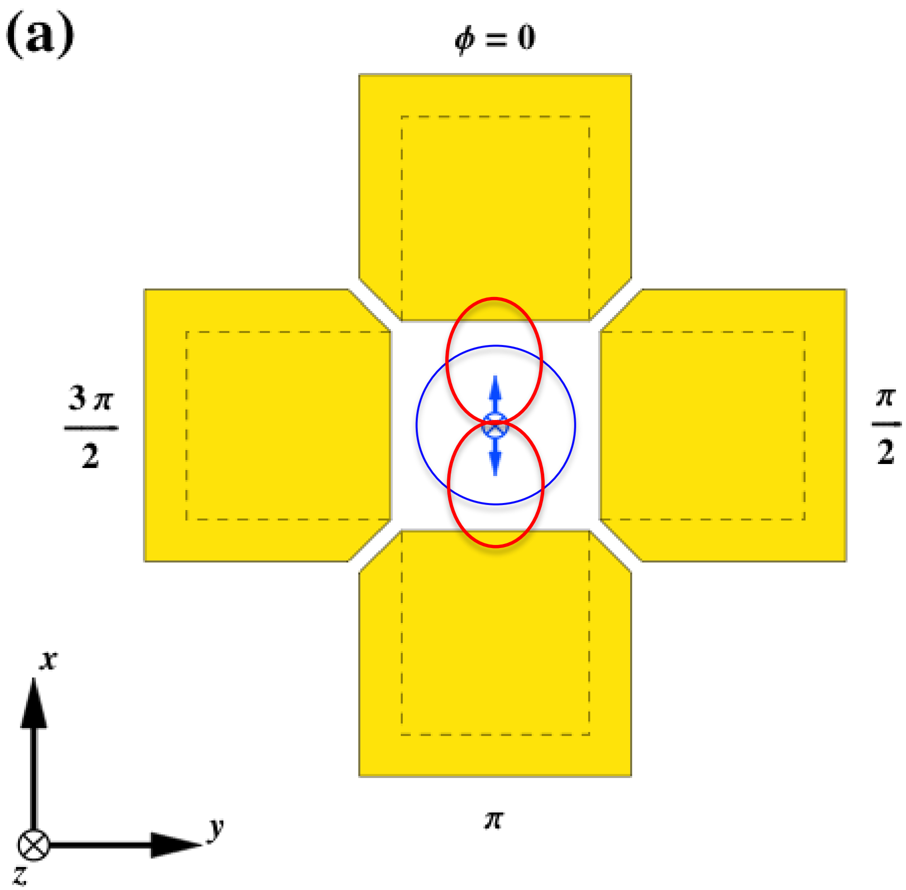

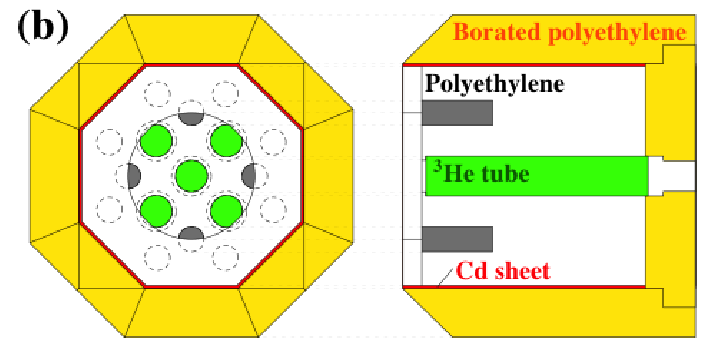

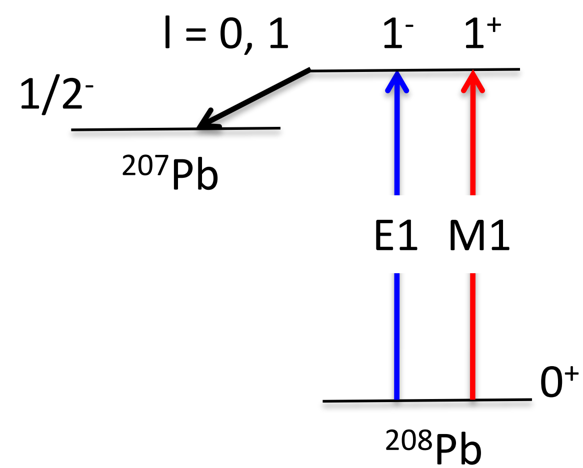

Neutron anisotropy detector for E1 & M1 (γ,n) cross section measurements

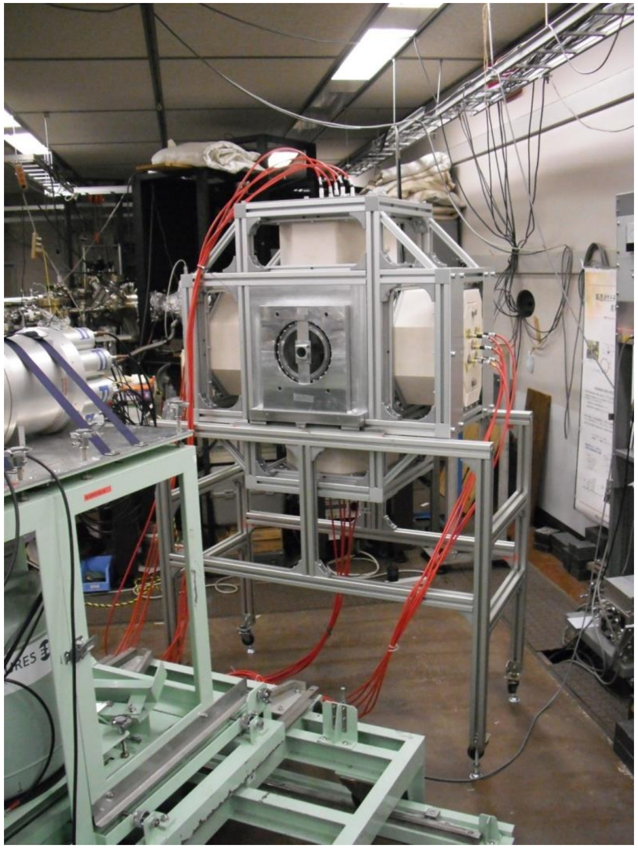

E1 cross sections for ^{208,207}Pb

HFB+QRPA E1 strength plus
pygmy E1 resonance
in Lorentzian shape

E_o = 7.5 MeV, Γ = 0.4 MeV
$\sigma_o \approx$ 20 mb for 208Pb
$\sigma_o \approx$ 15 mb for 207Pb

TRK sum rule
0.42% for 208Pb
0.32% for 207Pb

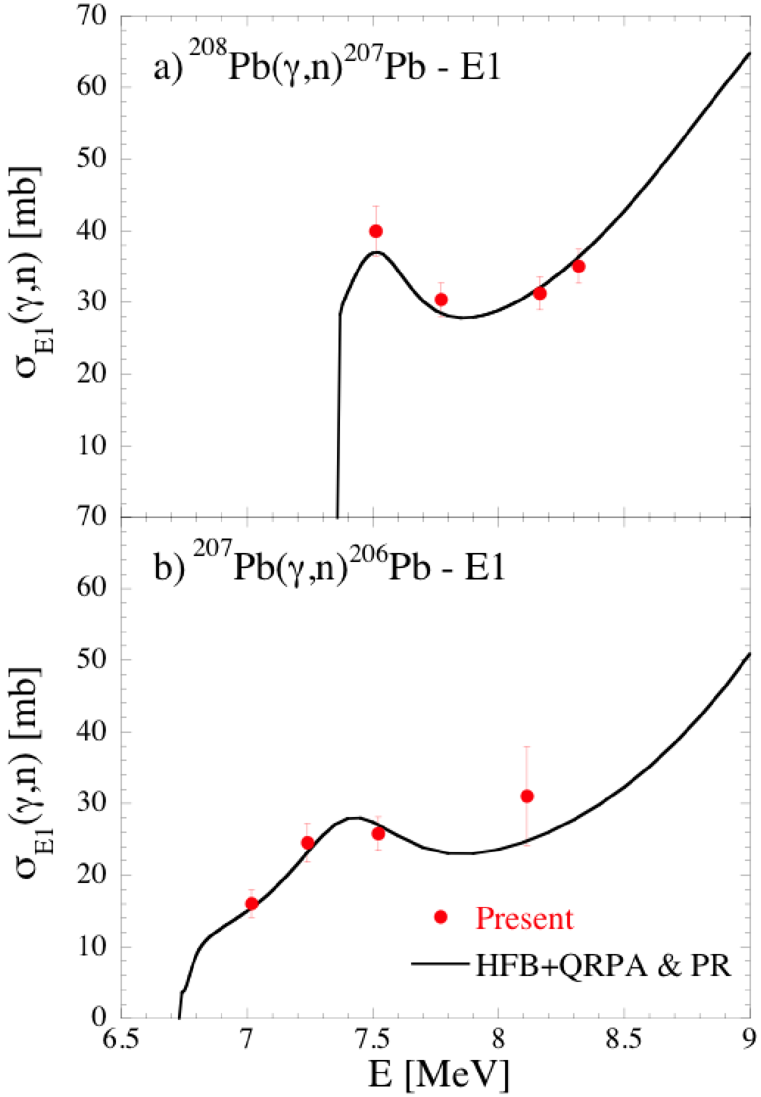

$B(E1)\uparrow$

208Pb

Present

$$B(E1)\uparrow = 0.82 \pm 0.09\ e^2 \cdot fm^2$$

$$E = 7.51 - 8.32\ MeV$$

(p,p') experiment

$$B(E1)\uparrow = 0.982 \pm 0.206\ e^2 \cdot fm^2$$

$$E = 7.515 - 8.430\ MeV$$

207Pb

$$B(E1)\uparrow = 0.88 \pm 0.17\ e^2 \cdot fm^2$$

$$E = 7.02 - 8.32\ MeV$$

M1 cross sections for ^{208,207}Pb

M1 resonance
in Lorentzian shape

208Pb
E_o = 8.06 MeV, Γ = 0.6 MeV
σ_o = 3.6 mb
B(M1)=4.2 ± 2.3 μ_N^2 E=7.51-8.32 MeV

207Pb
$E_o \approx$ 7.25 MeV, $\Gamma \approx$ 1 MeV
$\sigma_o \approx$ 3.2 mb
B(M1)=4.0 ± 1.9 μ_N^2 E=7.02-7.52 MeV

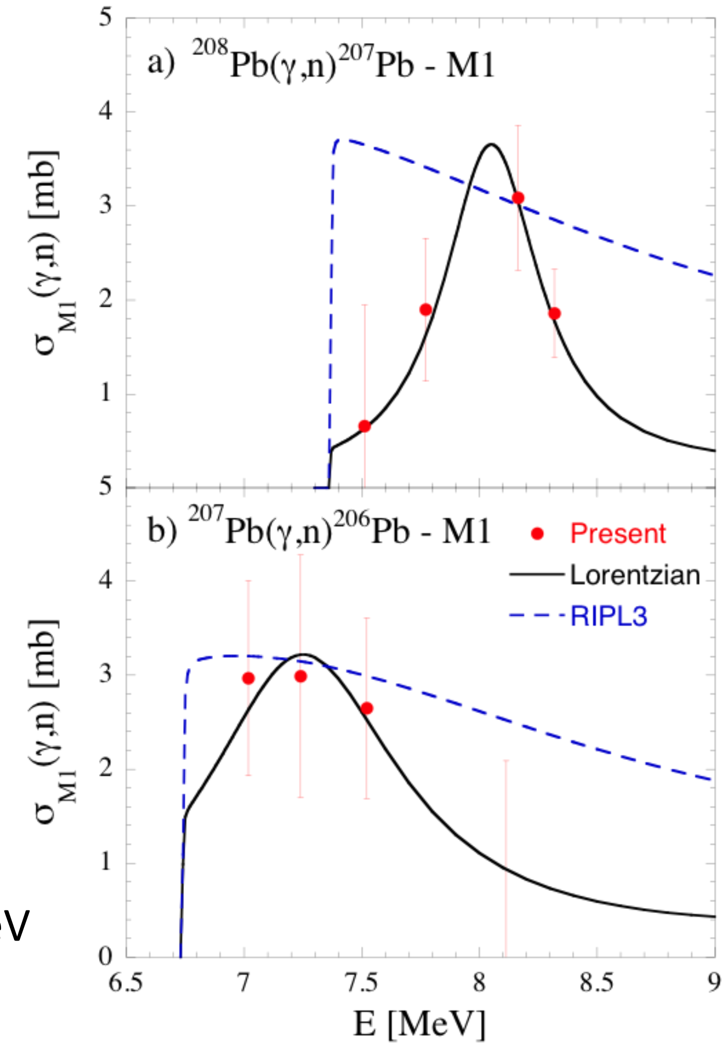

PDR study by (γ,n) measurements

1) Limited above neutron threshold (S_n)

2) Best suited to odd-A nuclei
   - low S_n

3) Determine partial strength
   - above S_n (complementary to (γ,γ'))
   - both discrete and continuum components

4) energy resolution
   - low with 4π neutron detector
   - high with TOF technique (future)

Nucleosynthesis of Heavy Elements
s-process, r-process and p-process

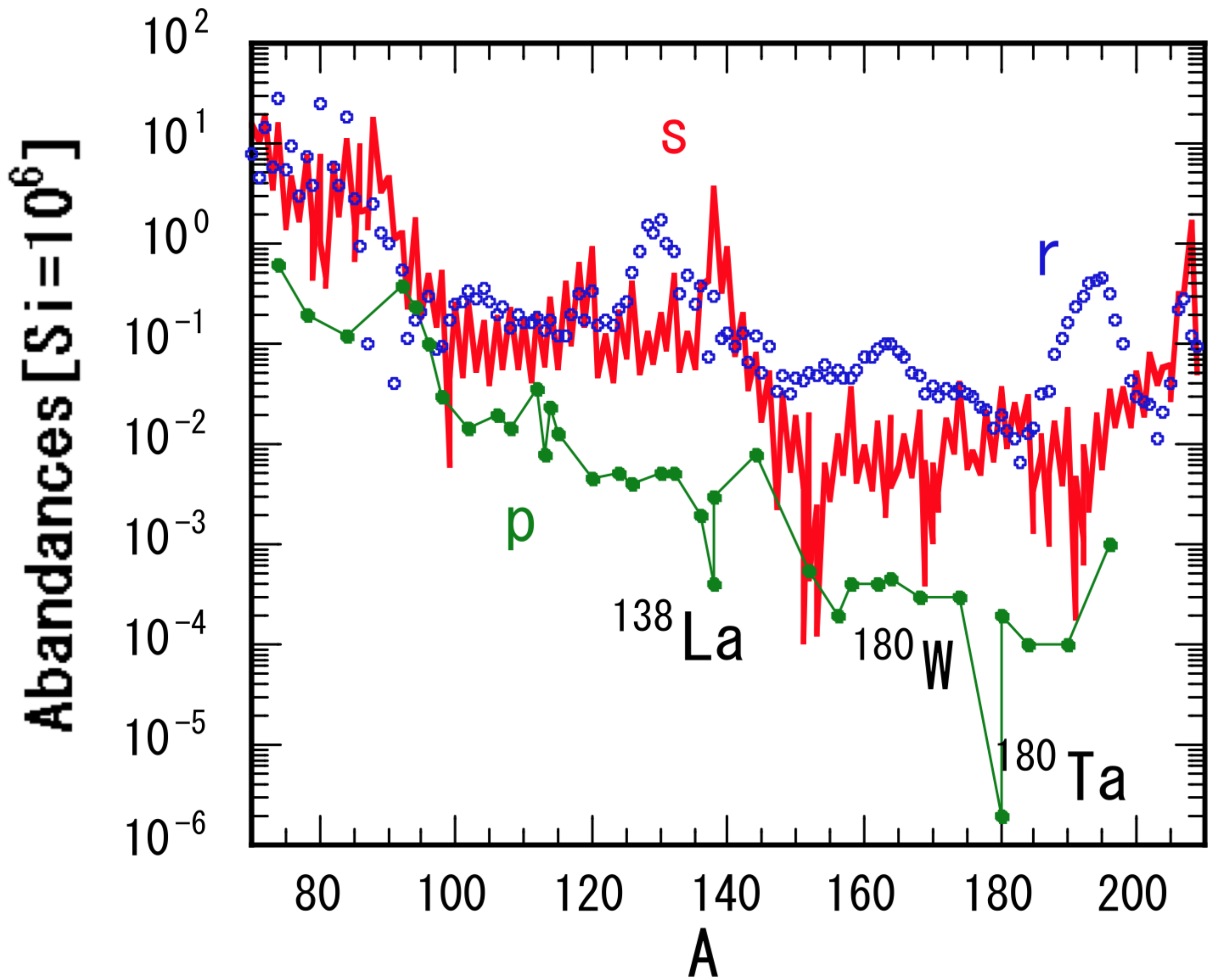

p-nuclei

35 neutron-deficient nuclei
from Se(Z=34) to Hg(Z=80)

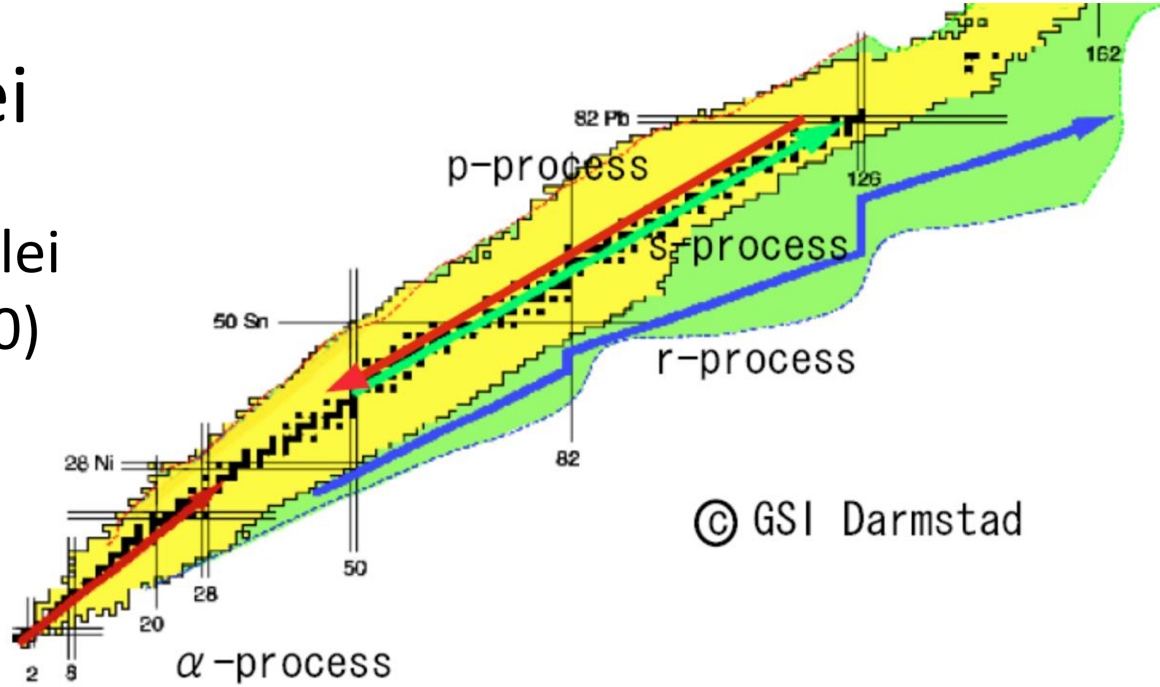

③ $(p,\gamma)+\beta-decay$

④ $(\gamma,n)+(\gamma,p)$

$(\gamma,n)+(\gamma,\alpha)+\beta-decay$

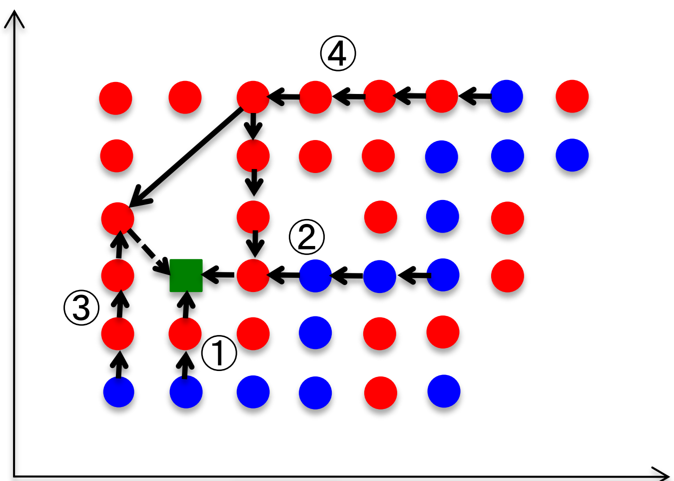

① (p,γ)

② (γ,n)

p-process nucleosynthesis

P. Mohr et al., Phys. Lett. B 488 (2000) 127
H. Utsunomiya et al., Nucl. Phys. A 777 (2006) 459

Photoreaction rates for gs

$$\lambda_{\gamma n}(T) = \int_0^\infty c n_\gamma(E,T)\sigma_{\gamma n}(E)dE$$

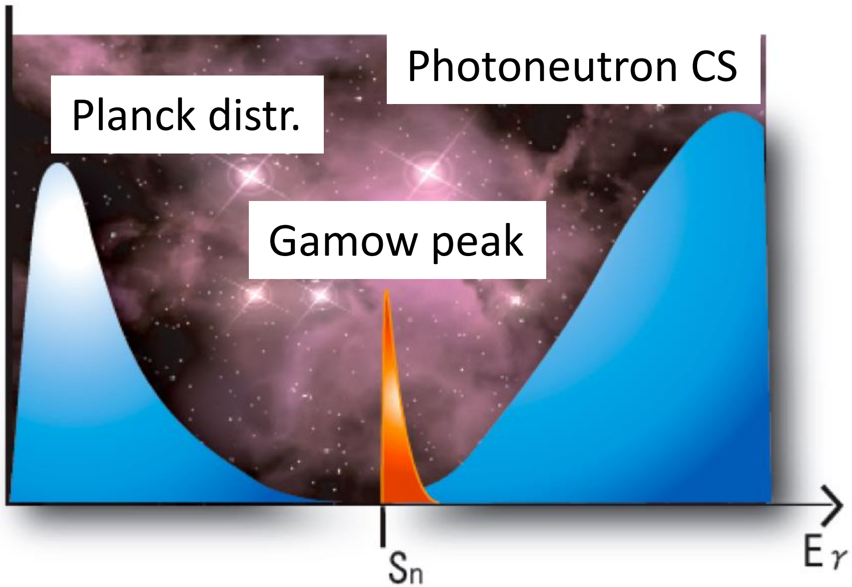

Planck distribution

$$n_\gamma(E,T)dE = \frac{1}{\pi^2}\frac{1}{(\hbar c)^3}\frac{E^2}{\exp(E/kT)-1}dE$$

Stellar photoreaction rate

Photoreaction rates for a state μ

$$\lambda_{\gamma n}^{\mu}(T) = \int_0^{\infty} c n_\gamma(E,T)\sigma_{\gamma n}^{\mu}(E)dE$$

$$\sigma_{\gamma n}^{\mu}(E_\gamma) = \pi \lambda\!\!\!^{-2}_\gamma \frac{1}{2(2j^\mu+1)} \sum_{J^\pi}(2J+1)\frac{T_\gamma^\mu(E_\gamma,J^\pi)T_n(E,J^\pi)}{T_{tot}(E,J^\pi)}$$

$$T_\gamma^\mu(E_\gamma,J^\pi) = 2\pi\varepsilon_\gamma^3 f_\gamma(E_\gamma)\uparrow$$ for E1 transition

Stellar photoreaction rate

$$\lambda_{\gamma n}^{*} = \frac{\sum_\mu (2j^\mu+1)\lambda_{\gamma n}^{\mu}(T)\exp(-\varepsilon_\mu/kT)}{\sum_\mu (2j^\mu+1)\exp(-\varepsilon_\mu/kT)}$$

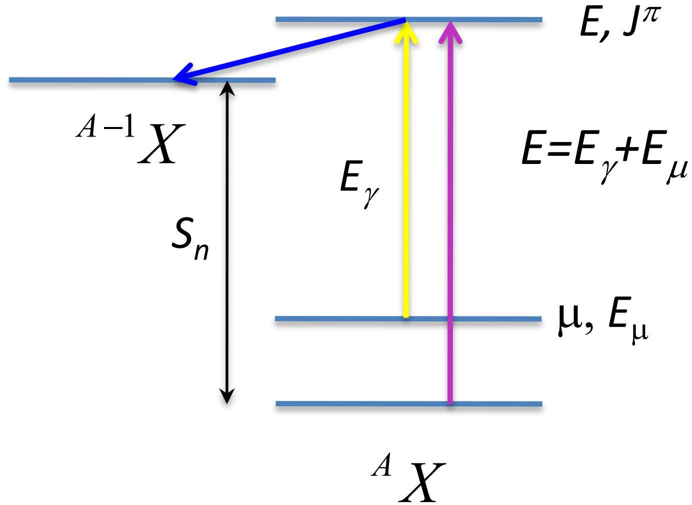

Key quantity:

γ-ray strength function $f_\gamma(E_\gamma)$

$E_\gamma > S_n$ for gs

$E_\gamma < S_n$ for excited states μ

Only naturally occurring isomer $^{180}Ta^{m}$

- Odd-odd Nucleus (Z=73, N=107)
- Neutron deficient nucleus (classified as one of p-nuclei)
- Solar Abundance ; 2.48×10^{-6}(the rarest)
- Half Life > 1.2×10^{15}y
- E_x = 75keV
- $J^{\pi} = 9^{-}$

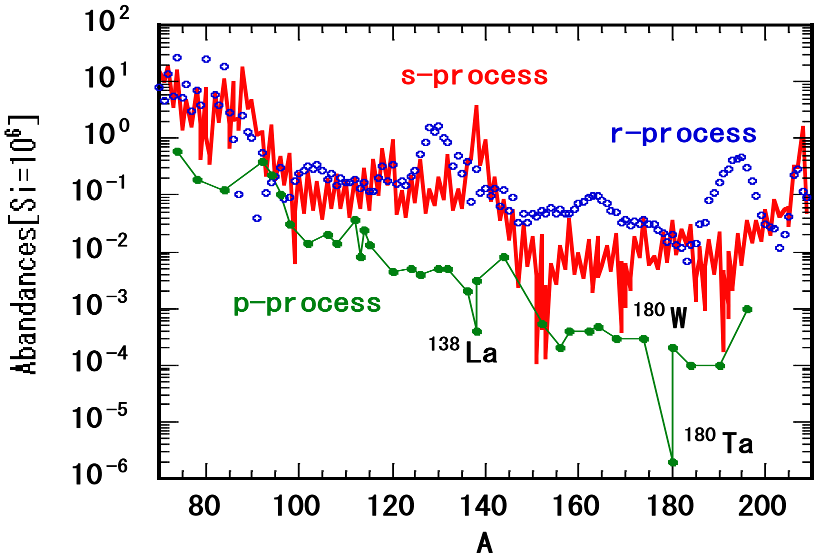

$^{180}Ta^{gs}$

- Half Life = 8.152h
- $J^{\pi} = 1^{+}$

Network of nucleosynthesis

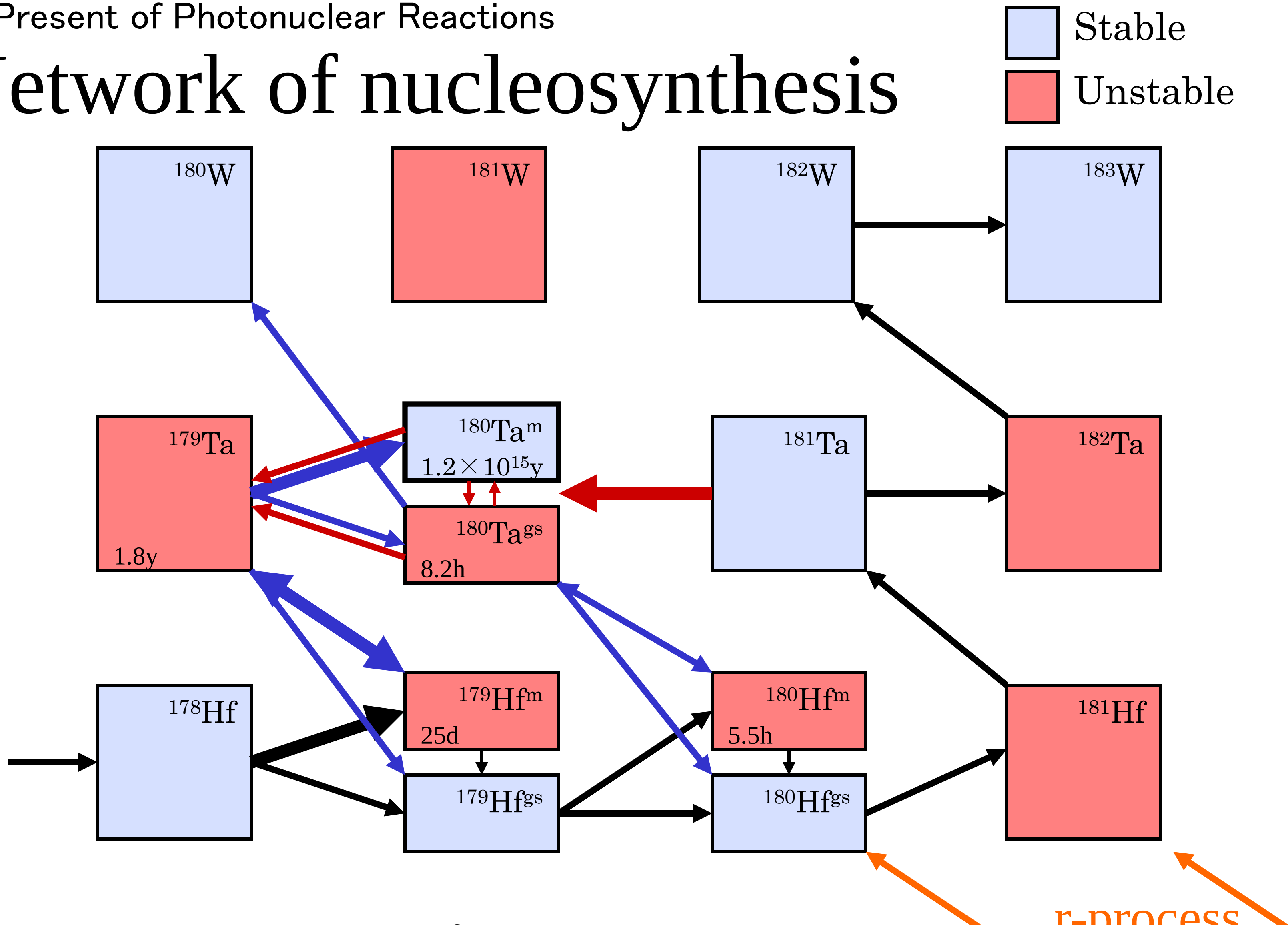

Primary s-process flow ${}^{A}_{Z}X(n,\gamma){}^{A+1}_{Z}X(\beta^-){}^{A+1}_{Z+1}X'$

p-process ${}^{181}Ta(\gamma,n){}^{180}Ta(thermal\ equilibrium){}^{180}Ta^m$

Weak branching s-process ${}^{179}Hf^m(\beta){}^{179}Ta(n,\gamma){}^{180}Ta^m$

Nucleosynthesis of $^{180}Ta^m$

- p-process in the pre-supernova phase of massive stars or during their explosions as type-Ⅱ supernovae

  Temperature ; $1.8 \leqq T[10^9 K] \leqq 3.0$

  Peak photon energy ; 200[keV]

  $^{181}Ta(\gamma,n)^{180}Ta$(thermal equilibrium) $^{180}Ta^m$

- s-process in the Low-mass AGB star

  Temperature ; $2.9 \leqq T[10^8 K] \leqq 3.3$

  (Zs. Nèmeth, F. Käppeler, G. Reffo; 1992)

  Typical neutron energy ; 25[keV]

  $^{179}Hf^m(\beta)^{179}Ta(n,\gamma)^{180}Ta^m$

$^{181}Ta(\gamma,n)^{180}Ta$

H. Utsunomiya et al., Phys. Rev. C 67, 015807 (2003)

Extra E1 γ-ray strength near Sn

Pygmy Dipole Resonance
N. Paar, D. Vretenar, E. Khan, G. Colò
Rep. Prog. Phys. ***70 691*** (2007)

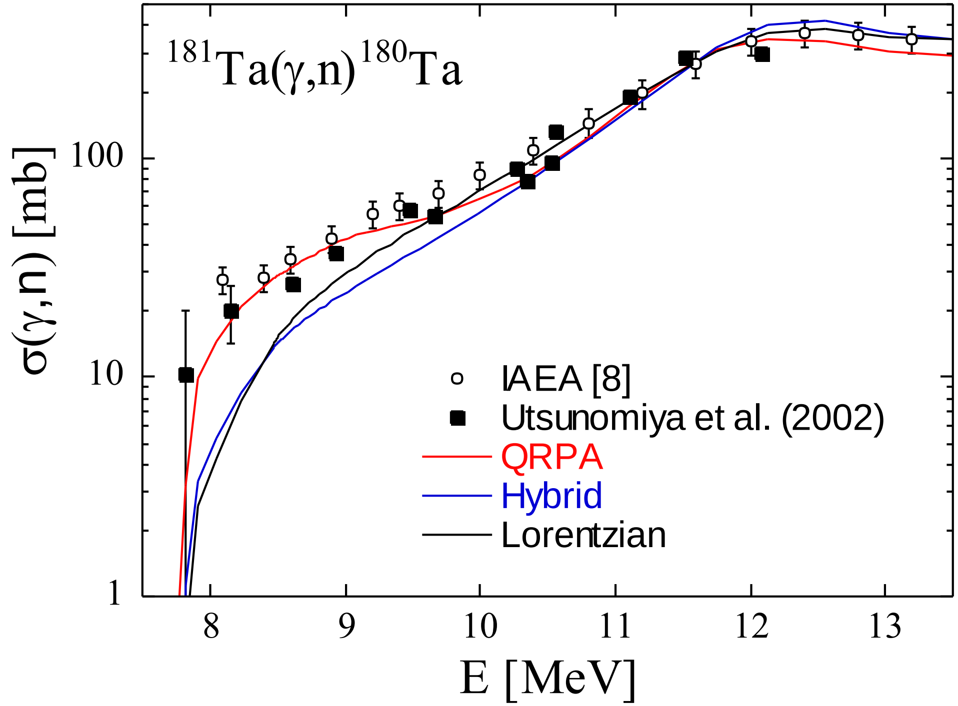

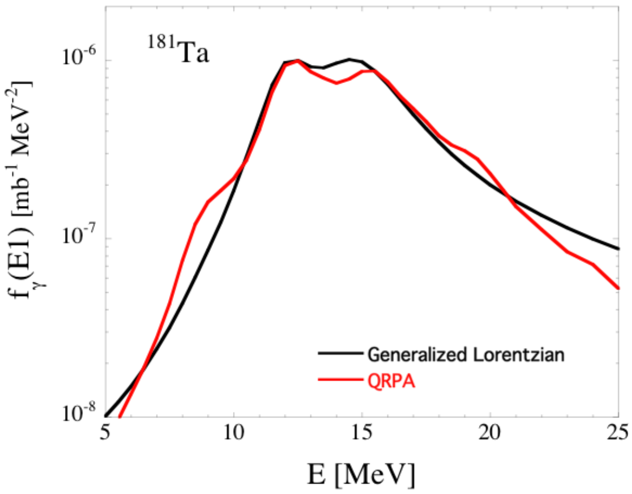

Model calculation of the p-process nucleosynthesis

H. Utsunomiya et al., Phys. Rev. C 67, 015807 (2003)

S. Goriely, ULB

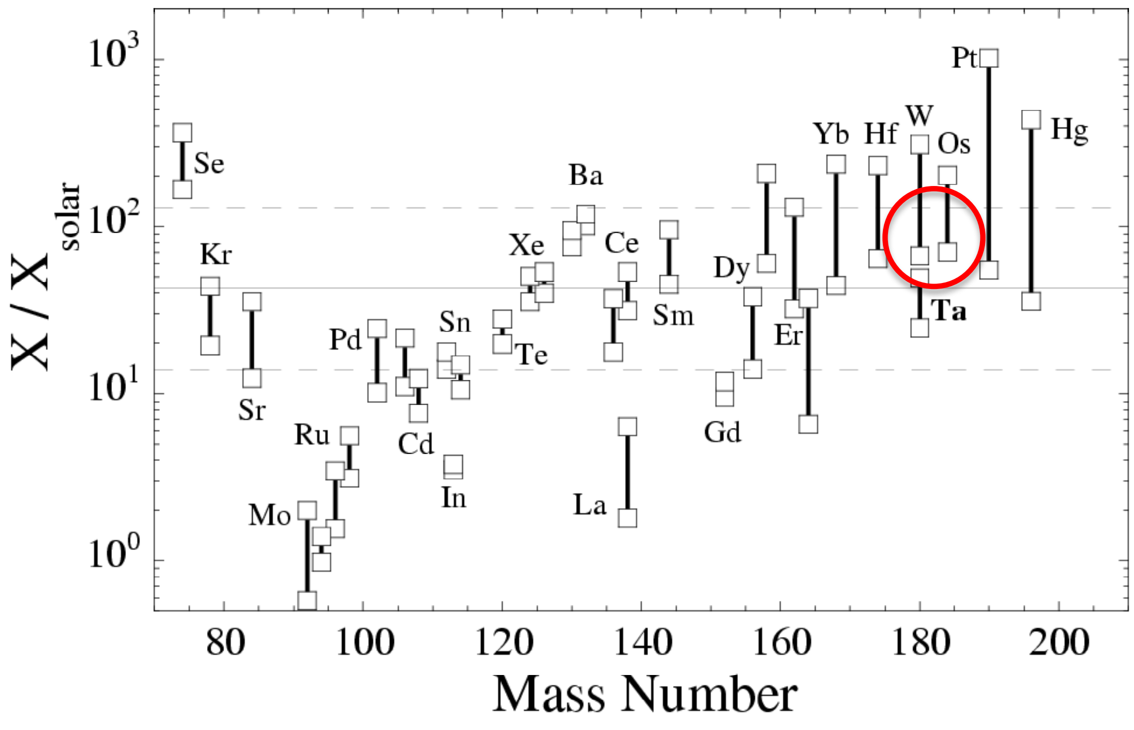

Nuclear Level Density of ^{180}Ta

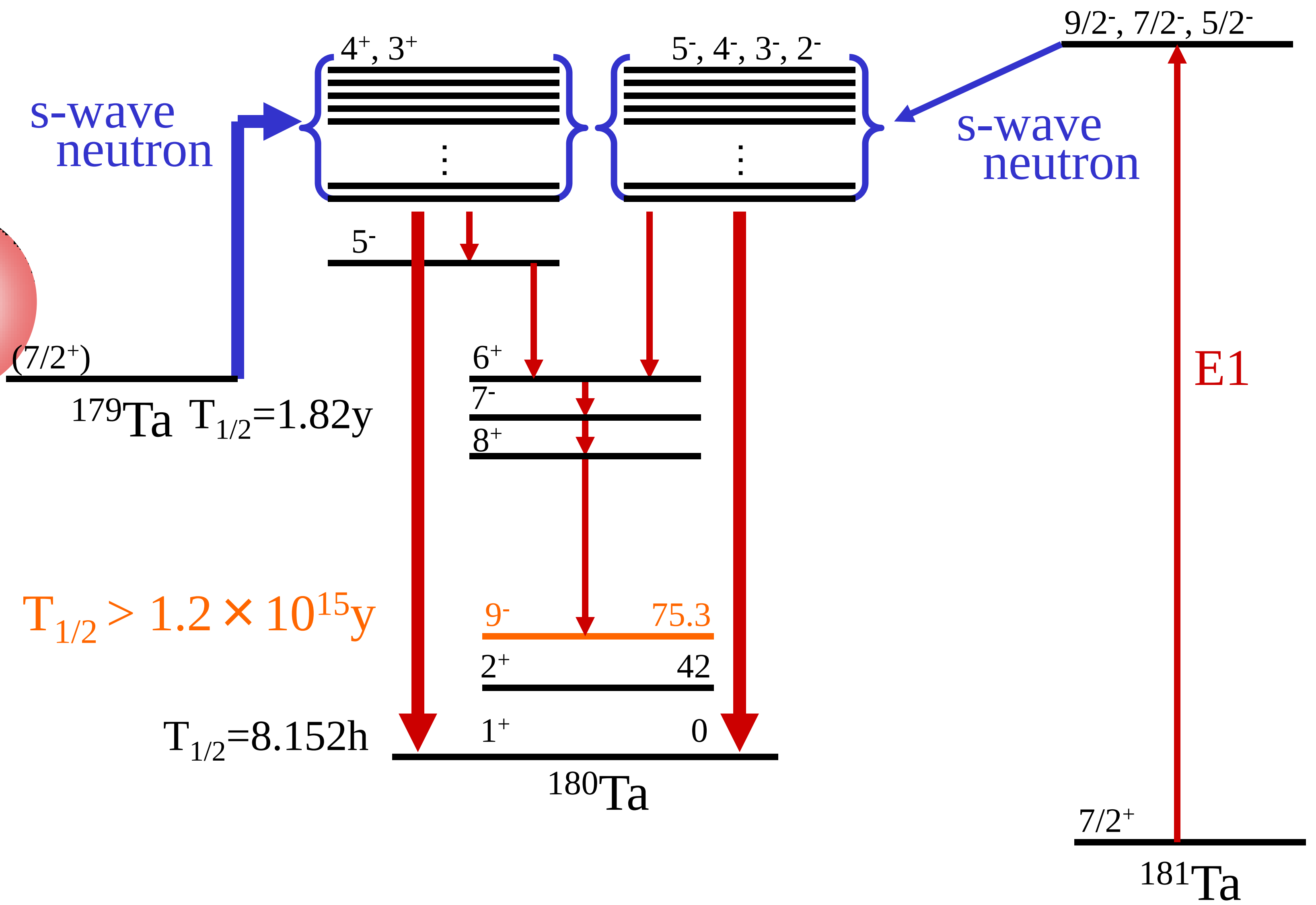

Progress of the reactions

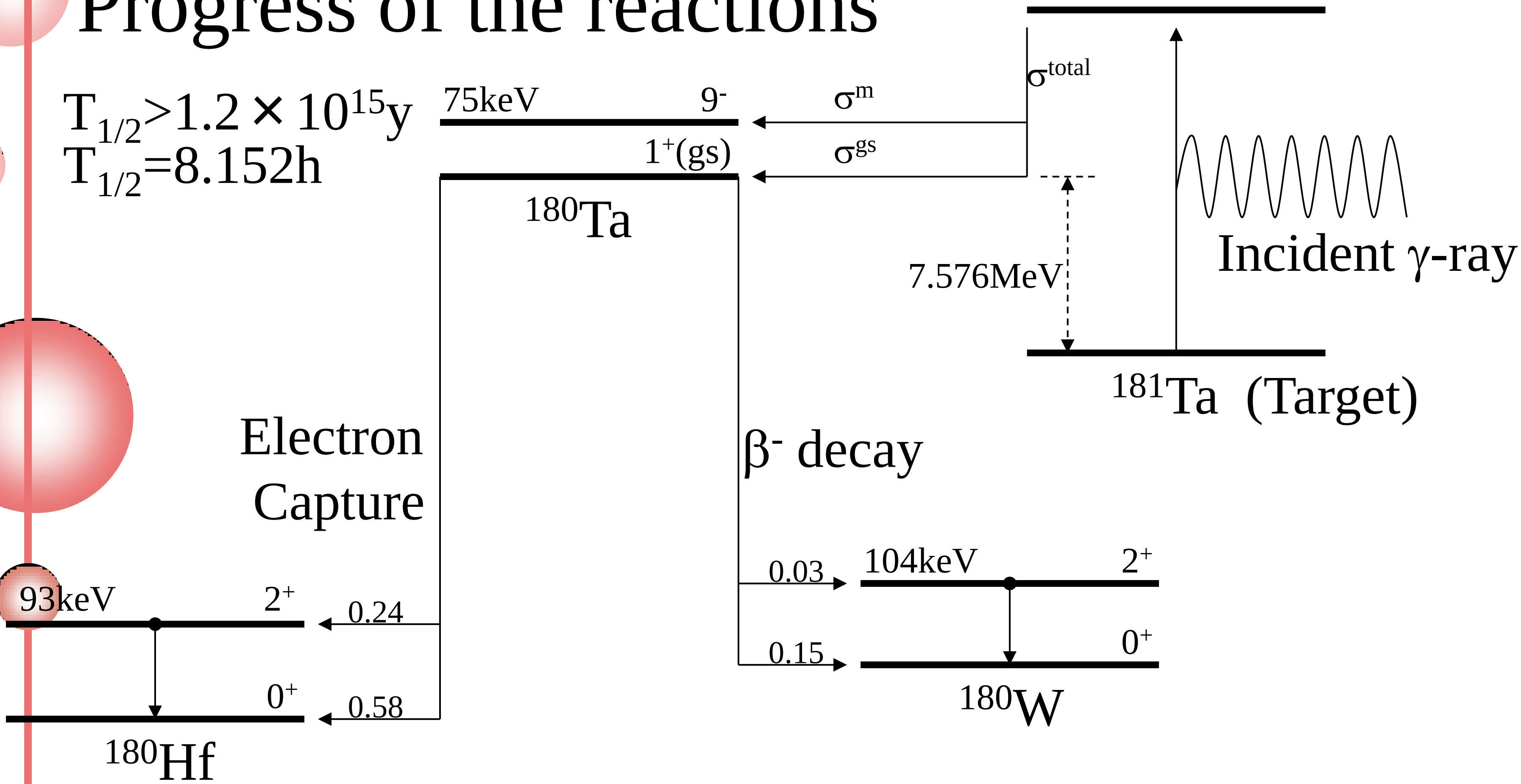

per 1 decay of $^{180}Ta^{gs}$	
93keV γ-ray	4.665%
55.8keV $K_{\alpha1}$	33.12%
54.6keV $K_{\alpha2}$	19.20%

$$\sigma^{m} = \sigma^{total} - \sigma^{gs}$$

Experimental Set-up

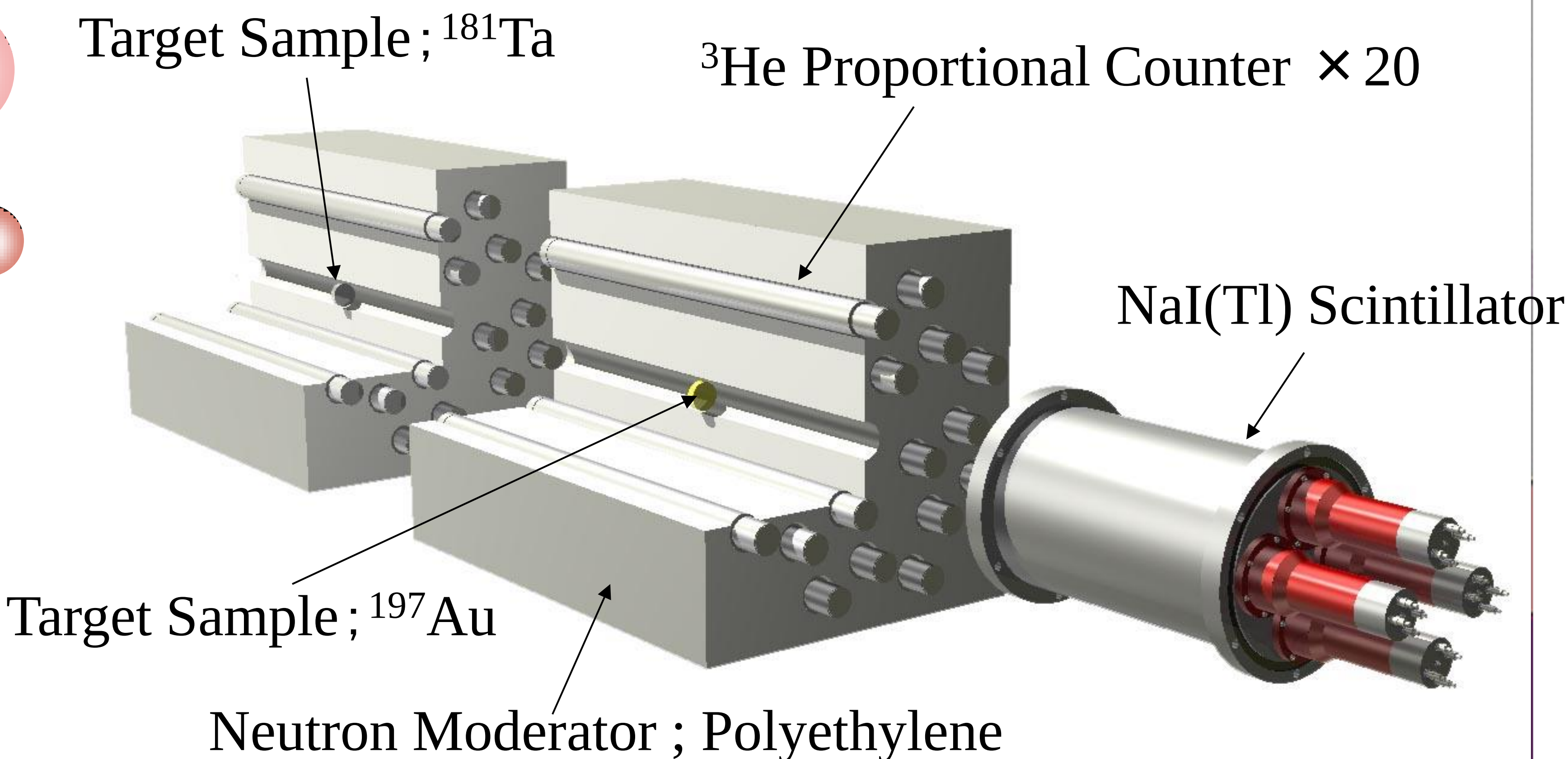

Ge Detector Set-up

Activated Ta foils
on the acrylic cap

$^{180}Ta^{gs} \rightarrow {}^{180}Hf$; Electron Capture

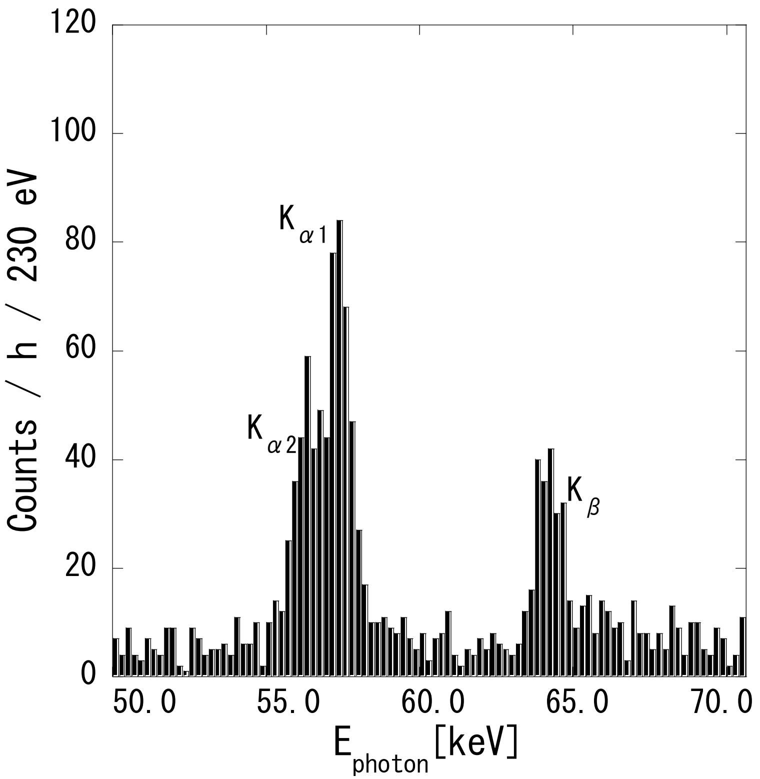

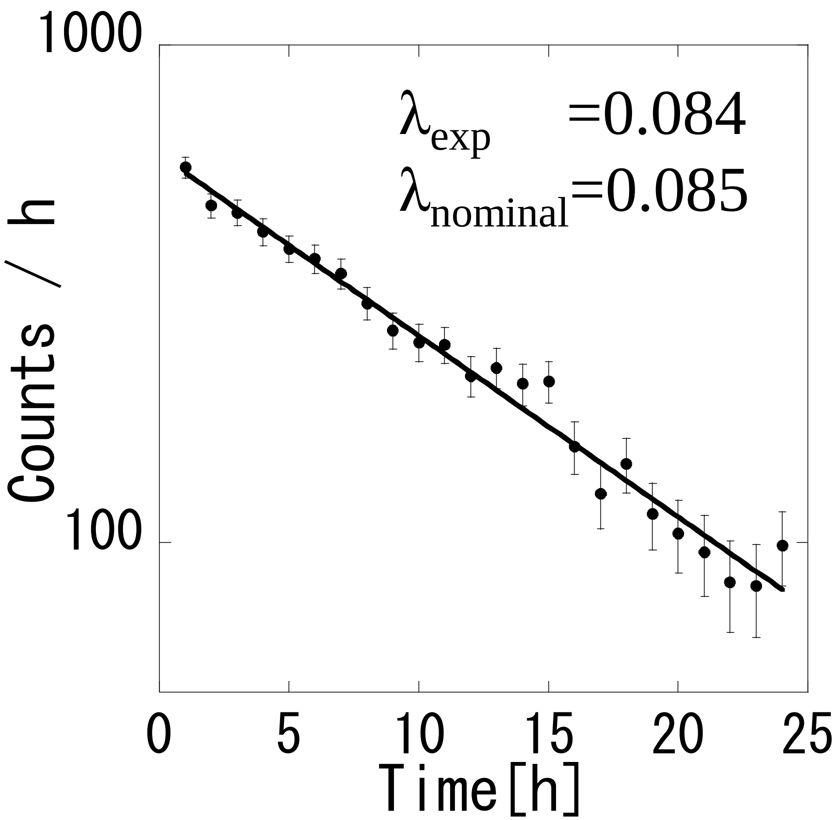

Experimental results, and comparison with theoretical models

Goko et al. Phys. Rev. Lett. 96, 192501 (2006)

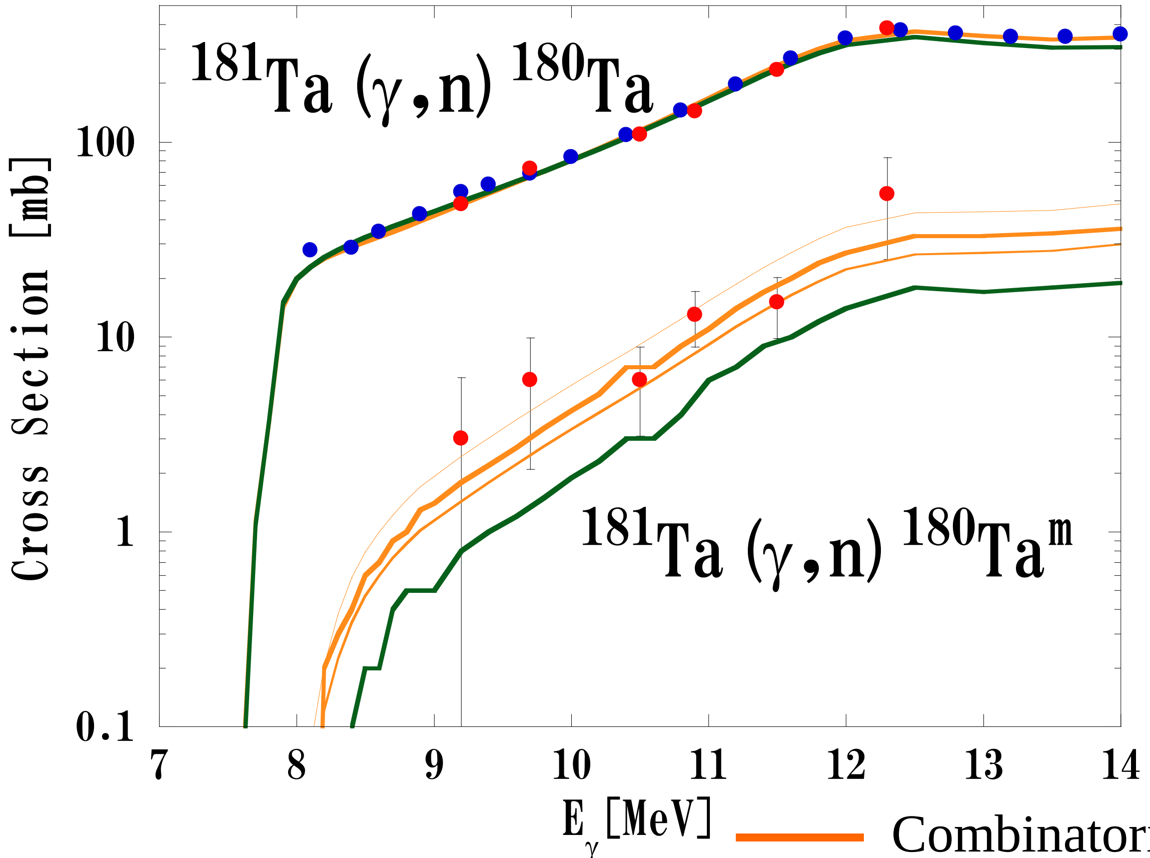

Systematic uncertainties 10～26%

● Present work (2006)

● IAEA : Lee et al. (1998)

HF model calculations by S.Goriely (ULB)

$^{179}Ta(n,\gamma)^{180}Ta^{m}$ for the s-process $^{180}Ta^{m}$ production

Goko et al.
Phys. Rev. Lett. 96, 192501 (2006)

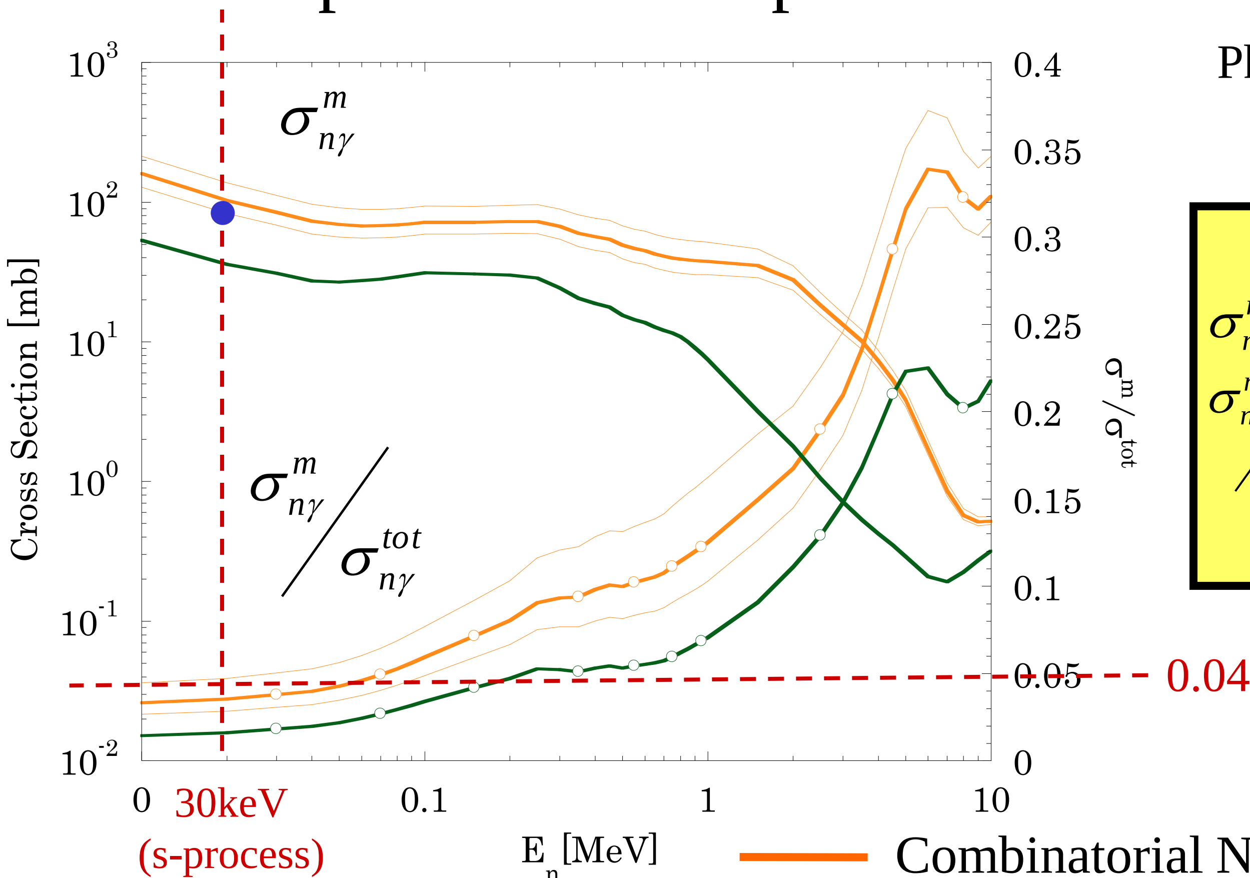

Combinatorial NLD model
Statistical NLD model
HF model calculations by S.Goriely (ULB)

Present results

$\sigma^{m}_{n\gamma} = 90 \pm 22 mb$

$\sigma^{m}_{n\gamma} / \sigma^{tot}_{n\gamma} = 0.04 \pm 0.01$

at 30 keV

Previous Predictions

σ^{m} : ● 44mb (Zs. Nèmeth, F.Käppeler, G.Reffo ;1992)

σ^{m}/σ^{tot} : 0.02〜0.09 (K.Yokoi, K.Takahashi ;1983)

0.043±0.008 (Zs. Nèmeth, F.Käppeler, G.Reffo ;1992)

Radiative neutron capture - $^{A}X(n,\gamma)^{A+1}X$

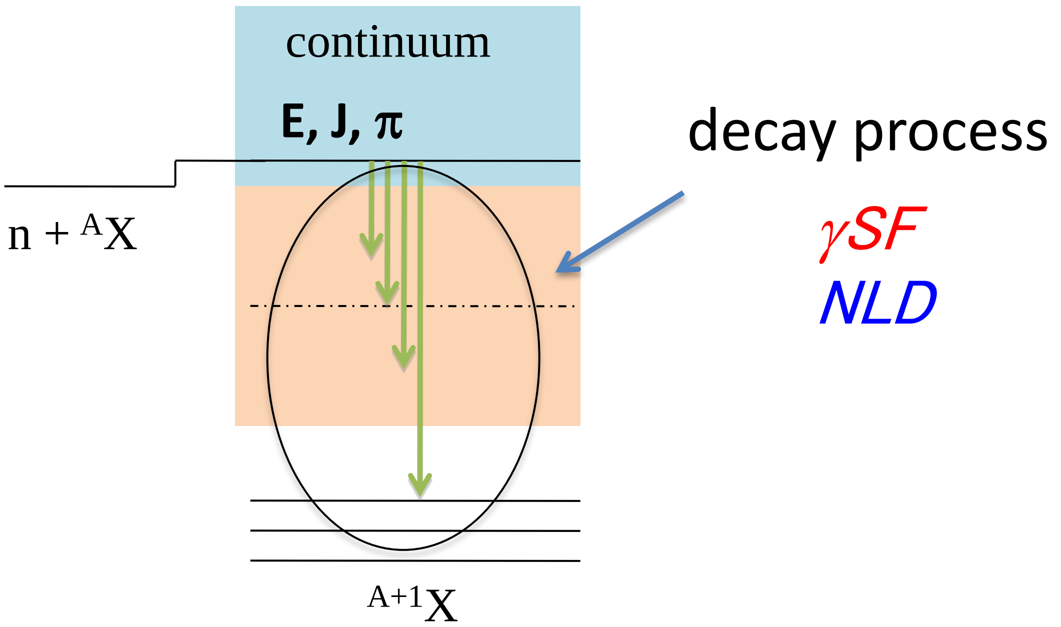

Hauser-Feshbach model cross section for $^{A}X(n,\gamma)^{A+1}X$

$$\sigma_{n\gamma}(E) = \frac{\pi}{k_n^2}\sum_{J,\pi} g_J \frac{T_\gamma(E,J,\pi)\, T_n(E,J,\pi)}{T_{tot}} \cong \frac{\pi}{k_n^2}\sum_{J,\pi} g_J T_\gamma(E,J,\pi)$$

$$T_{tot} \approx T_n(E,J,\pi)$$

Total γ transmission coefficient

After integrating over J and π

$$T_\gamma(E,J,\pi) = \sum_{\nu,X,\lambda} T^{\nu}_{X\lambda}(\varepsilon_\gamma) + \sum_{X,\lambda}\int T_{X\lambda}(\varepsilon_\gamma)\,\rho(E-\varepsilon_\gamma)\,d\varepsilon_\gamma$$

X=E, M

λ=1, 2, …

γ-ray strength function

$$T_{X\lambda}(\varepsilon_\gamma) = 2\pi\varepsilon_\gamma^{2\lambda+1} f_{X\lambda}(\varepsilon_\gamma)\downarrow$$

nuclear level density

$$\rho(E-\varepsilon_\gamma)$$

neutron resonance spacing

low-lying levels

(n,γ) and (γ,n) are interconnected through the γ-ray strength function and the nuclear level density in the Hauser-Feshbach model.

Radiative neutron capture

$^{A}X(n,\gamma)^{A+1}X$

$n+{}^{A}X$

$$f_{X\lambda}(\varepsilon_\gamma)\downarrow = \varepsilon_\gamma^{-(2\lambda+1)} \frac{\langle \Gamma_{X\lambda}(\varepsilon_\gamma)\rangle}{D_\ell}$$

$$\varepsilon_\gamma < S_n$$

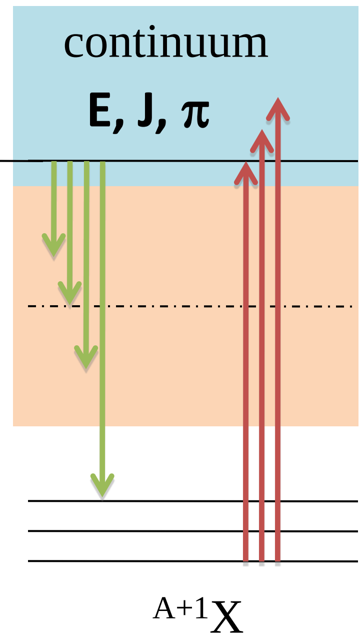

Photoneutron emission

$^{A+1}X(\gamma,n)^{A}X$

$$f_{X\lambda}(\varepsilon_\gamma)\uparrow = \frac{\varepsilon_\gamma^{-2\lambda+1}}{(\pi\hbar c)^2} \frac{\langle \sigma_{X\lambda}^{abs}(\varepsilon_\gamma)\rangle}{2\lambda+1}$$

$$\varepsilon_\gamma > S_n$$

Brink Hypothesis

$$\boxed{f_{X\lambda}(\varepsilon_\gamma)\uparrow \cong f_{X\lambda}(\varepsilon_\gamma)\downarrow}$$

γ-ray Strength Function Method

H. Utsunomiya et al., Phys. Rev. C 80, 055806 (2009)

Indirect determination of (n, γ) cross sections for unstable nuclei based on a unified understanding of (γ,n) and (n, γ) reactions through the γ-ray strength function

The best understanding of the γ SF with PDR and M1 resonance is obtained by integrating

- (γ, n) data
- (γ, γ') NRF data
- Particle-γ coin. data , Oslo Method
- Existing (n, γ) data

Applications of the γ-ray Strength Function Method

1. Nuclear Astrophysics

s-process branch-point nuclei: unstable nuclei along the line of β-stability

F. Käppeler *et al*., Rev. Mod. Phys. **83**, 157 (2011)

63Ni, 79Se, 81Kr, 85Kr, 95Zr, 147Nd, 151Sm, 153Gd, 185W

2. Nuclear Data for Nuclear Engineering

Applications

LLFP (long lived fission products) nuclear waste (orange circle)

Astrophysical significance (blue circle)

Present (©,n) measurements (yellow arrow)

Existing (n,©) data (black arrow)

(n,©) c.s. to be deduced (red arrow)

H. Utsunomiya et al., PRC80 (2009)

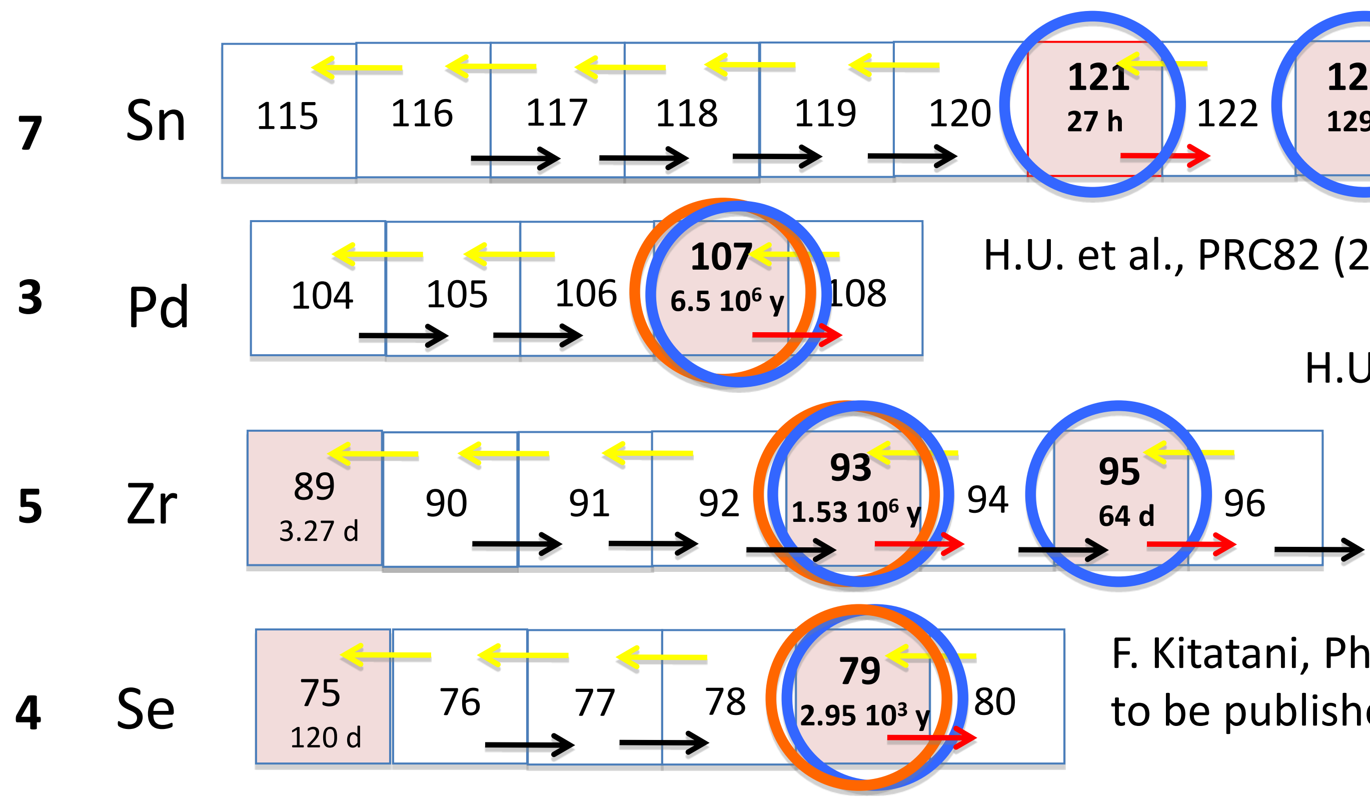

H.U. et al., PRC82 (2010)

H.U. et al., PRL100(2008) PRC81 (2010)

F. Kitatani, Ph.D. thesis, to be published

H.U. et al., PRC88 (2013)

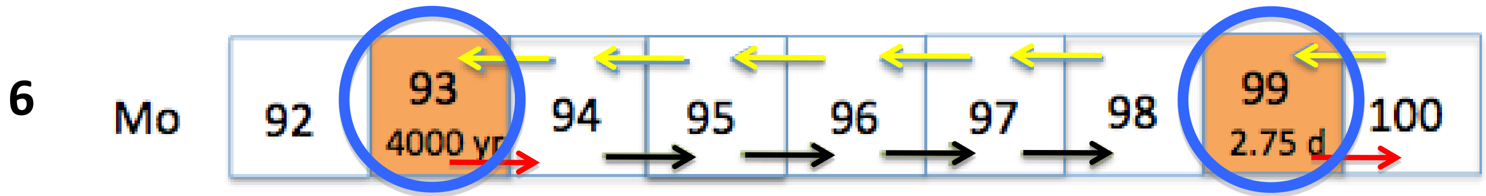

In collaboration with Univ. Oslo etc.

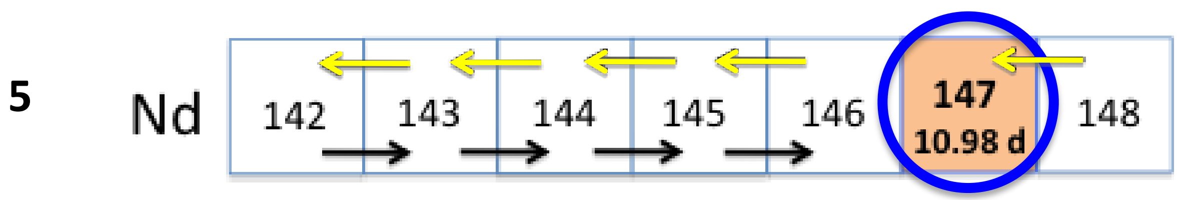

In collaboration with ELI-NP etc.

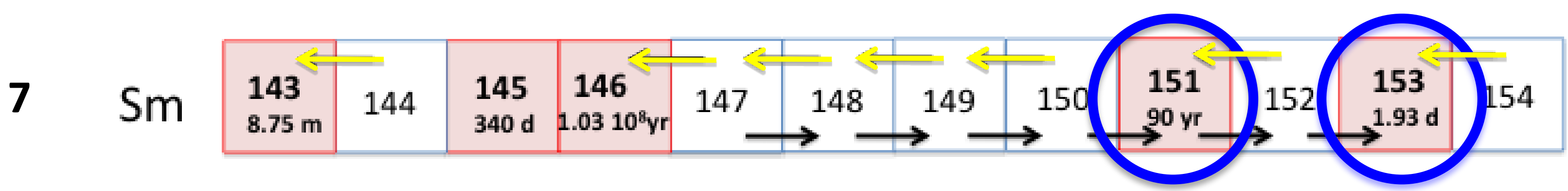

Structure of γ-ray strength function

Extra strengths

6 – 10 MeV

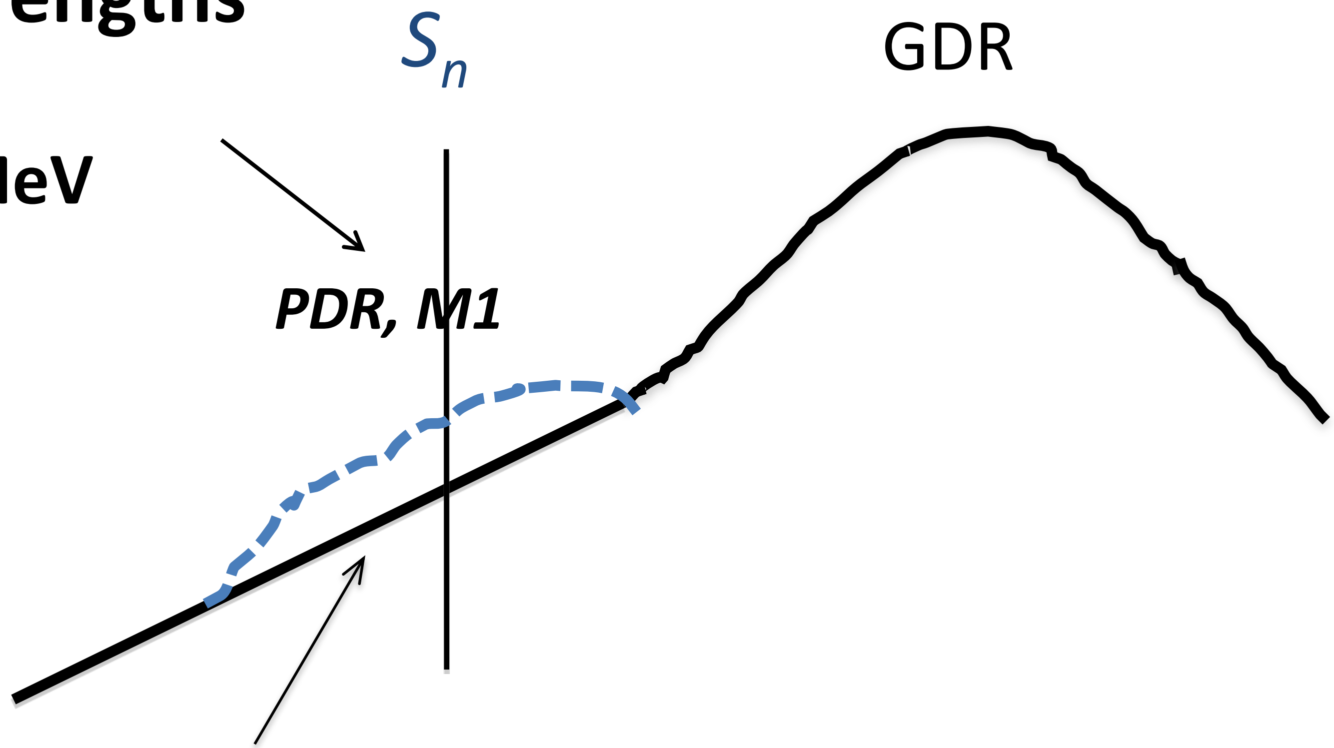

E1 strength of the low- energy tail of GDR

Experimental determination of γ-ray strength function

$^{A-1}X(n, \gamma)^{A}X$

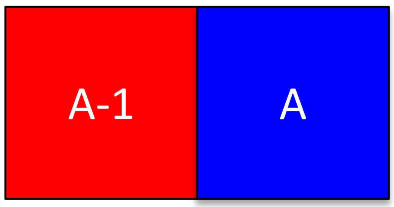

Statistical model calculation of $^{A-1}X(n, \gamma)^{A}X$ cross sections with experimental γSF

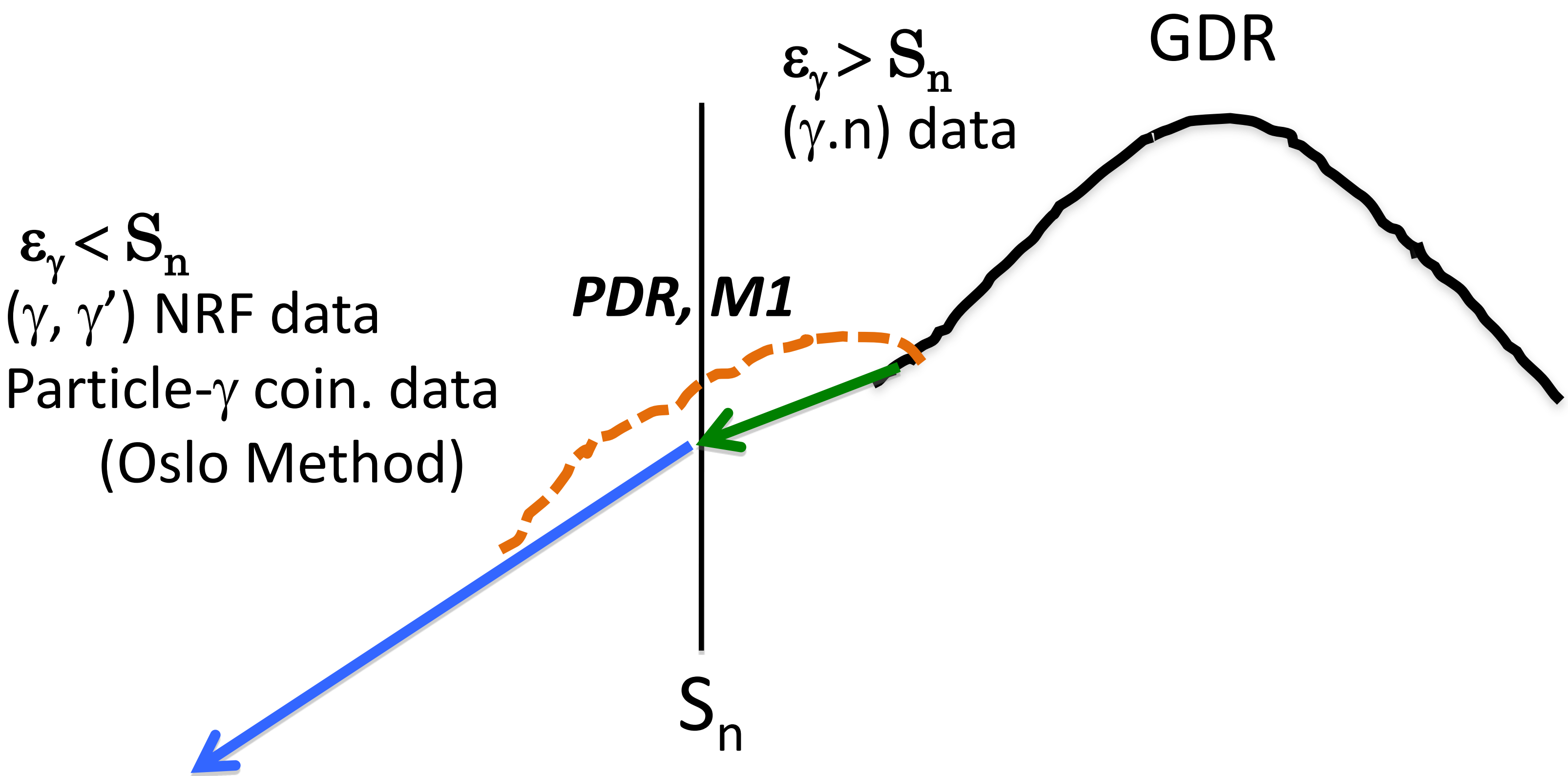

Theoretical extrapolation of γ-ray strength function

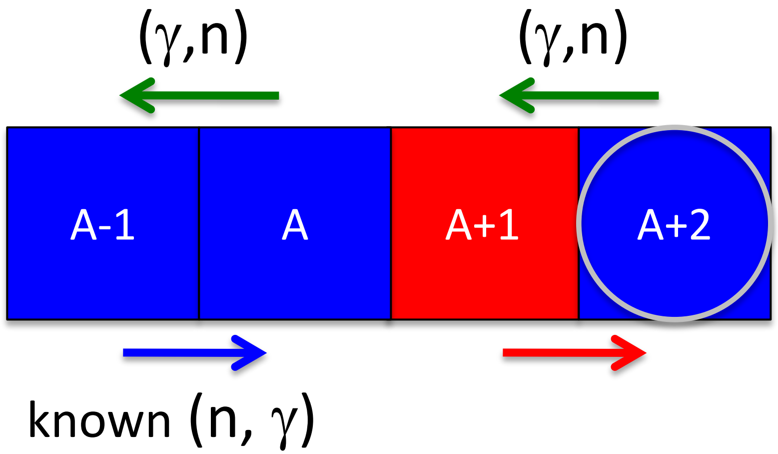

Statistical model calculation of $^{A+1}X(n,\gamma)^{A+2}X$ cross sections with experimentally-constrained γSF

1. $\varepsilon_\gamma > S_n$
(γ.n) data

2. $\varepsilon_\gamma < S_n$
Extrapolation by
<u>microscopic model</u>

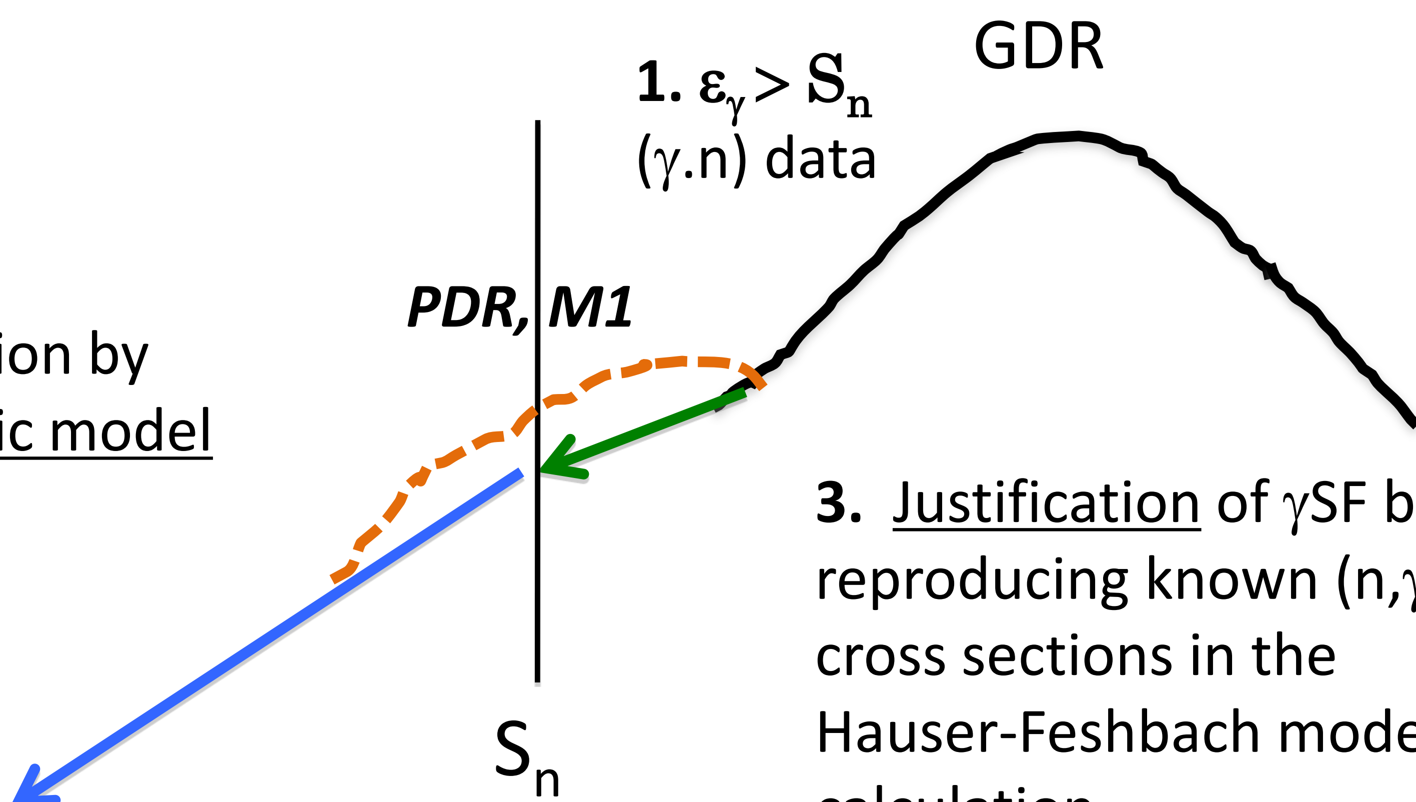

3. <u>Justification</u> of γSF by reproducing known (n,γ) cross sections in the Hauser-Feshbach model calculation

Sn isotopes

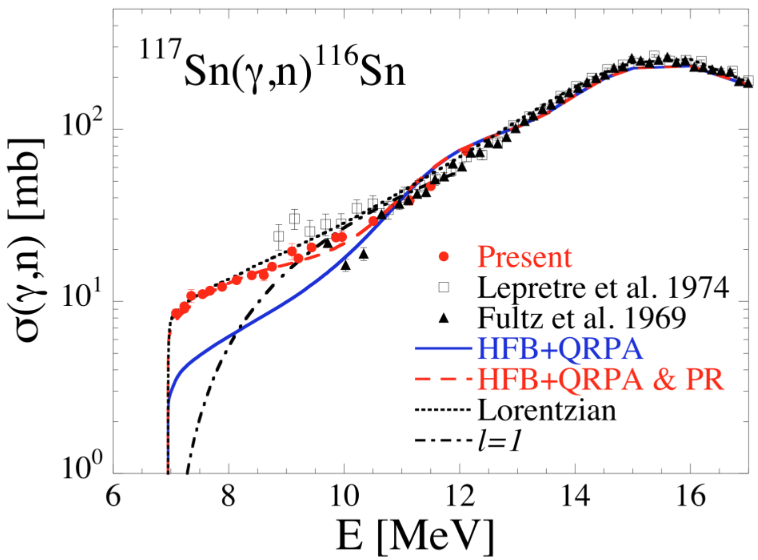

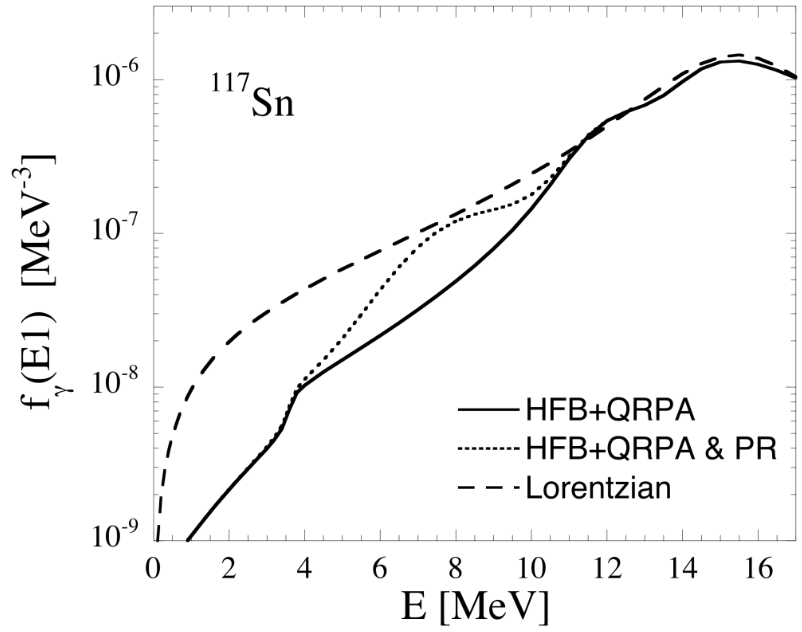

HFB+QRPA E1 strength supplemented with a pygmy E1 resonance in Gaussian shape

$E_o \approx 8.5$ MeV, $\Gamma \approx 2.0$ MeV, $\sigma_o \approx 7$ mb

∼ 1% of TRK sum rule (E1 strength)

γ**SF** for Sn isotopes

(γ,n) data

H. Utsunomiya et al., PRC84 (2011)

Oslo data

(3He, αγ）, (3He, 3He’ γ）

Toft et al., PRC 81 (2010); PRC 83 (2011)

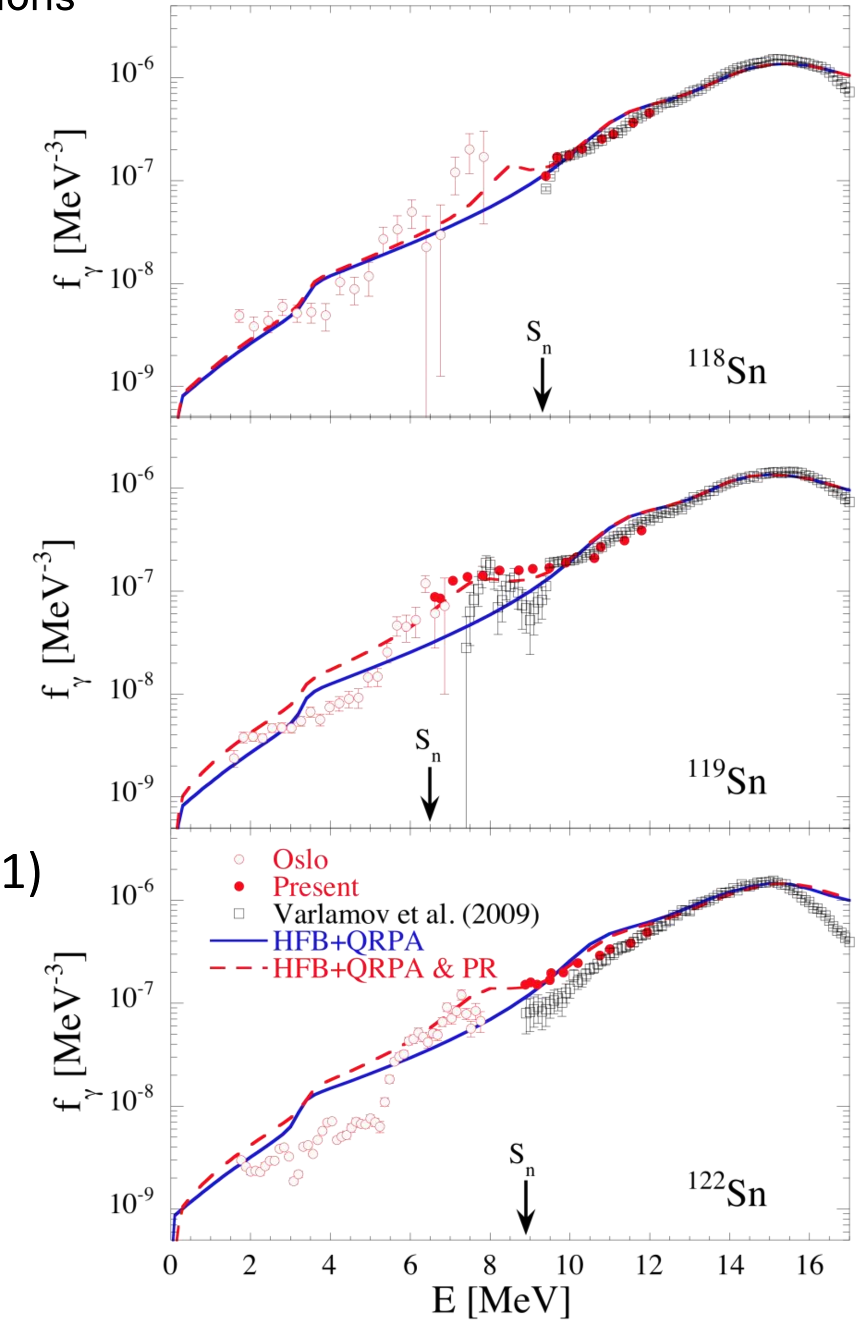

(n,γ) CS for Sn isotopes

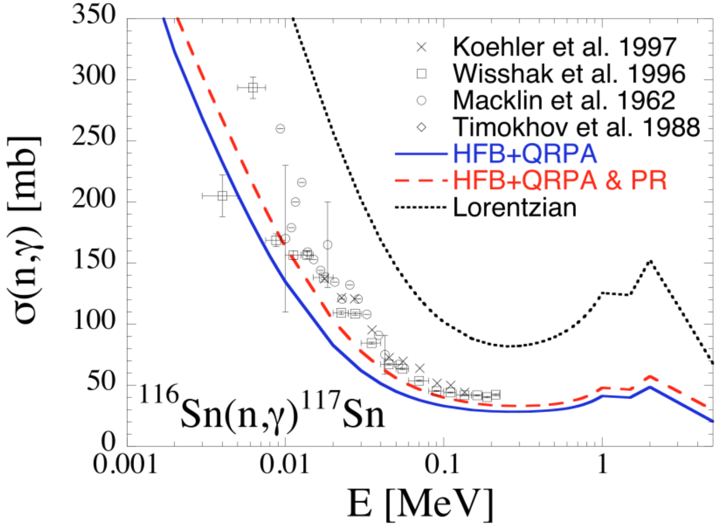

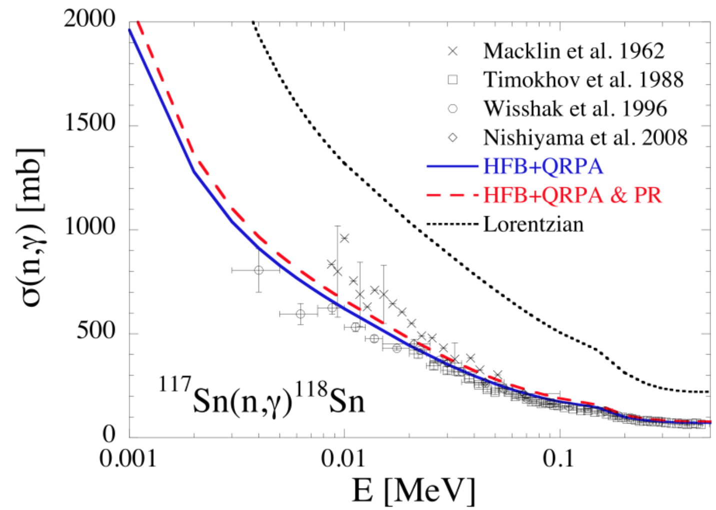

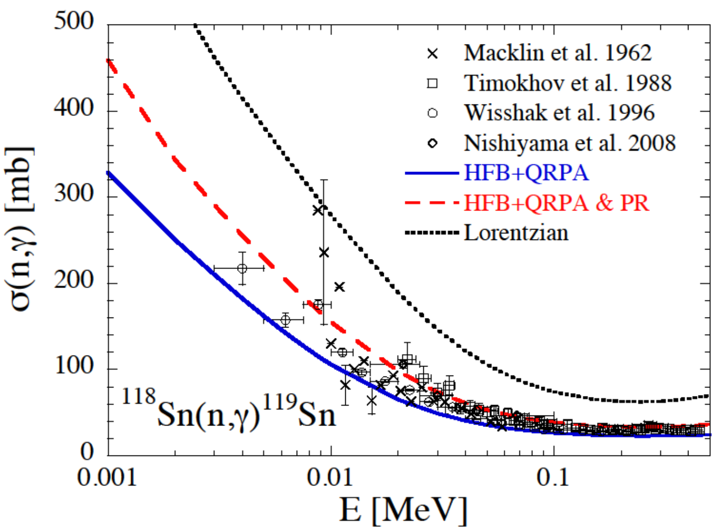

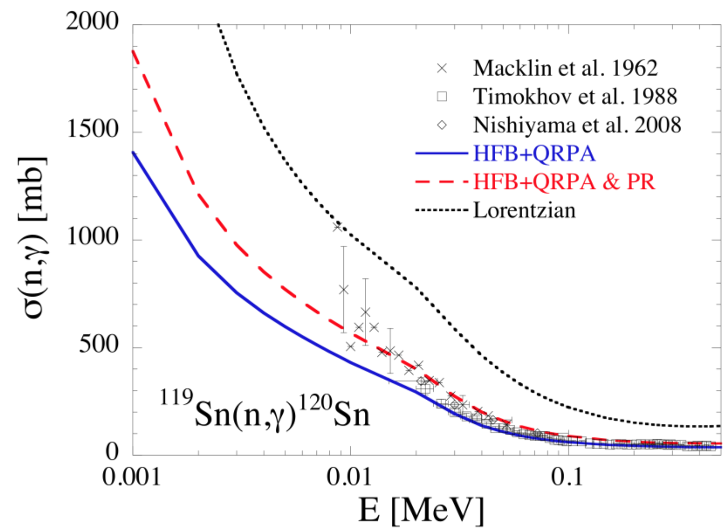

(n,γ) CS for unstable Sn isotopes

^{121}Sn[$T_{1/2}$=27 h]

^{123}Sn[$T_{1/2}$=129 d]

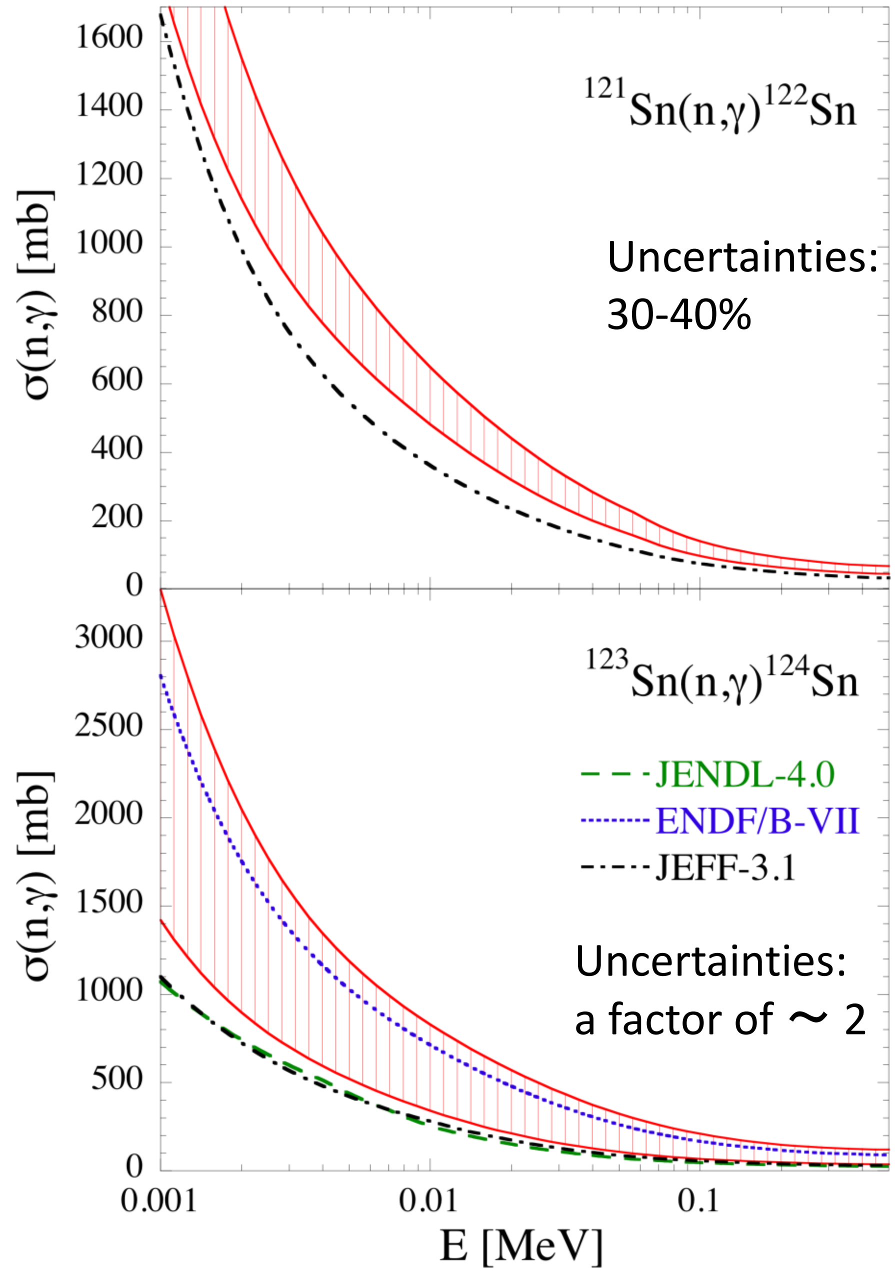

Mo isotopes

(γ,n) data

H. Utsunomiya et al., PRC 88 (2013)

Oslo data

(3He, αγ), (3He, 3He’γ)

M. Guttormsen et al., PRC71 (2005)

(γ,γ’) data

G. Rusev et al., PRC77 (2008)

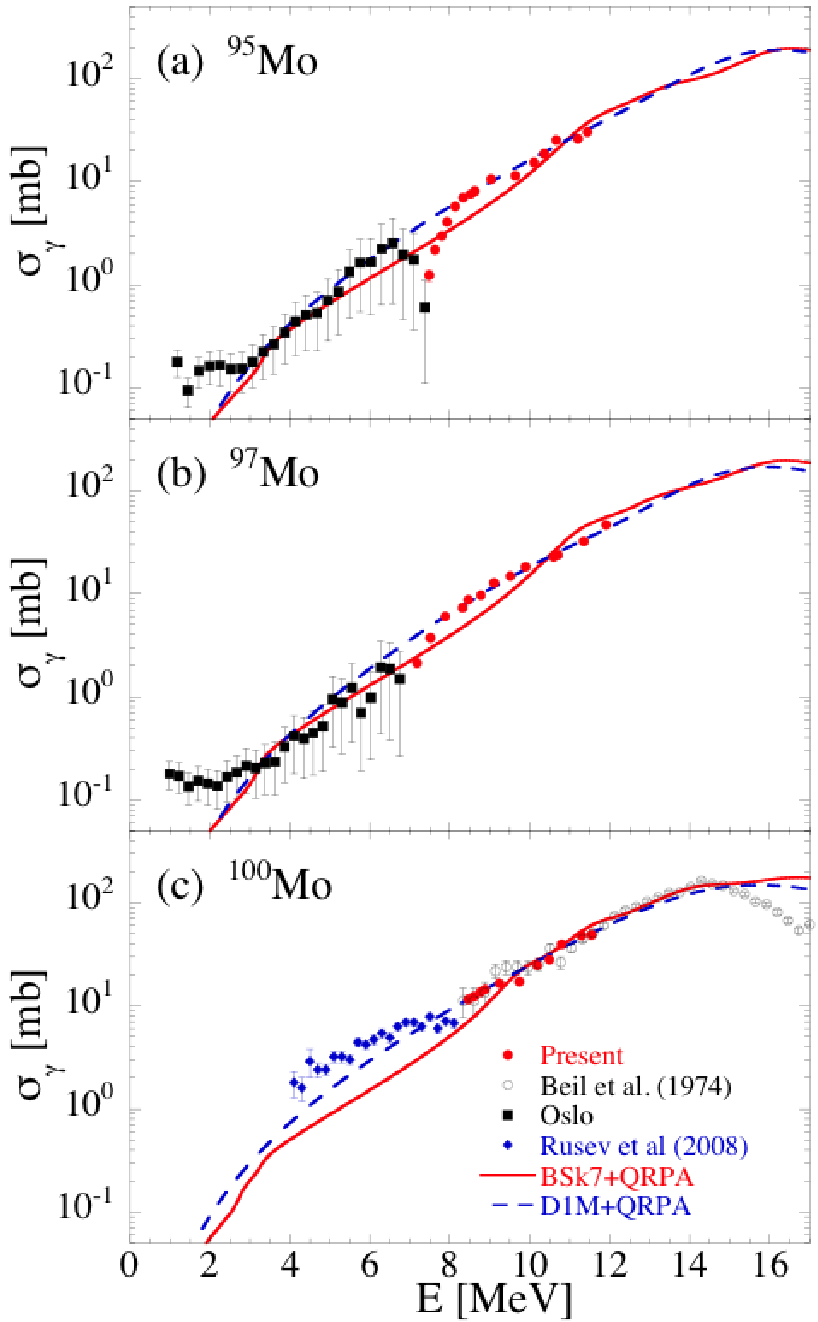

(n,γ) CS for Stable Mo isotopes

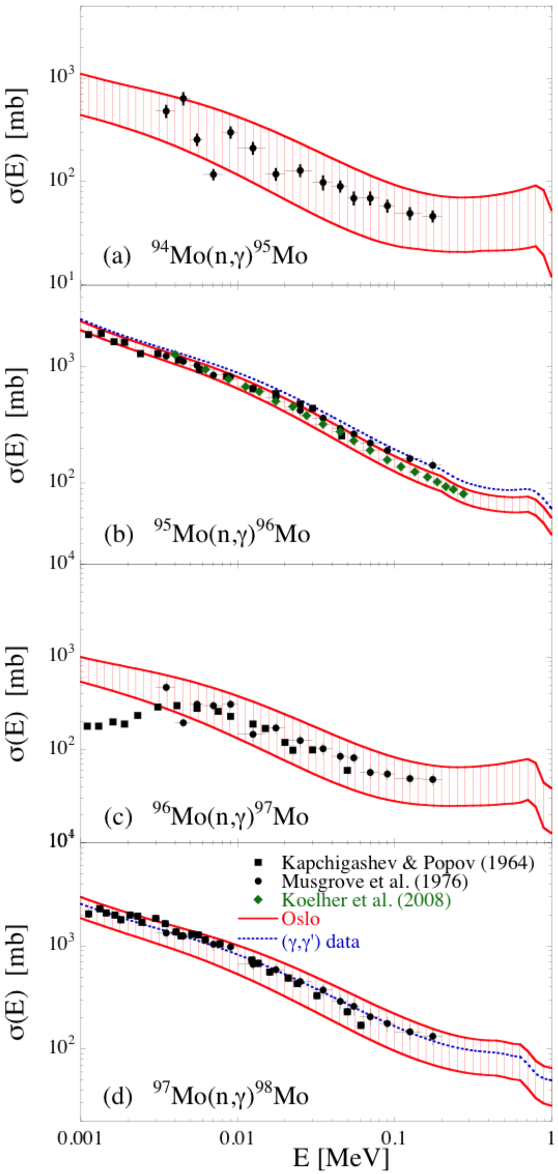

(n,γ) CS for Unstable Mo isotopes

^{93}Mo

$T_{1/2}$=4000 yr

^{99}Mo

$T_{1/2}$=2.75 d

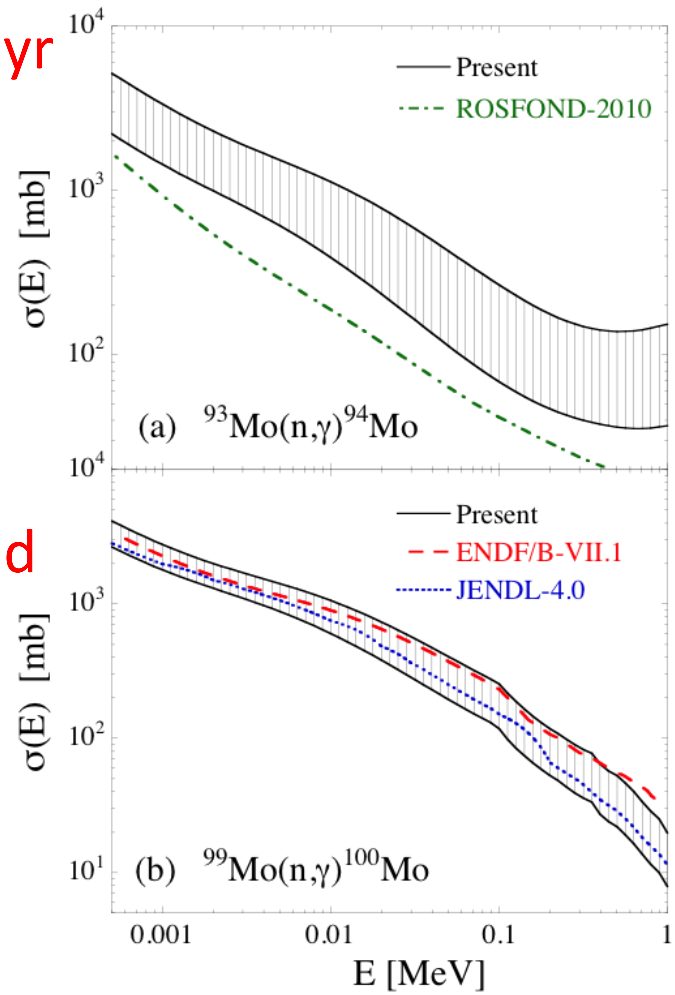

Lecture 3

Present and Future of Photonuclear Reactions

2.3 Nuclear Astrophysics (continued)
  c. reciprocity theorem – photodisintegration of D, ^{9}Be, ^{16}O
2.4 Evaluated Nuclear Data Library – ENDF, JEFF, JENDL, RIPL

3. ELI-NP project
  3.1 ELI-NP vs HIGS and NewSUBARU
  3.2 p-process – rare isotopes
  3.3 Precision Era of Nuclear Physics
    a. PDR above neutron threshold
    b. GDR – (γ,γ), (γ,n) $(\gamma,2n)$, $(\gamma,3n)$ cross sections
  3.4 Special topic
    Photoreactions on isomers – laser-gamma combined experiment

Nucleosynthesis of light nuclei

Reciprocity Theorem

A + a → B + b + Q

B + b → A + a – Q   Q value

$$\frac{\sigma(b \to a)}{(2I_A+1)(2i_a+1)p_a^2} = \frac{\sigma(a \to b)}{(2I_B+1)(2i_b+1)p_b^2}$$

Neutron Channel

a=n, b=γ $p_\gamma = \hbar k = \frac{E_\gamma}{c}$ $p_n^2 = 2\mu E_n$ $2j_b+1 \to 2$

Equivalency between (n, γ) and (γ,n)

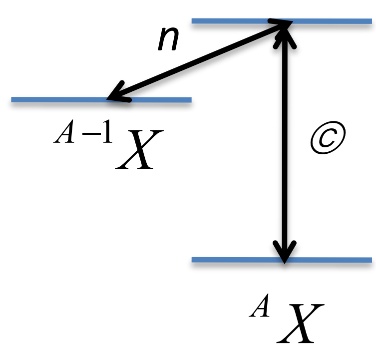

Examples

D Big Bang Nucleosynthesis: $p(n,\gamma)D$ vs $D(\gamma,n)p$

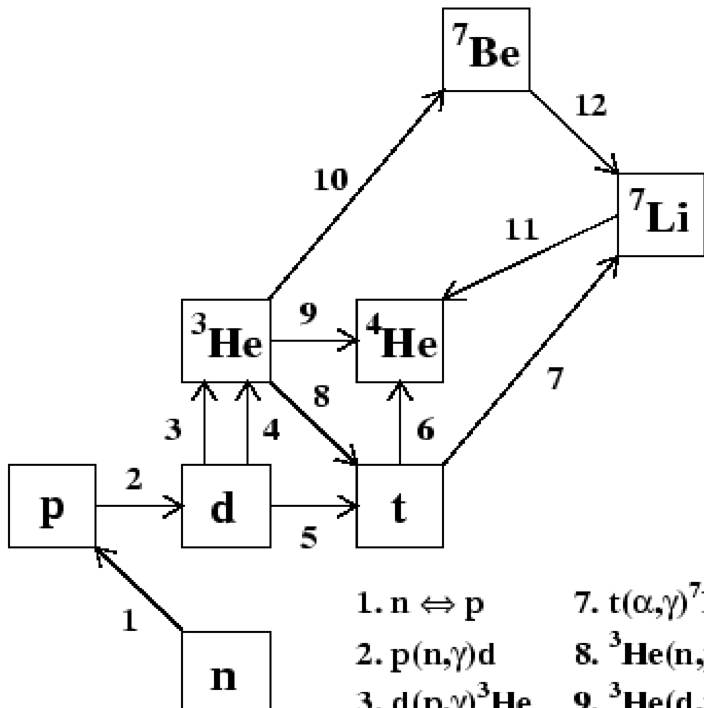

1. $n \Leftrightarrow p$
2. $p(n,\gamma)d$
3. $d(p,\gamma)^3He$
4. $d(d,n)^3He$
5. $d(d,p)t$
6. $t(d,n)^4He$
7. $t(\alpha,\gamma)^7Li$
8. $^3He(n,p)t$
9. $^3He(d,p)^4He$
10. $^3He(\alpha,\gamma)^7Be$
11. $^7Li(p,\alpha)^4He$
12. $^7Be(n,p)^7Li$

Examples

D Big Bang Nucleosynthesis: p(n,γ)D vs D(γ,n)p

K.Y. Hara et al., PRD 68, 072001 (2003)

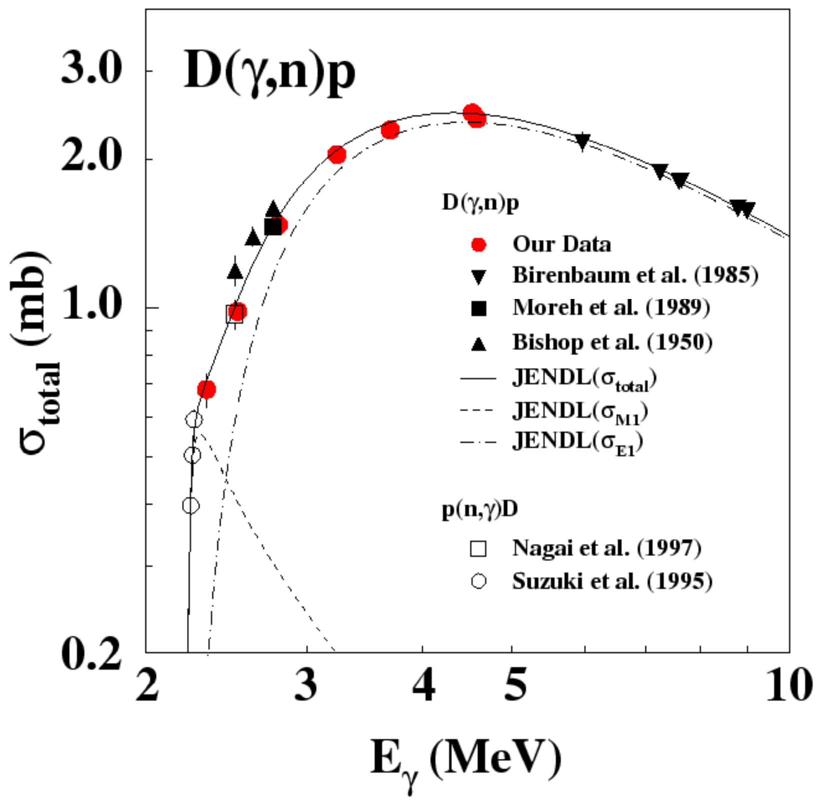

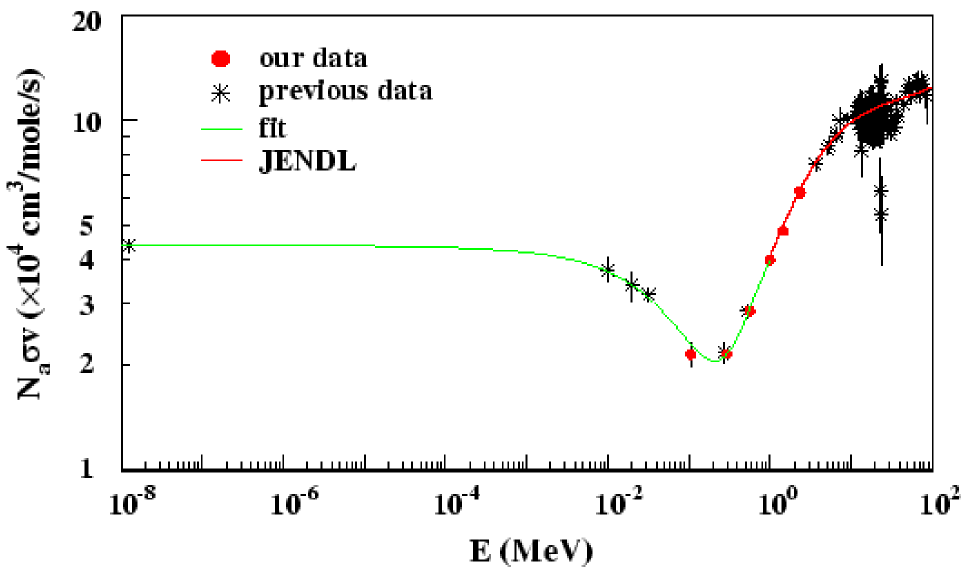

Examples

9Be Supernova Nucleosynthesis

$$\alpha\ \alpha \rightleftarrows {}^{8}\mathrm{Be}(n,\gamma)\,{}^{9}\mathrm{Be} \quad \text{vs} \quad {}^{9}\mathrm{Be}(\gamma,n)\,{}^{8}\mathrm{Be}$$

Neutrino-Driven Wind

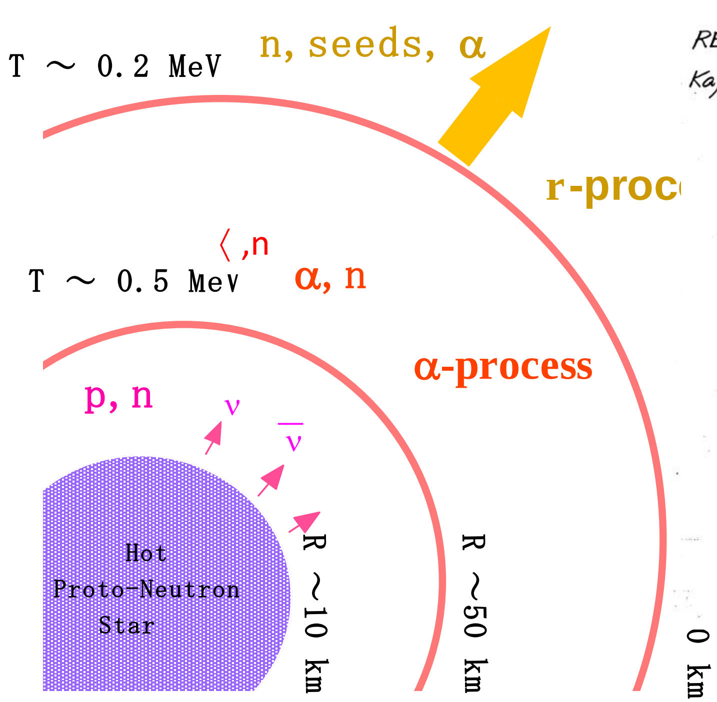

Type II Supernova

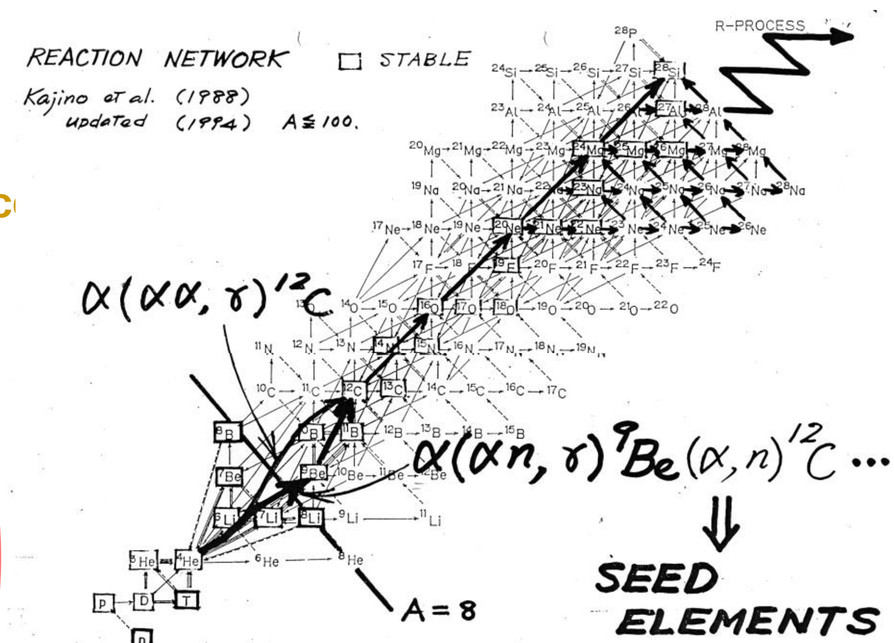

Examples

9Be Supernova Nucleosynthesis

$\alpha\ \alpha \rightleftarrows {}^{8}Be(n,\gamma)\,{}^{9}Be$ vs ${}^{9}Be(\gamma,n){}^{8}Be$

H. Utsunomiya *et al.* PRC 63, 018801 (2001)
K. Sumiyoshi *et al*. NPA709, 467 (2002)

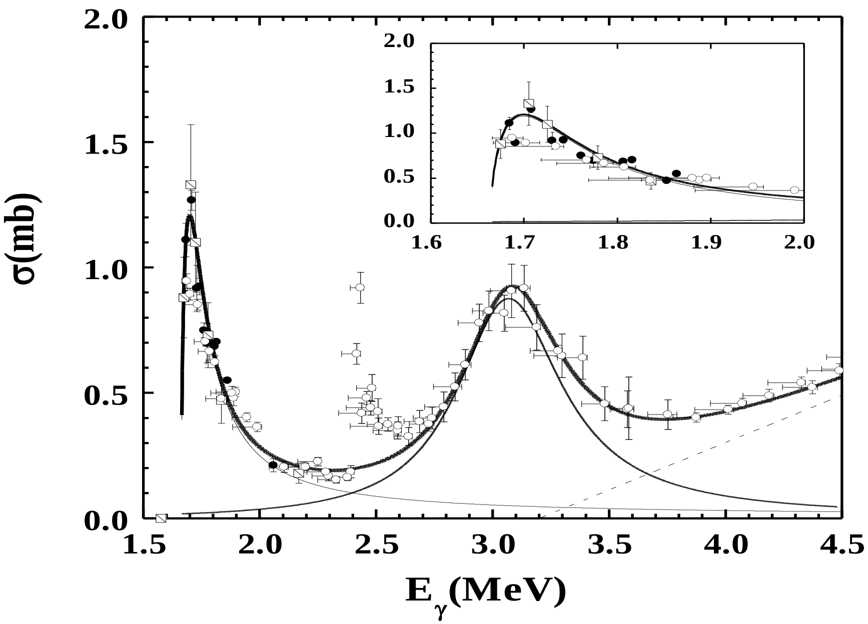

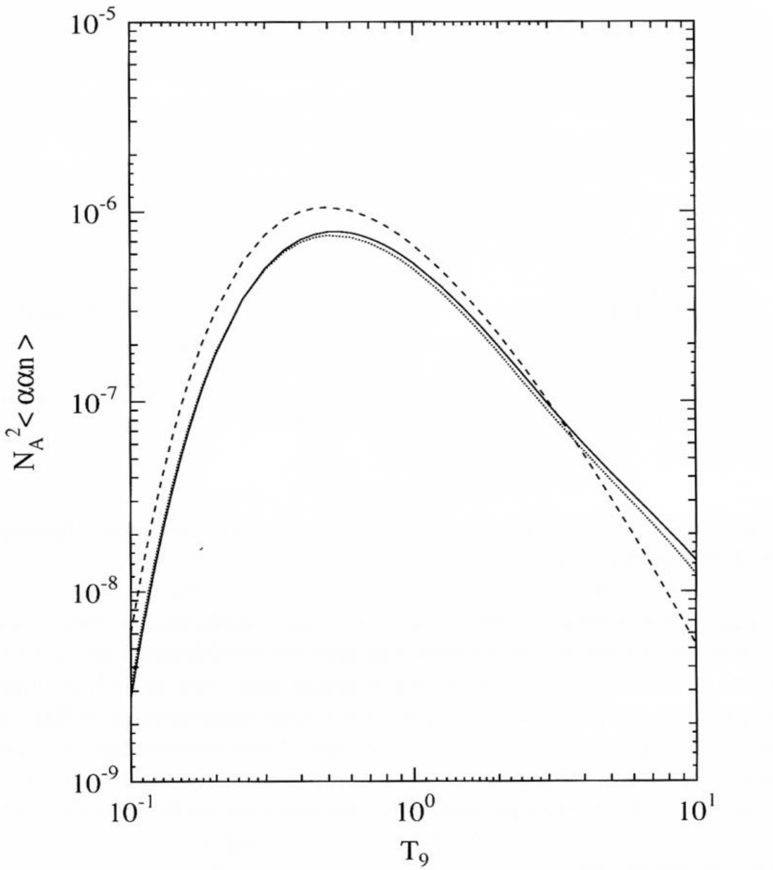

Examples

9Be

Supernova Nucleosynthesis

$\alpha\ \alpha \rightleftarrows {}^{8}Be(n,\gamma)\,{}^{9}Be$ vs ${}^{9}Be(\gamma,n){}^{8}Be$

C.W. Arnold *et al*. PRC 85, 044605 (2012)

HIGS

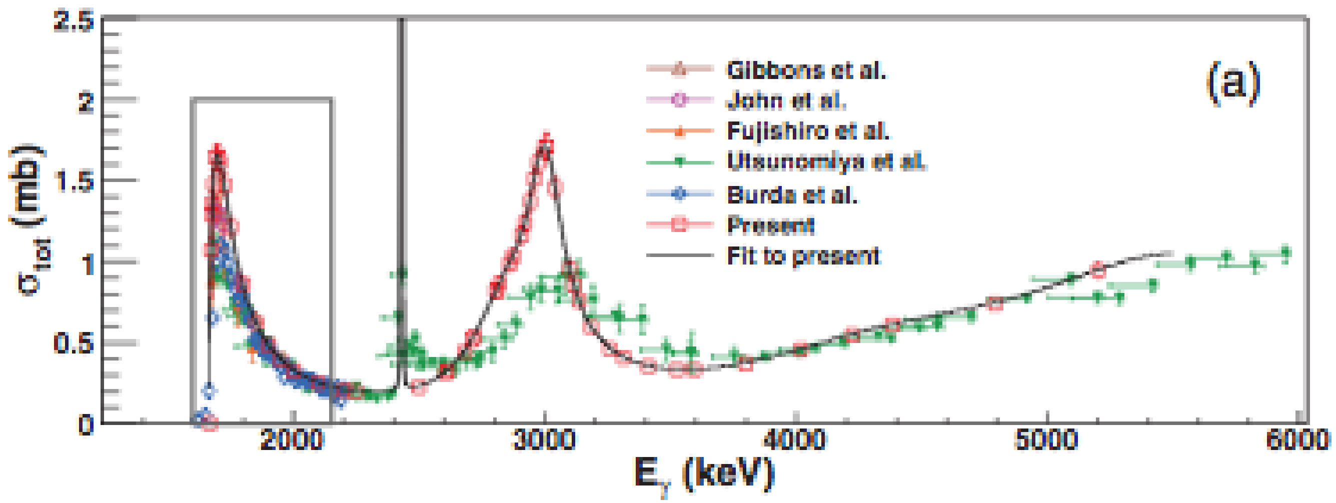

A new measurement has been done by Konan University and CNS, University of Tokyo etc. at the NewSUBARU synchrotron radiation facility and data reduction is in progress.

Courtesy by C. Ugalde

Application $^{16}O(\gamma, \alpha)^{12}C$

Reciprocal advantage:
a factor of 100

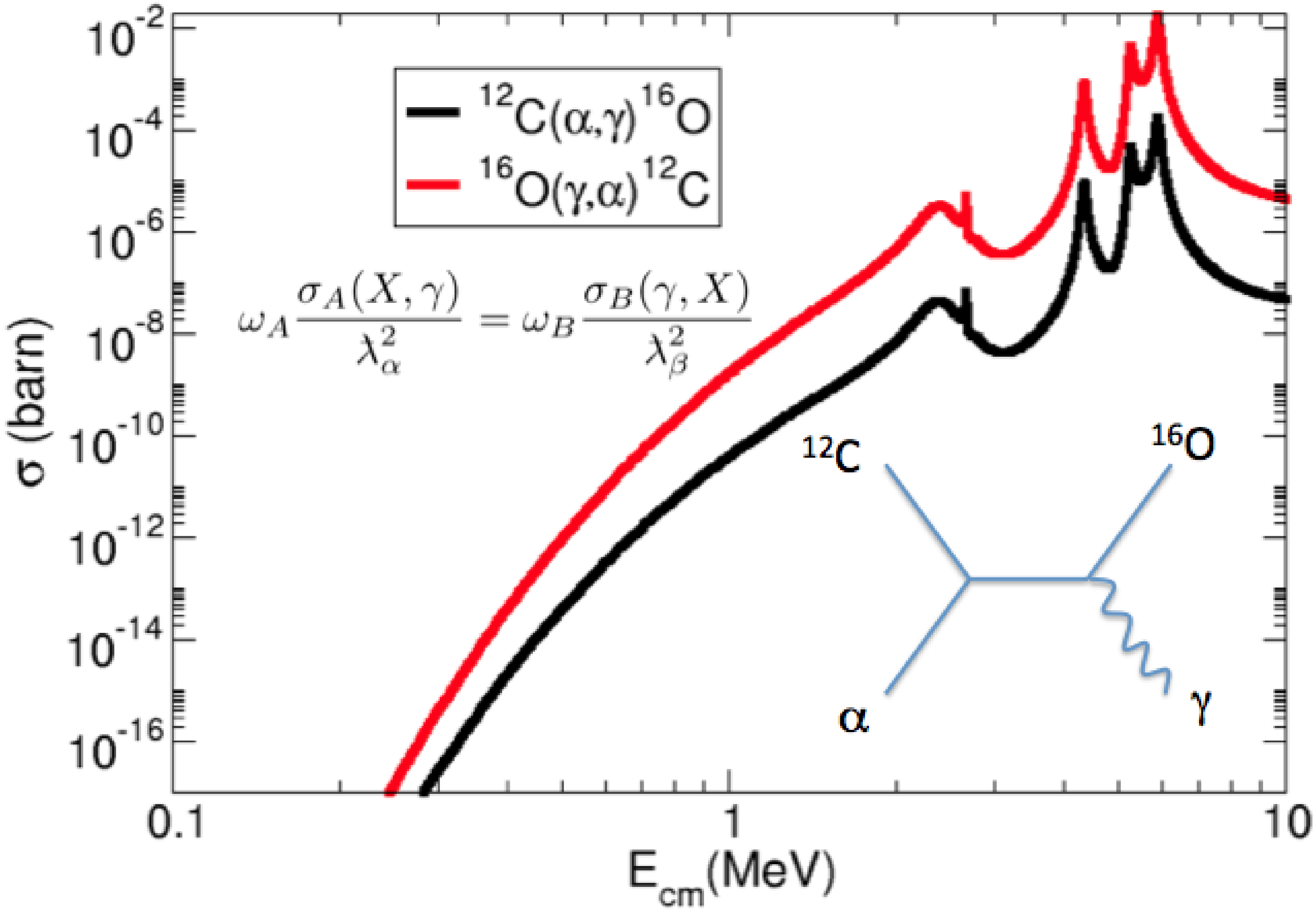

Application
$^{16}O(\gamma, \alpha)^{12}C$

Claudio Ugalde, The University of Chicago

STAR

Bubble Chamber

Superheated Target for Astrophysics Research (STAR)

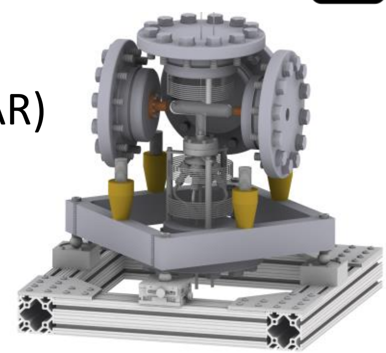

Moshe Gai, U. Conn. and Yale

Optical Readout TPC

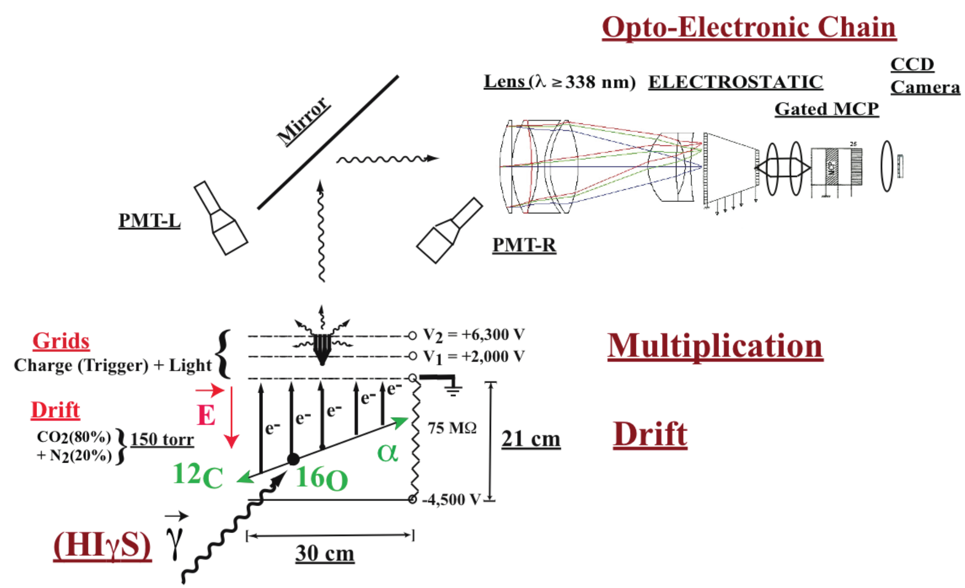

Evaluated Nuclear Data Library

- ENDF (USA)

  http://t2.lanl.gov/nis/data/endf/index.html
- JEFF (Europe)

  http://www.oecd-nea.org/dbforms/data/eva/evatapes/jeff_32/
- JENDL (Japan)

  http://wwwndc.jaea.go.jp/jendl/j40/J40_J.html

Reference Input Parameter Library (RIPL-3)

https://www-nds.iaea.org/RIPL-3/

ELI-NP (Europe)

(Extreme Light Infrastructure- Nuclear Physics)

Magurele-Bucharest, Romania

Approved by the European Commission in 2012

First Experiments in 2018

E_γ = 0.2 -19 MeV

$I_\gamma \geq 10^{11}$ (s^{-1} mm^{-2} $mrad^{-2}$ $0.1\%^{-1}$)

$\Delta E/E \leq 0.5\%$

HIGS (USA)

(High Intensity Gamma-Ray Source)

Duke Free Electron Laser Laboratory

E_γ = 1 -100 MeV
$I_\gamma > 10^8$ s^{-1} cm^{-2} on target
$\Delta E/E > 1\%$

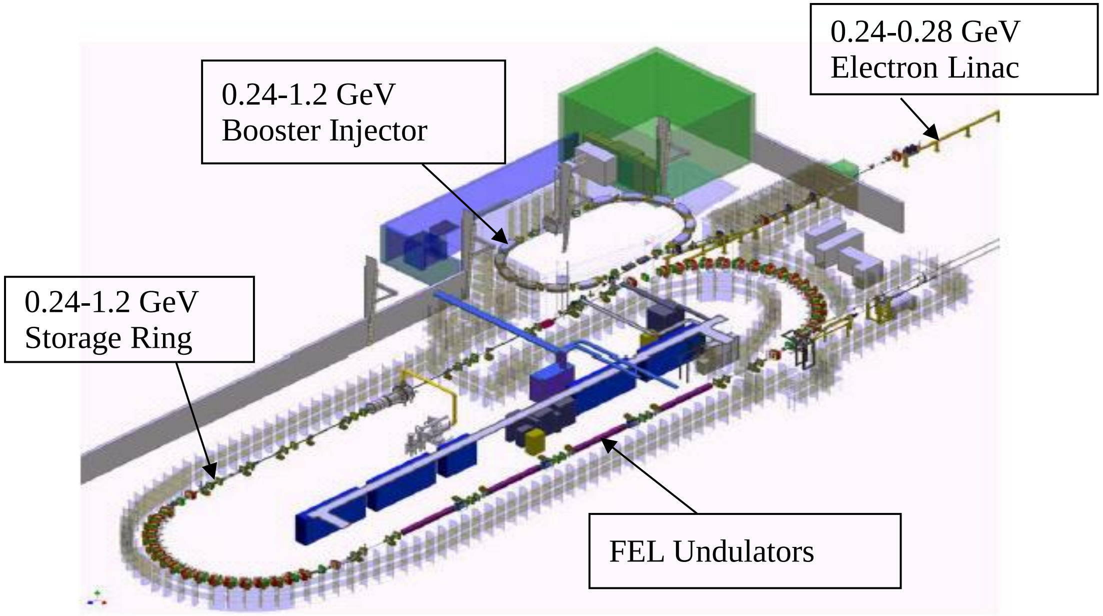

AIST Electron Accelerator Facility

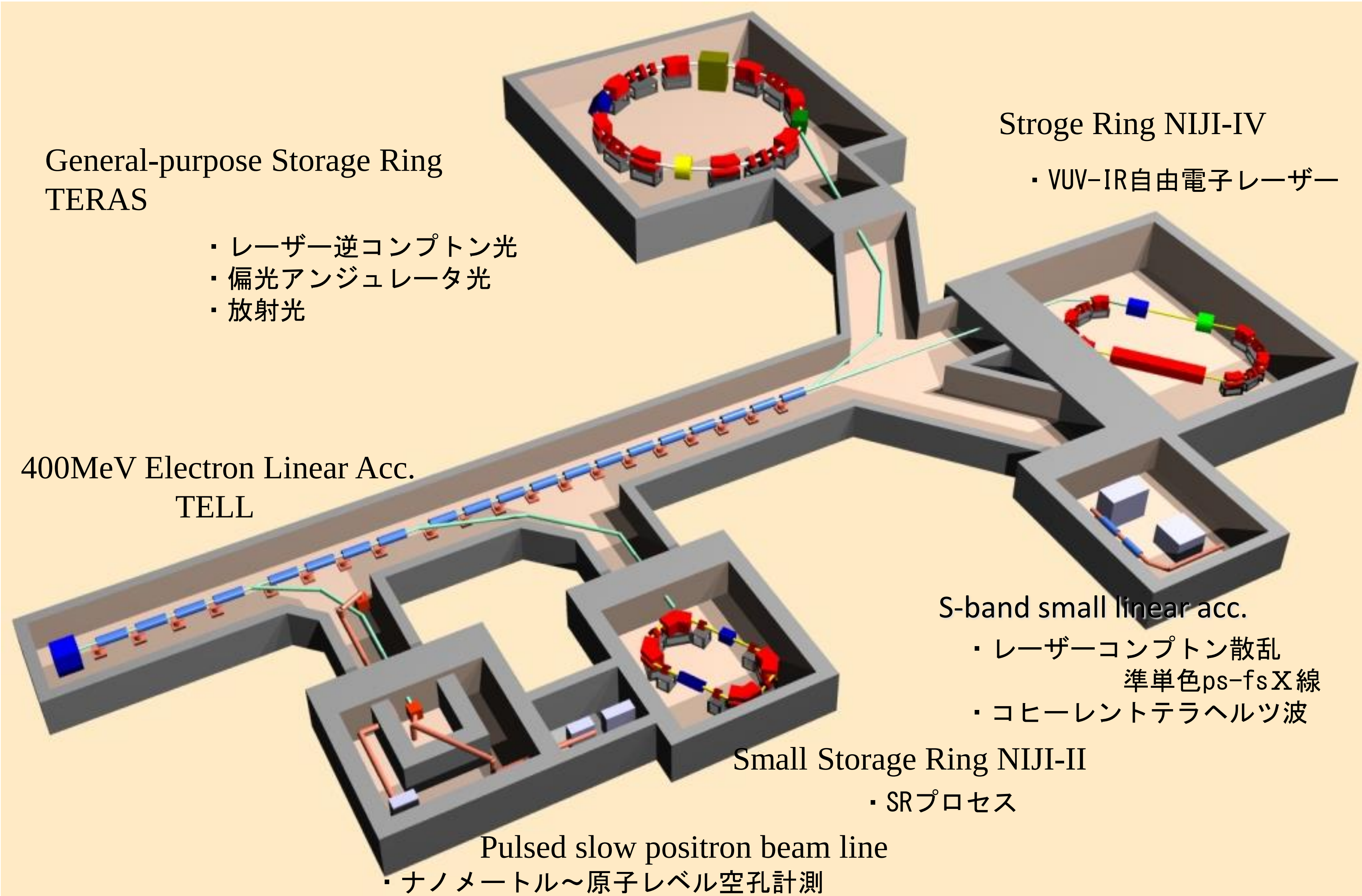

AIST : National Institute for Advanced Industrial Science and Technology
TERAS (Tsukuba Electron Ring for Acceleration and Storage)

closed in April 2012

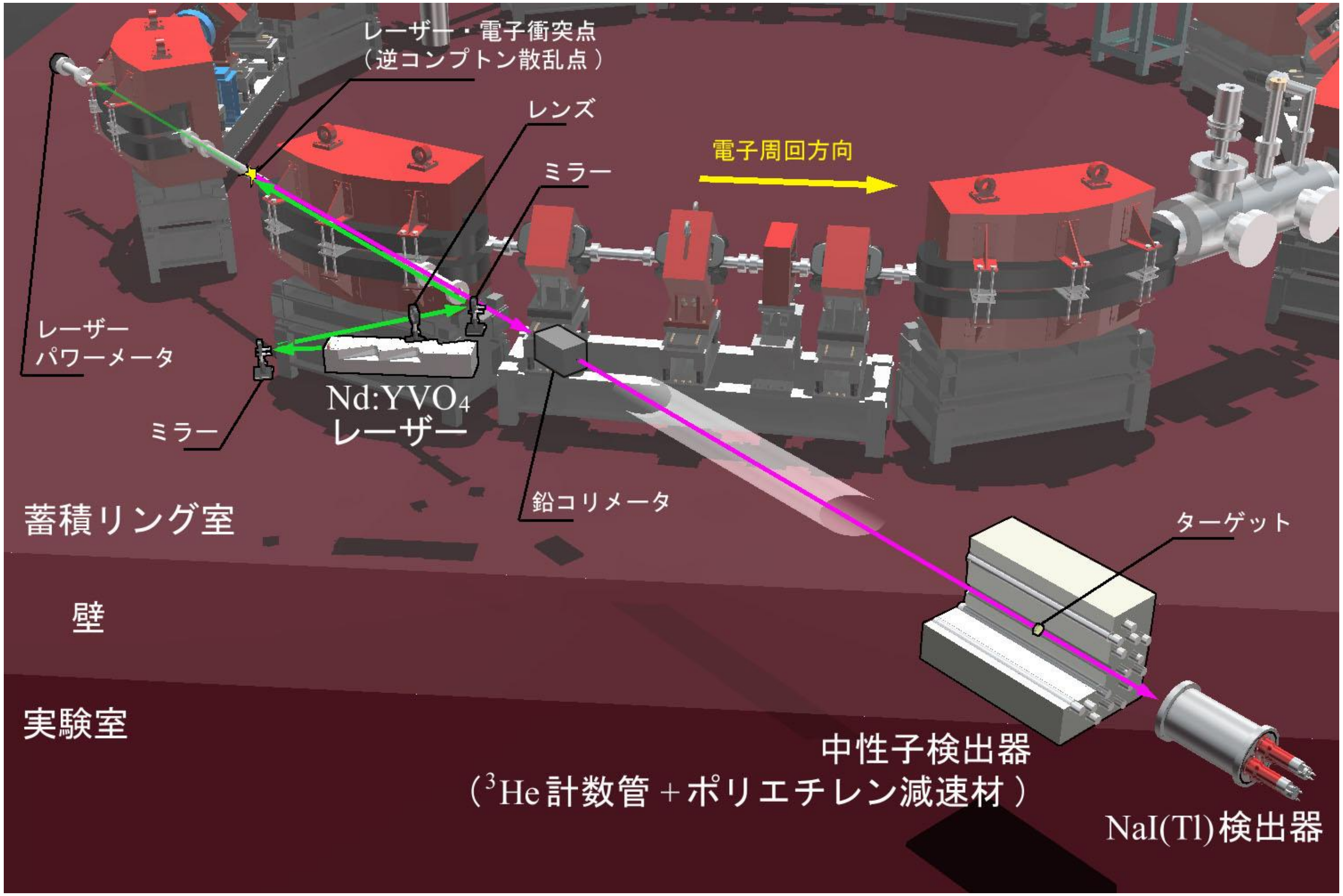


LEPS, LEPS2
GeV γ
SPring8 8 GeV e- storage ring
SACLA
8 GeV e- linac
8 GeV e- synchroton
1 GeV e- Linac
NewSUBARU
MeV γ

NewSUBARU (Japan)

0.55 – 1.5 GeV storage ring

E_γ=0.5 – 76 MeV

$I_\gamma = 10^6 - 10^7\ s^{-1}$

(3 – 6 mm dia.)

$\Delta E/E > 2\%$

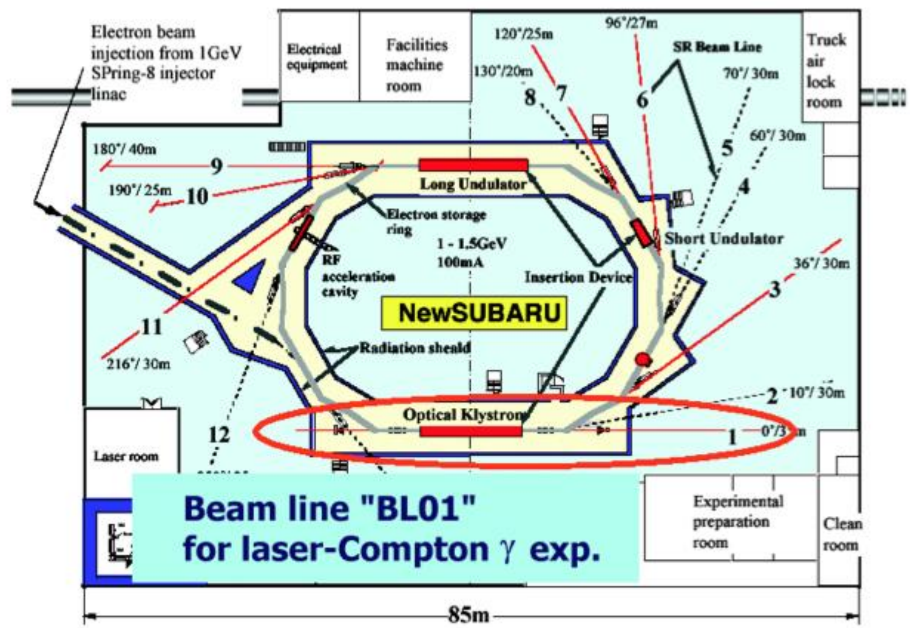

Experimental Hutch GACKO (Gamma Collaboration Hutch of Konan University)

Table-top Lasers

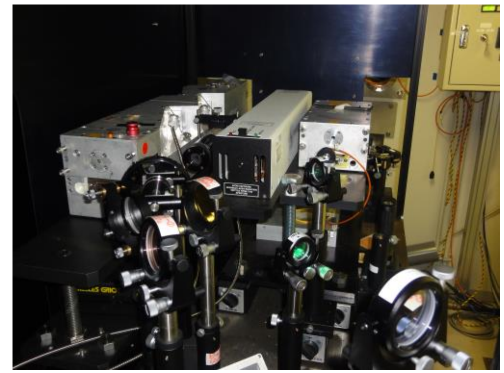

I. Physics and Experiments with a 4π Neutron Detector

Physics

Rare isotope measurements for the p-process nucleosynthesis

p−nuclei are very rare.

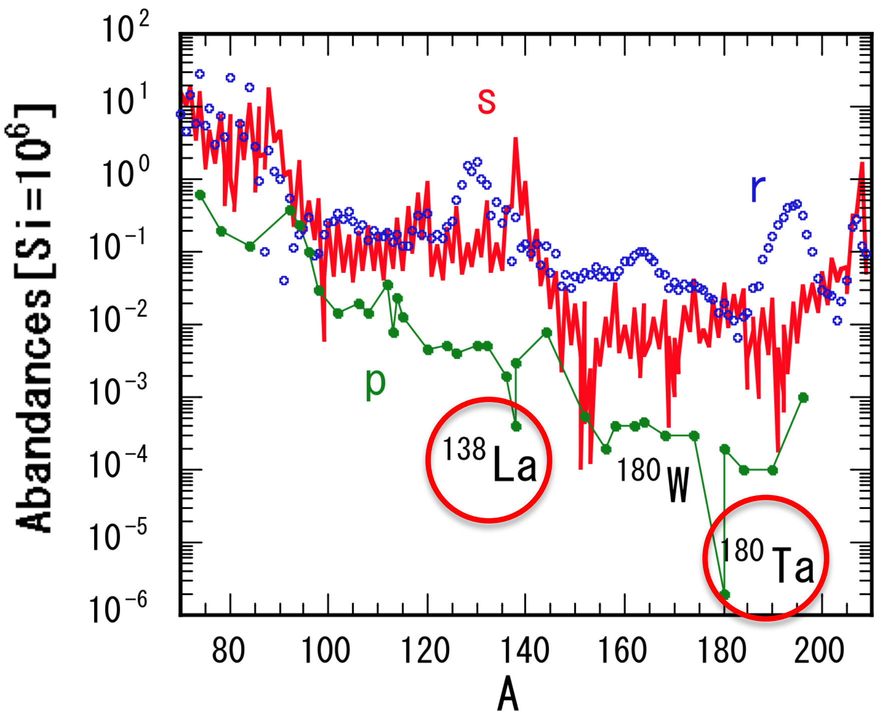

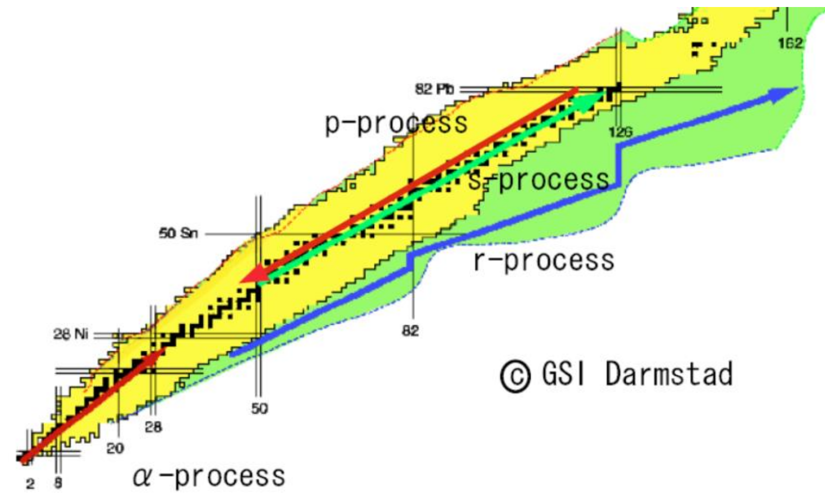

- Highest intensity and monochromatic γ-ray beam
- 1mg samples of rare isotopes

Rarest element
Only naturally–occurring isomer

Production	vs	Destruction
181Ta(γ,n)<u>180Ta</u>		<u>180Ta</u>(γ,n)179Ta
139La(γ,n)<u>138La</u>		<u>138La</u>(γ,n)137La
measured!		Not so ever

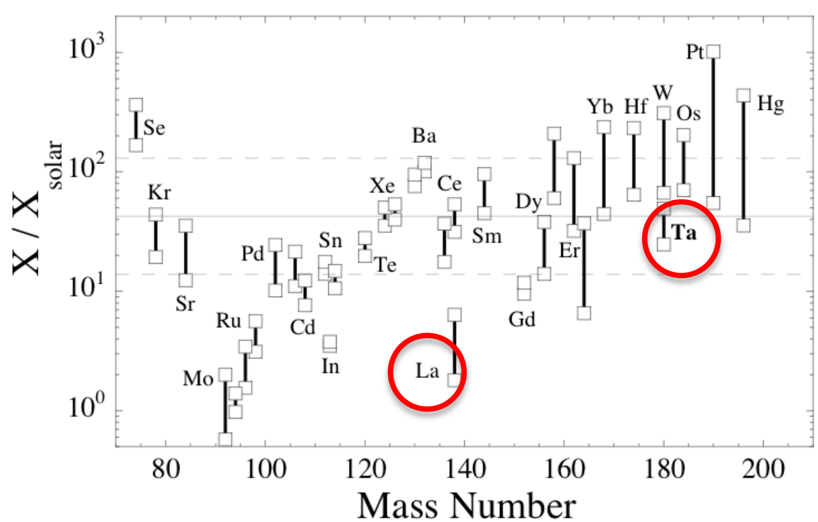

H. Utsunomiya et al., PRC67, 015807 (2003)

Day 1 Experiment #1

^{180}Ta(γ,n) & ^{138}La(γ,n) measurement

20 ^{3}He proportional counters
embedded in polyethylene moderator
Triple-ring configuration
- 1st ring of 4 counters
- 2nd ring of 8 counters
- 3rd ring of 8 counters

4π Neutron Detector

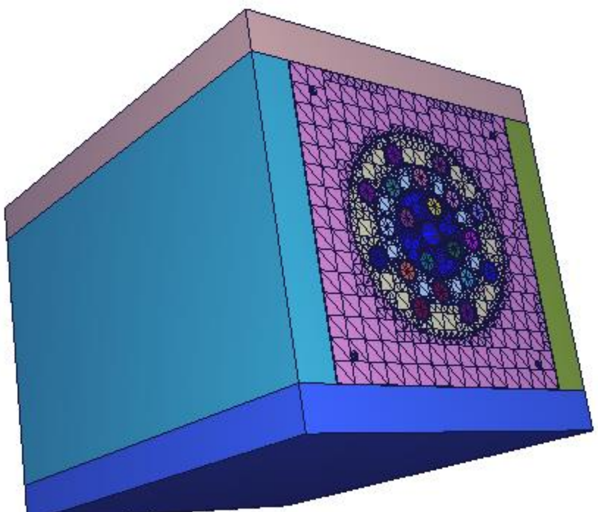

^{180}Ta vs ^{181}Ta (Isotopic Impurity)

A ^{180}Ta sample with **rather low enrichment** may contain a large amount of ^{181}Ta.

$S_n(^{181}\text{Ta:7576.8 keV}) - S_n(^{180}\text{Ta: 6641.2 keV}) = 935.6$ keV

Similarly,

$S_n(^{139}\text{La:8778 keV}) - S_n(^{138}\text{La: 7495 keV}) = 1283$ keV

We have to be careful about the amount of chemical impurities of ^{180}Ta and ^{138}La samples as well.

Rare isotopes to be studied

35 p-nuclei
Neutron-deficient isotopes

Nucleus	Natural abundance (%)	Abundance (10^6 Si) Anders&Grevesse
180Ta	0.012	2.48E-06
190Pt	0.014	0.00017
184Os	0.02	0.000122
156Dy	0.06	0.000221
120Te	0.09	0.0043
124Xe	0.09	0.00571
126Xe	0.09	0.00509
138La	0.09	0.000409
158Dy	0.1	0.000378
132Ba	0.101	0.00453
130Ba	0.106	0.00476
180W	0.12	0.000173
168Yb	0.13	0.000322
162Er	0.14	0.000351
196Hg	0.15	0.00048
174Hf	0.16	0.000249
136Ce	0.185	0.00216
152Gd	0.2	0.00066
138Ce	0.251	0.00284
115Sn	0.34	0.0129
78Kr	0.35	0.153
84Sr	0.56	0.132
114Sn	0.66	0.0252
74Se	0.89	0.55
108Cd	0.89	0.0143
112Sn	0.97	0.0372
102Pd	1.02	0.0142
106Cd	1.25	0.0201
164Er	1.61	0.00404
98Ru	1.87	0.035
144Sm	3.07	0.0008
113In	4.29	0.0079
96Ru	5.54	0.103
94Mo	9.25	0.236
92Mo	14.84	0.378

Realm of Nuclear Photonics

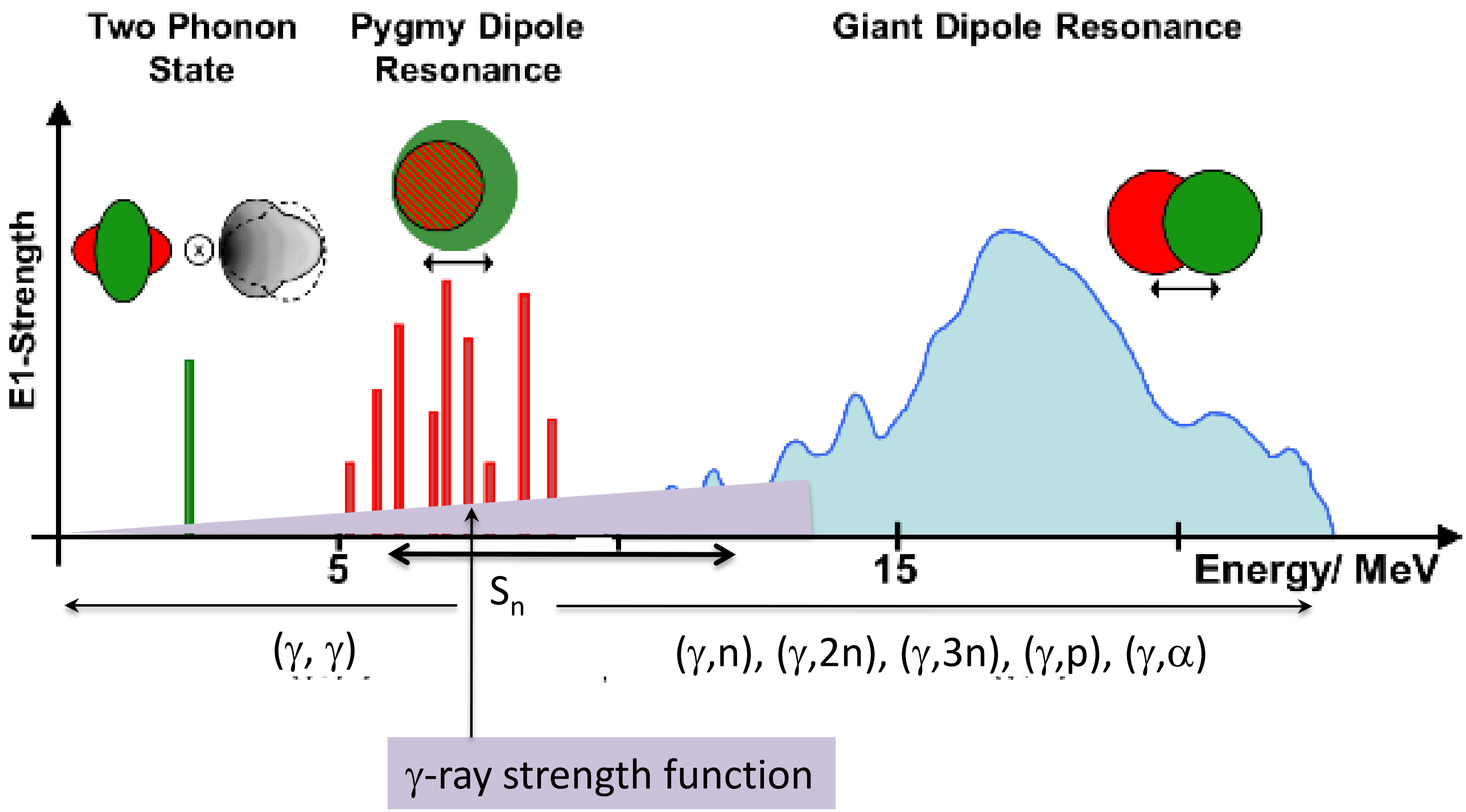

Nucleosynthesis (p-process, s-process)

modified by H. Utsunomiya

Norbert Pietralla, TU Darmstadt ELI Workshop

Resonances above S_n

Threshold Photoneutron Technique
Bremsstrahlung + n-TOF

C.D. Berman et al., PRL25, 1302 (1970)
R.J. Baglan et al., PRC3, 2475 (1971)

$^{207}Pb(\gamma,n)$

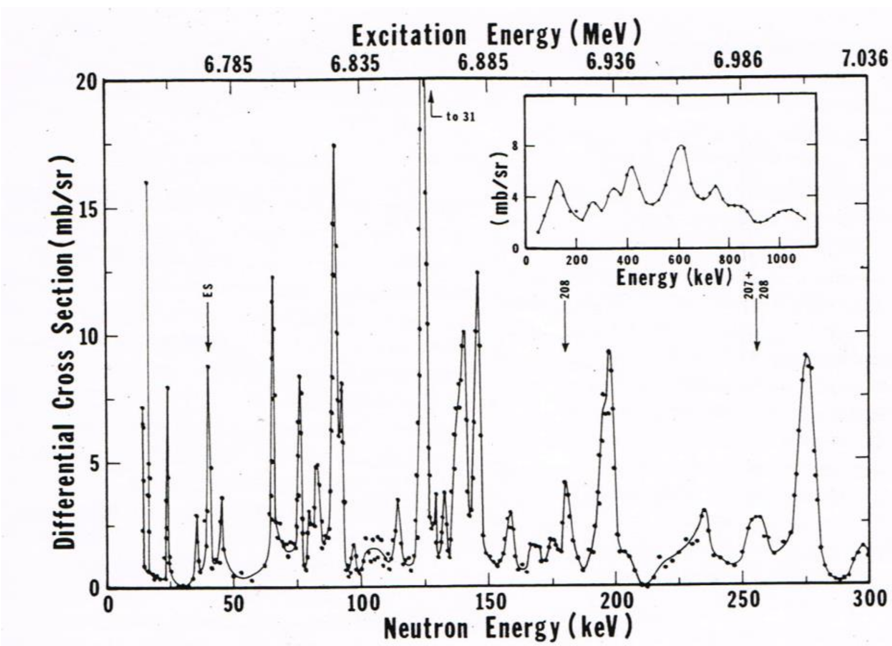

$^{208}Pb(\gamma,n)$

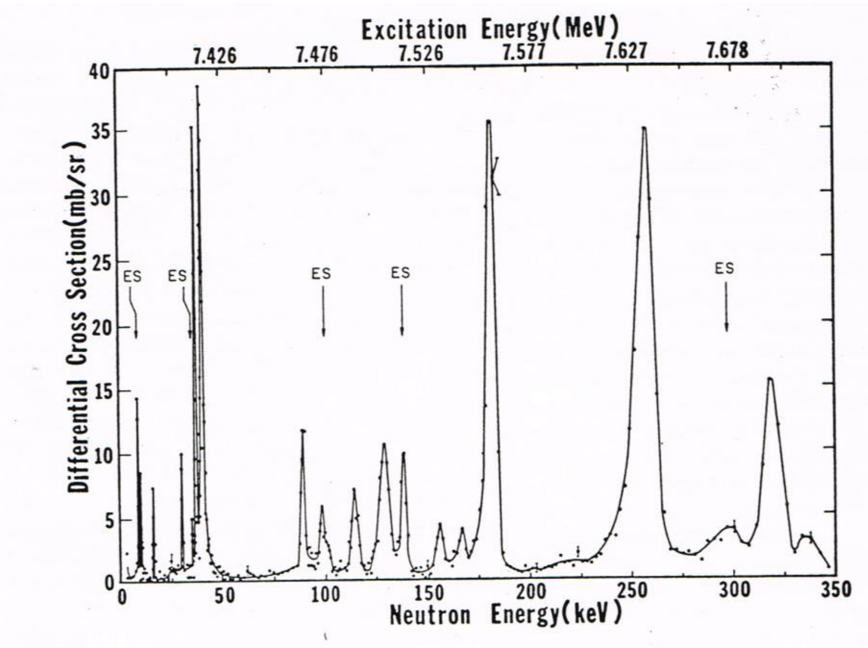

$^{57}Fe(\gamma,n)$

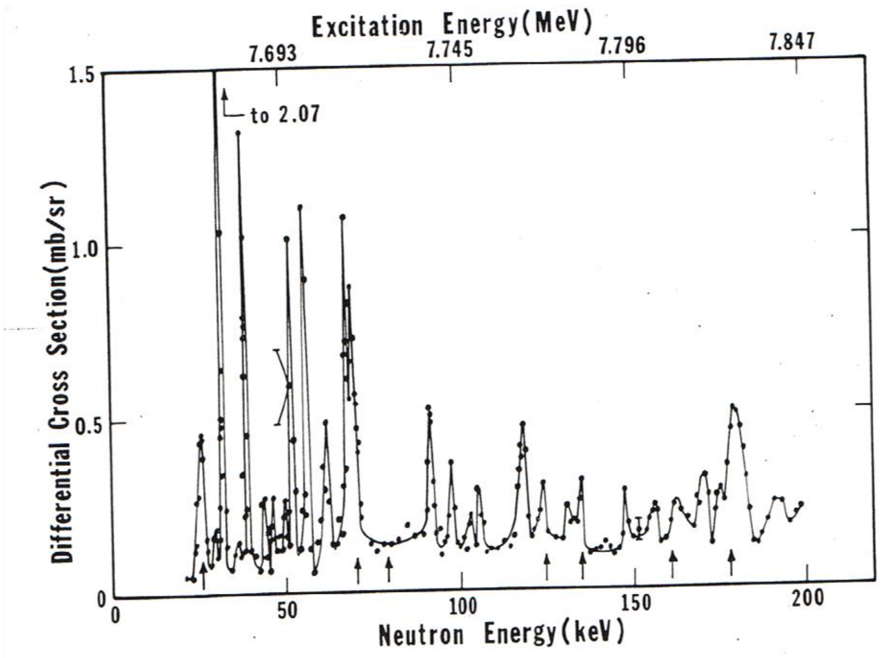

$^{53}Cr(\gamma,n)$

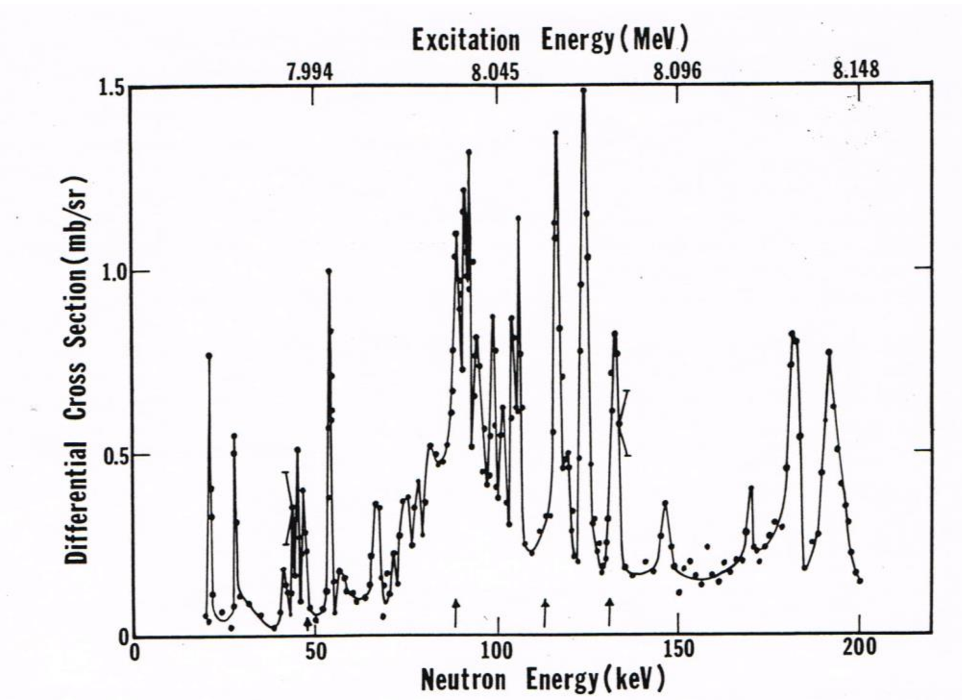

Day 1 Experiment #2

PDR and M1 resonance in ^{207}Pb

- ^{207}Pb(γ,n) measurement -

Liquid Scintillation and $LaBr_3$(Ce) Detector Array

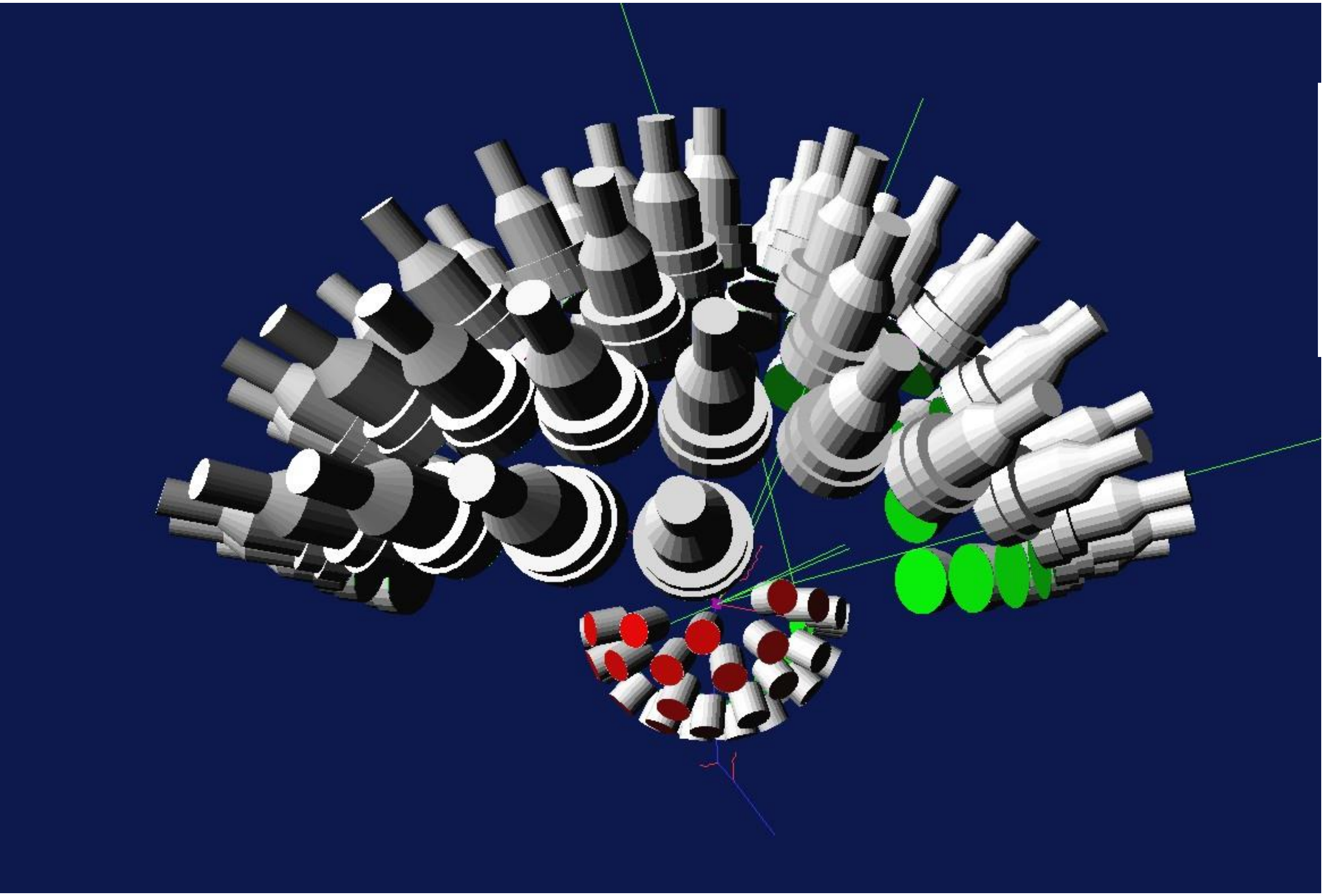

62

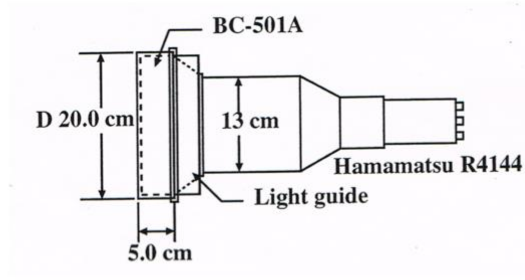

34

$LaBr_3$(Ce), 3” x 3”

Day 1 Experiment #3

Exclusive neutron decays of GDR in ^{159}Tb

in collaboration with Vladimir Varlamov

- **^{159}Tb(γ,xn) x= 1, 2, 1g/cm^2**
- S_n = 8.133 MeV
- S_{2n} = 14.911 MeV

IAEA –TECDOC-1178

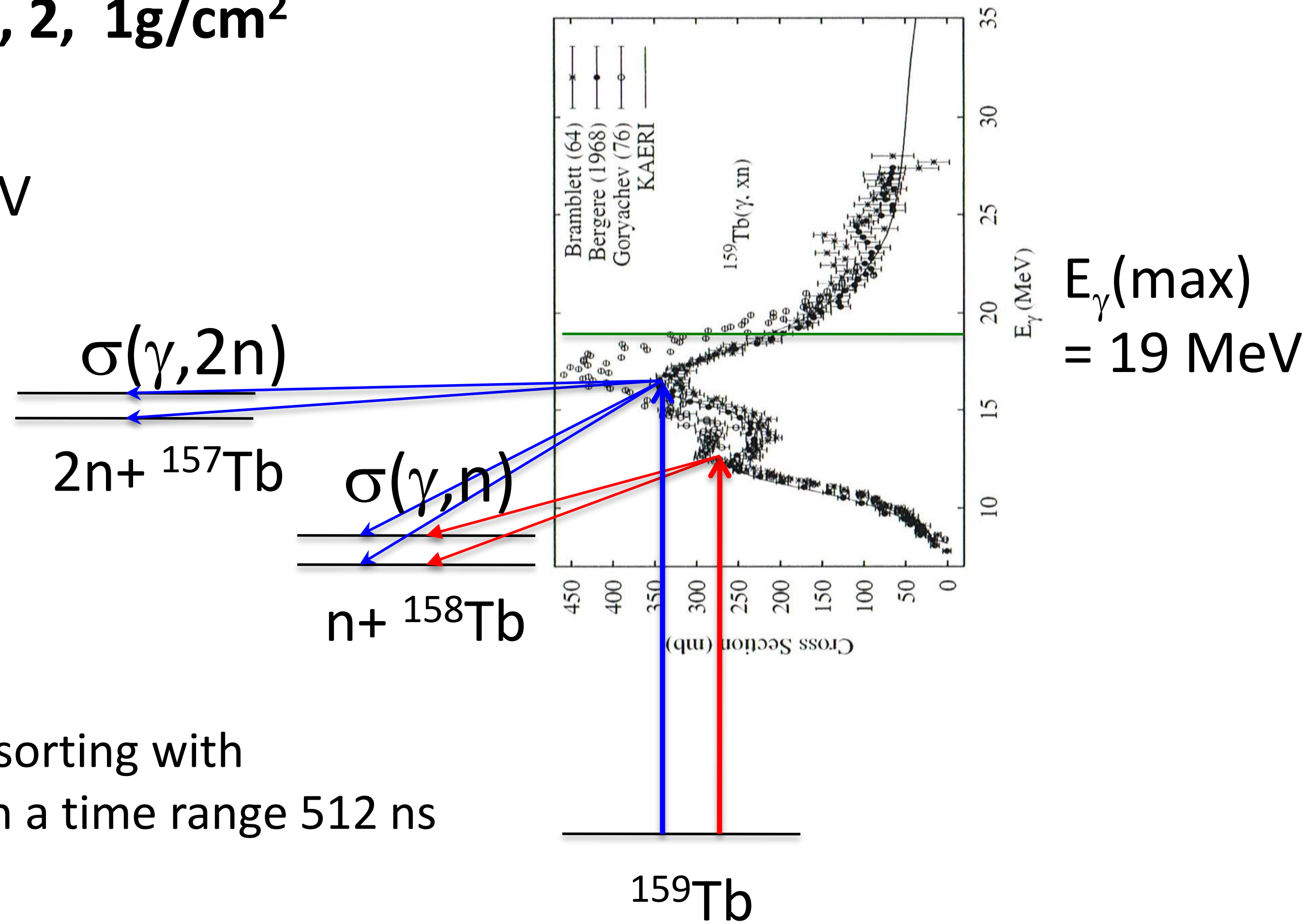

Neutron multiplicity sorting with
a multi-stop TDC with a time range 512 ns

Day 1 Experiment #4-1

<u>Production</u> of long-lived Isomers by 2 x 10PW lasers at <u>E7</u>

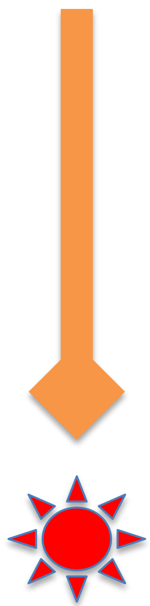

Laser

2 x 10 PW

Laser acceleration of heavy ions that undergo nuclear excitations induced by electrons.

^{189}Os: 9/2^{-}, 30.8 keV, 5.81h

^{176}Lu: 1^{-}, 123 keV, 3.66h

Experimental setup for Laser acceleration of Fe ions

Private communication with Dr. Nishiuchi of JAEA-KIZU

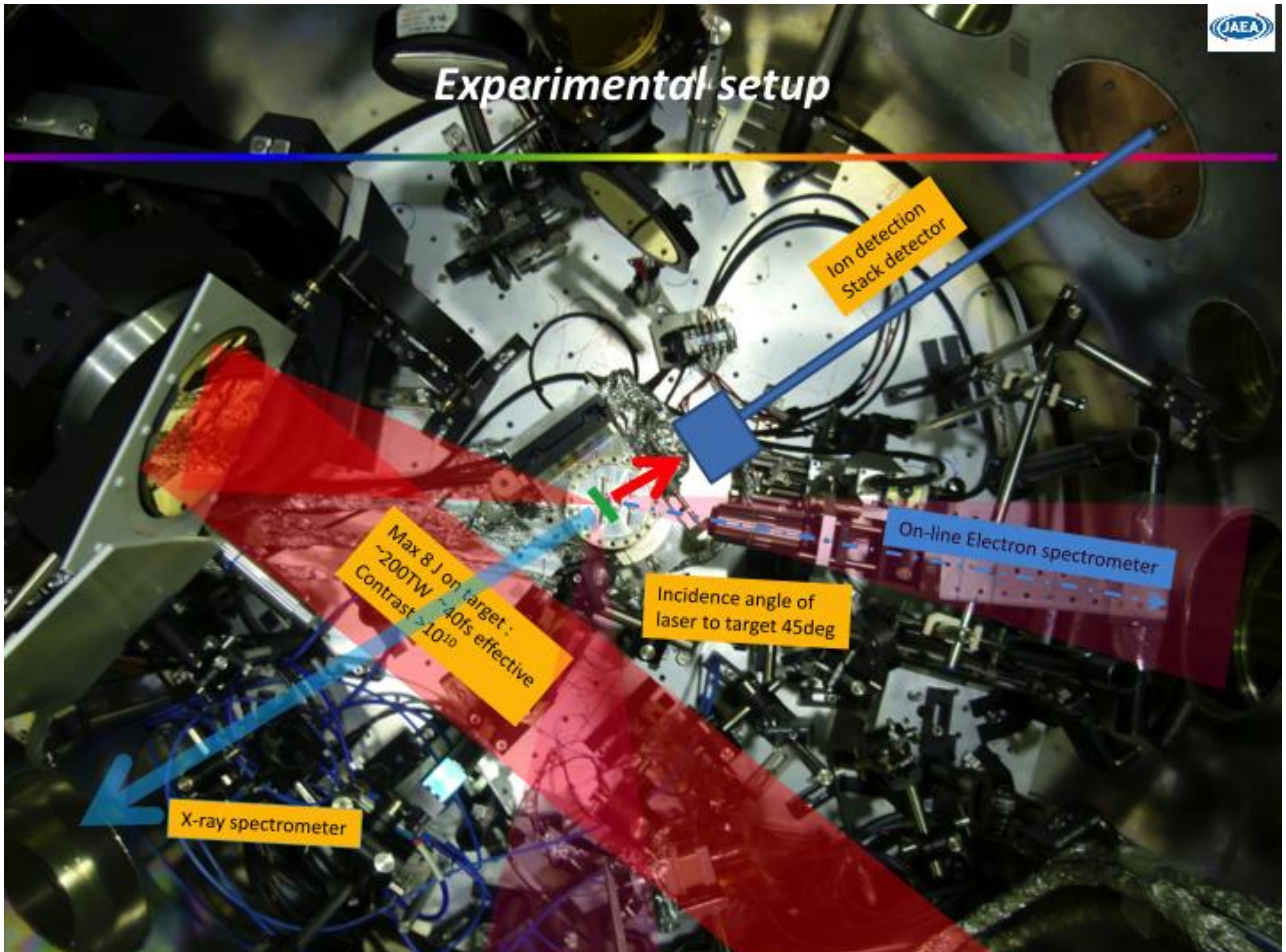

Acceleration mechanism (Target Normal Sheath Acceleration)

Extension of the classical case of plasma expansion into vacuum driven by ambipolar electric field

$$E \sim \frac{T_e}{e\lambda_D}$$

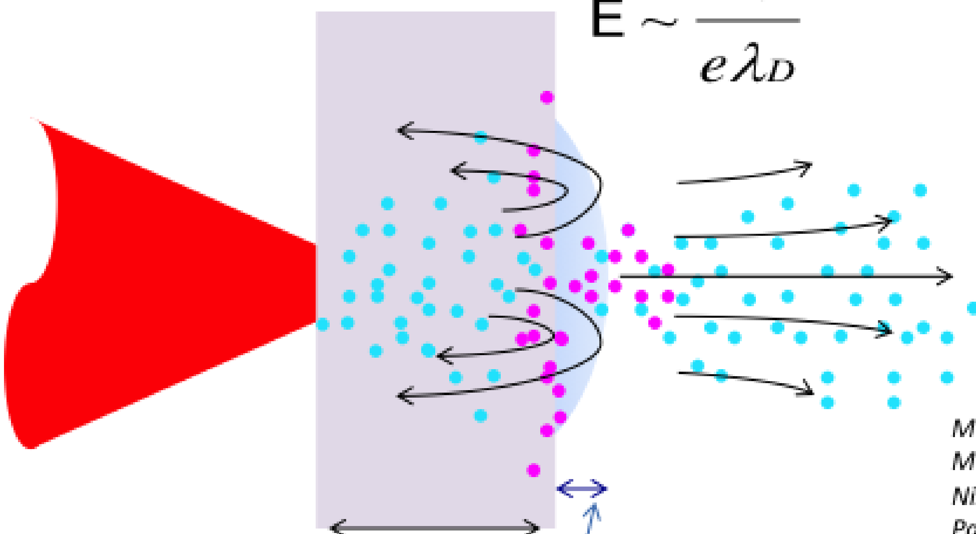

Target ~μm

λ_D<1μm

>10TV/m

Boltzmann dist. for electron

$$n_e = n_{e0} \exp(e\Phi / T_e)$$

Poisson eq.

$$\varepsilon_0 \frac{\partial^2 \Phi}{\partial^2 x} = e(n_e - n_p)$$

*Mora, PRL **90**, 185002 (2003), Mora, PRE **72**, 056401 (2005)*
*Murakami and Basko, PoP **13** 012105 (2006)*
*Nishiuchi PLA **357** 339 (2006)*
*Passoni and Lontano LPB **22** 163 (2004),*
Lontano and Passoni PoP 13 042102 (2006)
*Passoni and Lontano PRL **101** 115001 (2008),*

Proton energy at shock front

$$E_i \propto f(t_{acc}, l_{acc}) \times T_e$$

Day 1 Experiment #4-2

Photoexcitation of long-lived isomers at E8

^{189}Os: 9/2$^-$, 30.8 keV, 5.81h

^{176}Lu: 1$^-$, 123 keV, 3.66h

We can confirm photo-excitation of isomers by detecting neutrons.

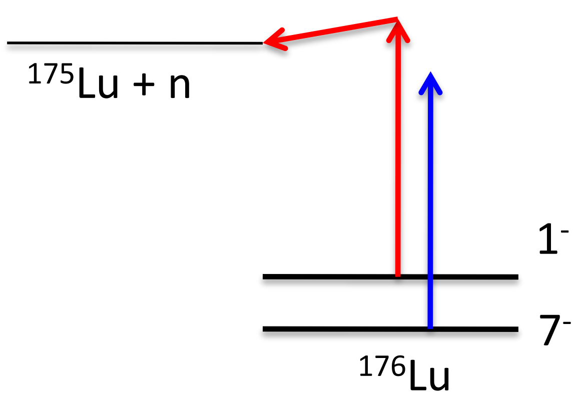

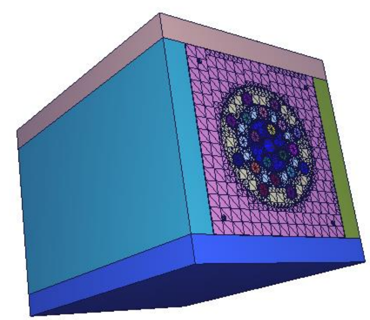

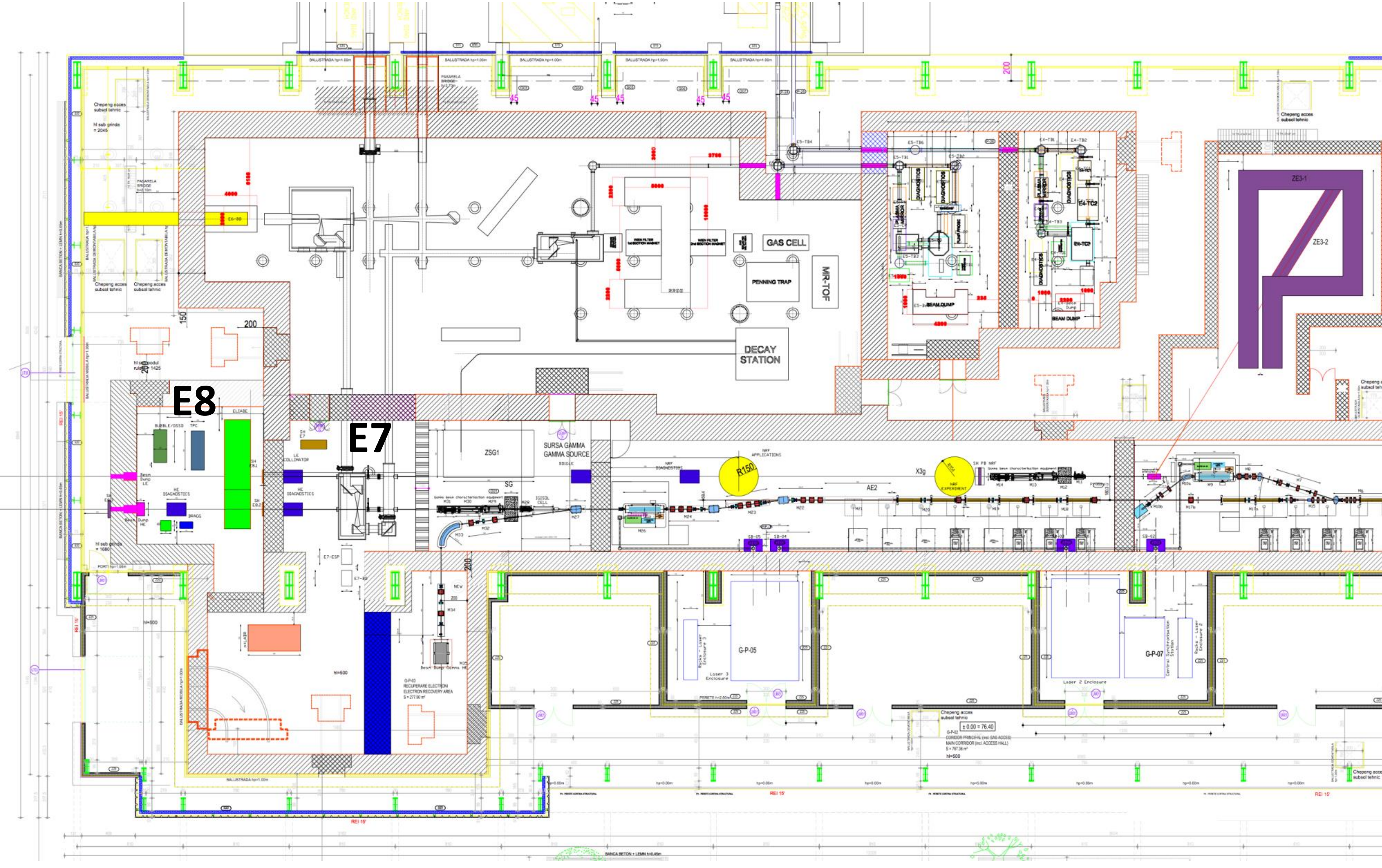
E8
E7
ELIADE
ZSG1
SURSA GAMMA
GAMMA SOURCE
GAS CELL
PENNING TRAP
MR-TOF
DECAY
STATION
BEAM DUMP
R150
X3g
AE2
ZE3-1
ZE3-2
G-P-05
G-P-07

Summary

- Following pioneering developments at HIGS, AIST, and NewSUBARU, ELI-NP will open up a new era of nuclear science with intense gamma and laser photon beams.
- Please join photon physics at different facilities worldwide.

Imagination is more important than knowledge.

— A. Einstein